

Dissertation zur Erlangung des Doktorgrades der Fakultät für
Biologie der Ludwig-Maximilians-Universität München

Inhibition of PLK1-dependent phosphorylation of
EBNA2 promotes EBV-induced carcinogenesis in
humanized mice



Xiang Zhang

München, February 2021

Diese Dissertation wurde angefertigt
unter der Leitung von Prof. Dr. Bettina Kempkes
in der Abteilung Genvektoren
am Helmholtz Zentrum München, Deutsches Forschungszentrum für Gesundheit und
Umwelt (GmbH)

Erstgutachter: Prof. Dr. Bettina Kempkes

Zweitgutachter: Prof. Dr. Wolfgang Enard

Tag der Abgabe: 02.02.2021

Tag der mündlichen Prüfung: 28.06.2021

Zusammenfassung

Über 95% der erwachsenen Bevölkerung weltweit sind asymptomatisch und dauerhaft mit dem Epstein-Barr-Virus (EBV) infiziert. EBV ist mit einer Vielzahl von Erkrankungen sowohl lymphoiden als auch epithelialen Ursprungs assoziiert, darunter infektiöse Mononukleose, Hodgkin-Lymphom, Burkitt-Lymphom und Nasopharynxkarzinom. Ein Schlüssel-EBV-Protein ist der Transkriptionsfaktor EBV nukleäre Antigen 2 (EBNA2), der die B-Zell-Proliferation durch Aktivierung viraler und zellulärer Zielgene initiiert. In dieser Arbeit wurde die Bindung der mitotischen Polo-like Kinase 1 (PLK1) an EBNA2 charakterisiert, PLK1 phosphoryliert die EBNA2 Transaktivierungsdomäne und inhibiert deren Aktivität. EBNA2 Mutationen, die die PLK1-Bindung beeinträchtigen oder die Phosphorylierung durch PLK1 blockieren, sind Funktionsgewinnmutanten. Sie erhöhten die Transaktivierungskapazitäten, beschleunigen die Proliferation infizierter B-Zellen und förderten die Entwicklung von Lymphomen in humanisierten Mäusen. Zusammengefasst koordiniert PLK1 die Aktivität von EBNA2, um das Risiko von Tumorinzidenzen zugunsten der Entstehung einer Latenz im infizierten Wirt zu verringern.

.

Abstract

Over 95% of the adult population worldwide is asymptotically and persistently infected with Epstein-Barr virus (EBV). EBV is associated with a diverse range of diseases of both lymphoid and epithelial origin, including infectious mononucleosis, Hodgkin's lymphoma, Burkitt's lymphoma, and nasopharyngeal carcinoma. A key EBV protein is the transcription factor EBV nuclear antigen 2 (EBNA2), which initiates B cell proliferation by activating viral and cellular target genes. In this thesis, the complex of EBNA2 and polo-like kinase 1 (PLK1) was characterized. PLK1 phosphorylated the transactivation domain of EBNA2, and thereby inhibited its transactivation activity. EBV mutants that impair PLK1 binding or block phosphorylation by PLK1 are gain of function mutants. They have enhanced transactivation capacities, they accelerate the proliferation of infected B cells, and they promote the development of lymphomas in humanized mice. In conclusion, PLK1 coordinates the activity of EBNA2 to attenuate the risk of tumor incidences in favor of the establishment of latency in the infected host.

Table of Content

1. Introduction.....	1
1.1. Epstein-Barr virus.....	1
1.1.1. EBV genome	2
1.1.2. The life cycle of EBV	4
1.1.3. EBV-associated diseases	6
1.2. EBNA2.....	8
1.2.1. EBNA2 features and its binding proteins.....	8
1.2.2. Posttranscriptional modification of EBNA2 and its function.....	9
1.3. Polo-like kinase family	10
1.3.1. PLK1 function	11
1.3.2. Substrate phosphorylation by PLK1	11
1.3.3. PLK1: an oncogene or tumor suppressor gene?.....	12
1.4. Association of EBV pathogenesis with PLK1	13
1.5. Objective.....	13
2. Material	15
2.1. Human donor samples	15
2.2. Mouse models	15
2.3. Human primary B cells.....	15
2.4. Cell lines	15
2.5. Bacterial strains.....	17
2.6. Recombinant DNA	18
2.7. Oligonucleotides.....	22
2.8. Peptides	22
2.9. Antibodies	22
2.10. Cell culture materials.....	23
2.11. Bacterial culture materials.....	24
2.12. Chemicals and reagents	24
2.13. Kits.....	26
2.14. Laboratory equipment.....	26
2.15. Bioinformatics tools	27
3. Methods.....	28
3.1. Mammalian cell culture methods.....	28
3.1.1. Cell culture	28
3.1.2. Long term cell storage.....	28
3.1.3. Generation of clonal recombinant EBV producer cell lines	29

3.1.4.	Production and concentration of recombinant EBV	30
3.1.5.	Titration of recombinant EBV	30
3.1.6.	Preparation of human primary B cells from adenoids	31
3.1.7.	Establishment of LCLs by recombinant EBV	31
3.1.8.	Cell proliferation assays	32
3.2.	Bacterial culture methods	32
3.2.1.	Propagation and storage of bacteria.....	32
3.2.2.	Preparation of chemically competent bacteria.....	33
3.2.3.	Preparation of electro-competent bacteria SW105.....	33
3.2.4.	Heat shock transformation of <i>E.coli</i>	34
3.2.5.	Electroporation of <i>E.coli</i>	34
3.2.6.	Cloning and mutagenesis of plasmids	34
3.2.7.	Isolation of plasmids.....	44
3.2.8.	BAC recombineering	44
3.2.9.	Isolation of BACmids.....	46
3.3.	DNA related techniques	47
3.3.1.	Isolation of genomic DNA from mammalian cells	47
3.3.2.	Polymerase chain reaction (PCR).....	47
3.3.3.	Restriction endonuclease digestion of DNA	48
3.3.4.	5'-phosphorylation of oligonucleotides.....	48
3.3.5.	Oligo annealing to form linkers	48
3.3.6.	DNA gel electrophoresis	48
3.3.7.	Purification of DNA fragments.....	48
3.3.8.	Determining the concentration of DNA	48
3.3.9.	Sanger sequencing of DNA	49
3.3.10.	EBV diagnosis by PCR	49
3.4.	Protein biochemistry related techniques.....	49
3.4.1.	Recombinant protein expression	49
3.4.2.	Recombinant protein purification	49
3.4.3.	Generation of whole mammalian cell extracts.....	50
3.4.4.	Bradford assay	51
3.4.5.	Dual-luciferase assay.....	51
3.4.6.	Co-immunoprecipitation	51
3.4.7.	GST pull-down assay	52
3.4.8.	Kinase assay <i>in vitro</i>	52
3.4.9.	Dephosphorylation of protein	52
3.4.10.	Sodium dodecyl sulfate-polyacrylamide gel electrophoresis (SDS-PAGE)	52
3.4.11.	Coomassie brilliant blue staining	53
3.4.12.	Gel drying	53
3.4.13.	Phosphorimaging	53

3.4.14.	Western blotting (WB).....	53
3.4.15.	Liquid chromatography-tandem mass spectrometry (LC-MS/MS).....	55
3.5.	Protein biophysics related techniques	54
3.5.1.	Isothermal titration calorimetry (ITC)	54
3.5.2.	Nuclear magnetic resonance (NMR) spectroscopy	54
3.6.	Animal study	55
3.6.1.	Generation of humanized mice	55
3.6.2.	Infection of huNSG mice with recombinant EBV	55
3.6.3.	The whole blood and spleen preparations for immunophenotyping.....	55
3.6.4.	Viral loads detection in blood and spleen in infected humanized mice	57
3.7.	Statistical analyses.....	57
4.	Results.....	58
4.1.	Characterization of the interaction of EBNA2 and PLK1	58
4.1.1.	EBNA2 and PLK1 interact with each other in EBV-transformed B cells.	58
4.1.2.	PLK1 binds to two regions of EBNA2	59
4.1.3.	Phosphorylated S379 in EBNA2 PDS1 serves as a canonical PLK1 docking site primed by CDK1.	61
4.1.4.	PDS2 binding to PLK1 PBD does not require priming by cellular kinases.....	62
4.1.5.	Impact of PLK1 docking sites on EBNA2 transactivation activities	64
4.2.	EBNA2: a novel viral substrate of PLK1.	65
4.2.1.	EBNA2 is a novel substrate of PLK1.	65
4.2.2.	Identification of phosphorylation sites of EBNA2 by PLK1 using LC-MS/MS	66
4.2.3.	S457 and T465 are the major phosphorylation sites of EBNA2 by PLK1	68
4.2.4.	Impact of PLK1-dependent phosphorylation on EBNA2's transactivation	69
4.3.	BACmid construction and recombinant EBV production.....	70
4.3.1.	Construction of HA-tagged EBNA2 WT, S379A, or S457A/T465V in the EBV genomes.....	70
4.3.2.	Recombinant EBV production and titration.....	73
4.4.	Characterization of human primary B cells infected with recombinant EBV	74
4.4.1.	EBV strains carrying EBNA2 mutants deficient for PLK1 docking or phosphorylation transform primary B cells <i>in vitro</i>	75
4.4.2.	EBV strains expressing EBNA2 mutants deficient for PLK1 docking or phosphorylation promote B cell proliferation.....	77
4.4.3.	Upregulation of LMP1 in LCLs established by EBV strains expressing EBNA2 deficient for PLK1 docking or phosphorylation.....	78
4.5.	Characterization of humanized mice infected with recombinant EBV	78
4.5.1.	EBV strains carrying EBNA2 mutants deficient for PLK1 phosphorylation induce more frequently lymphomas in humanized mice.....	79

4.5.2. EBV strains carrying EBNA2 mutants deficient for PLK1 phosphorylation induce an earlier immune response in humanized mice	80
5. Discussion	83
5.1. The interaction of EBNA2 and PLK1	83
5.2. The phosphorylation of EBNA2 by PLK1	83
5.3. Characterization of EBV expressing EBNA2 deficient for PLK1 binding or phosphorylation <i>in vitro</i> and <i>in vivo</i>	84
5.4. A proposed model	85
5.5. The relevance of this study for the use of PLK1 inhibitors in cancer treatment....	87
6. References	88
7. Appendices	99
7.1. Supplemental information	99
7.2. Comments on figures.....	116
7.3. Affirmation.....	117
7.4. Curriculum vitae	118

Registers

List of Figures

Figure 1. Diagram of EBV virion.	2
Figure 2. Schematic representation of the EBV genome.	4
Figure 3. Schematic representation of the EBV life cycle.	6
Figure 4. Schematic illustration of selected features of EBNA2.	9
Figure 5. The general structure of the PLK family.	10
Figure 6. Schematic diagram of the mechanism of PLK1 phosphorylation.	12
Figure 7. Endogenous EBNA2 and PLK1 interact with each other in EBV-transformed B cells. ..	58
Figure 8. Two C-terminal regions of EBNA2 serve as PLK1 docking sites (PDS1 and PDS2) to confer EBNA2/PLK1 interaction.	60
Figure 9. The phosphorylation of S379 by CDK1 activates PDS1 binding to PLK1.	61
Figure 10. The PDS2/PLK1 PBD binding is mediated by clusters A and C.	64
Figure 11. Inhibition of phosphorylation of the docking site S379 promotes EBNA2 transactivation activity.	64
Figure 12. PLK1 phosphorylates EBNA2.	65
Figure 13. Identification of PLK1-dependent phosphorylation sites of EBNA2.	67
Figure 14. S457 and T465 are the major phosphorylation sites of EBNA2 by PLK1.	68
Figure 15. The phosphorylation of EBNA2 by PLK1 suppresses its transactivation.	70
Figure 16. Construction of EBV genomic BACmids encoding C-terminal HA-tagged EBNA2 WT, S379A, or S457A/T465V.	72
Figure 17. Schematic workflow of recombinant EBV virus production.	74
Figure 18. Schematic process of the transformation of primary B cells by EBV.	75
Figure 19. EBV strains carrying EBNA2 mutants deficient for PLK1 docking or phosphorylation transform primary B cells <i>in vitro</i>	76
Figure 20. EBV strains expressing EBNA2 mutants deficient for PLK1 docking or phosphorylation promote B cell proliferation.	77
Figure 21. Expression of representative viral and cellular genes.	78
Figure 22. EBV strains expressing EBNA2 mutants deficient for PLK1 docking or phosphorylation cause more frequently lymphomas in humanized mice.	80
Figure 23. EBV strains expressing EBNA2 mutants deficient for PLK1 phosphorylation cause an earlier immune response in humanized mice.	81
Figure 24. A model explaining how PLK1 prevents EBV-induced tumorigenesis through phosphorylation of EBNA2.	86
Figure S1. Schematic diagram of overlap PCR-based mutagenesis.	106
Figure S2. EBNA2 423-474 (PDS2) is sufficient for its binding to PLK1.	107
Figure S3. S379 is a canonical PLK1 docking site.	107
Figure S4. S379 and Cluster A/C are involved in PLK1 binding.	108

Figure S5. Electrophoresis separation of EBNA2 for LC-MS/MS.	108
Figure S6. Identification of phosphorylation sites of EBNA2 treated with PLK1.	110
Figure S7. Identification of phosphorylation sites of EBNA2 fragment 453-474aa by PLK1.	112
Figure S8. Schematic diagram of positive/negative selection used in BAC recombineering.	112
Figure S9. Schematic overview of supercoiled BACmid isolation.	113
Figure S10. Recombinant EBV virus titration.	113
Figure S11. Preparation of human primary B cells.	114
Figure S12. FACS profiles of cell trace violet proliferation assay of B cells after infection.	115
Figure S13. Infection with EBV strains expressing EBNA2 mutants deficient for PLK1 docking or phosphorylation leads to earlier CD8 ⁺ T cell expansion.	115

List of Tables

Table 1. The transcription programs of EBV.	8
Table 2. General and commercially available cell lines.	15
Table 3. Recombinant EBV producer cell lines.	16
Table 4. Lymphoblastoid cell lines.	16
Table 5. Bacterial strains.	17
Table 6. Plasmids used in mammalian cells.	18
Table 7. Plasmids used in protein expression from <i>E.coli</i> or Sf21 insect cells.	19
Table 8. Plasmids used for other purposes.	21
Table 9. BACmids used in this thesis.	21
Table 10. Antibodies used in immunoprecipitation and primary antibodies used in western blotting.	22
Table 11. Secondary antibodies used in western blotting.	23
Table 12. Antibodies used in flow cytometry.	23
Table S1. Oligos used in plasmid construction.	100
Table S2. Oligos used in BAC recombineering.	104
Table S3. Oligos used in pathogen diagnosis.	106
Table S4. Collaborators' contributions to the figures in this thesis.	116
Table S5. My contributions to the figures provided by my collaborators.	116

List of Abbreviations

A	Alanine	LB	Luria-Bertani
[γ - ³² P]	Adenosine triphosphate labeled on the gamma phosphate group with ³² P	LC	Liquid chromatography
ATP	Adenosine triphosphate	LCL	Lymphoblastoid cell line
aa	Amino acid	LCV	Lymphocryptovirus
Ab	Antibody	LMP	Latent membrane protein
approx.	Approximate	λ PPase	Lambda protein phosphatase
APS	Ammonium persulfate	M	Molar
ATP	Adenosine triphosphate	m.o.i.	Multiplicity of infection
BAC	Bacterial artificial chromosome	mA	Milliampere
BARTs	BamHI A rightward transcripts	min	Minute(s)
BCR	B cell receptor	miRNA	Micro-Ribonucleic acid
BGLF4	BamH I G fragment leftward open reading frame 4	ml	Milliliter
BL	Burkitt's lymphoma	mM	Millimolar
bp	Base pair(s)	MOPS	3-(N-morpholino) propanesulfonic acid
BRLF1	BamH I R fragment leftward open reading frame 1	mRNA	messenger RNA
BSA	Bovine serum albumin	MS	Mass spectrometry
BYRF1	BamH I Y fragment rightward open reading frame 1	NaCl	Sodium chloride
BZLF1	BamH I Z fragment leftward open reading frame 1	NaOH	Sodium hydroxide
C	Cysteine	NC	Nitrocellulose
°C	Degree Celsius	ng	Nanogram
Cam	Chloramphenicol	NK cell	Natural killer cell
CBF1	C promoter binding factor 1	nm	Nanometer
CDK	Cyclin dependent kinase	NMR	Nuclear Magnetic Resonance
CK	Casein kinase	NP40	4-Nonylphenyl-polyethylene glycol
cm	Centimeter	NPC	Nasopharyngeal carcinoma
Co-IP	Co-Immunoprecipitation	ORF	Open reading frame
Cp	C promoter	ORF	Open reading frame
CsCl	Caesium chloride	OriLyt	Lytic Origin of replication
D	Aspartic acid	OriP	Latent Origin of replication
d	day(s)	P	Proline
d.p.i.	days post-infection	PBMC	Peripheral blood mononuclear cell
DIM	Dimerization domain	PBS	Phosphate buffered saline
DMEM	Dulbecco's Modified Eagle's Medium	PCR	Polymerase chain reaction
DMSO	Dimethyl sulfoxide	PK	Protein kinase
DNA	2'-deoxyribonucleic acid	PLK	Polo-like kinase
dNTP	Deoxyribonucleotide triphosphate	pmol	picomol
Dox	Doxycycline	PTLD	Post-transplant lymphoproliferative disorder
DTT	Dithiothreitol	PVDF	Polyvinylidene fluoride
<i>E.coli</i>	<i>Escherichia coli</i>	Qp	Q promoter
e.g.	for example	R	Arginine (reverse)
EBER	Epstein-Barr virus encoded RNA	RBPJ	Recombination signal binding protein for immunoglobulin kappa J region
EBNA	Epstein-Barr virus nuclear antigen	RNA	Ribonucleic acid
EBV	Epstein-Barr virus	RNase	Ribonuclease
EDTA	Ethylenediaminetetraacetic acid	rpm	Round per minute
END	EBNA2 N-terminal dimerization domain	RPMI	Roswell Park Memorial Institute
EtBr	Ethidium bromide	RT	Room temperature
F	Phenylalanine (forward)	S	Serine
FACS	Fluorescence-activated cell sorting	s	Second(s)
FBS	Fetal bovine serum	S.E.M.	Standard error of mean
G	Glycine	SD	Standard deviation
g	Gravitational constant	SDS	Sodium dodecyl sulfate
GAPDH	Glyceraldehyde 3-phosphate dehydrogenase	SDS-PAGE	SDS polyacrylamide gel electrophoresis
GC	Gastric carcinoma or germinal center	Strep	Streptomycin
GFP	Green fluorescence protein	T	Threonine
gp	Glycoprotein	TAD	Transactivation domain
GRU	Green Raji Unit	TAE	Tris acetate EDTA
GST	Glutathione S-transferase		

h	hour(s)	TBE	Tris base EDTA
HA	Hemagglutinin	TE	Tris EDTA buffer
HAT	histone acetyltransferase	TEMED	N,N,N',N'-Tetramethyl ethylenediamine
HCl	Hydrogen chloride	TR	Terminal repeat
HHV4	Human herpesvirus 4	Tris	Tris (hydroxymethyl) aminomethane
HHV8	Human herpesvirus 8	UniProt	Universal Protein Resource
HIV	Human immunodeficiency virus	UV	Ultraviolet
HL	Hodgkin's lymphoma	V	Valine or Volt
HLA	Human leukocyte antigen	Ω	Ohm
HRP	Horseradish peroxidase	W	Tryptophan
HRS	Hodgkin/Reed-Sternberg	WB	Western blotting
I	Isoleucine	Wp	W promoter
IARC	International Agency for Research on Cancer	WT	Wild-type
IgG	immunoglobulin G	Y	Tyrosine
IL	Interleukin	α	Alpha (anti)
IM	Infectious mononucleosis	β	Beta
IP	Immunoprecipitation	μCi	Microcurie
ITC	Isothermal titration calorimetry	μF	microfarad
Kan	Kanamycin	μg	Microgram
kb	kilobase pairs	μl	Microliter
kDa	kilodalton	μM	Micromolar

Acknowledgments

First of all, I would like to express my sincere gratitude to my supervisor Prof. Dr. Bettina Kempkes for providing guidance and feedback throughout this project, allowing me to further arrange the project freely, and establishing up to seven intranational and international collaborations with other wonderful laboratories, and for her continuous support and trust in my competencies.

I thank Prof. Dr. Wolfgang Enard for being my second referee for this thesis.

I would like to thank Prof. Dr. Dirk Eick and Prof. Dr. Angelika Böttger for their critical assessments and constructive suggestions in my TAC meetings to keep me on track.

I would also like to express my sincere gratitude to Prof. Dr. Wolfgang Hammerschmidt for his considerate guidance and thoughtful recommendations on producing recombinant Epstein-Barr viruses. I am also thankful to his lab members, Yen-Fu Adam Chen, Ezgi Akidil, Dagmar Pich, and so on for sharing biological samples and critical techniques. Without this, the research would not have been possible.

I would like to thank Prof. Dr. Christian Münz who provided an opportunity to characterize my virus mutants in humanized mice in his laboratory at Universität Zürich (UZH). In particular, I'm grateful to Dr. Anita Murer, who showed me the reconstitution and infection of humanized mice, and Patrick Schuhmachers, who was always available for questions.

I would also like to thank Prof. Dr. Michael Sattler and Dr. André Mourão for the stimulating questions on protein-protein interaction. The meetings with them were vital in inspiring me to think outside the box, from multiple perspectives to form a comprehensive and objective critique.

I would also like to thank Prof. Dr. Bernhard Küster and Dr. Piero Giansanti for processing the project using liquid chromatography with tandem mass spectrometry in their laboratory at Technische Universität München (TUM). Without this, the research would not have been possible.

I would also like to thank Prof. Dr. Klaus Strebhardt and Dr. Monika Raab from Universitätsklinikum Frankfurt for the critical discussion on polo-like kinase 1, one of the major subjects in this research.

I also thank my present labmates, Cornelia Kuklik-Roos, Sophie Beer, and Sayantani Bhattacharjee, and former colleagues Dr. Simone Rieger and Dr. Sybille Thumann for the stimulating discussions, sharing of techniques and reagents, and for the great atmosphere in the lab. Particular thanks to Cornelia (Conny) who provides the best technical support, and also emotional support. Thank Sophie for the active discussion on my project.

Last but not least, I want to thank my family for their love and unconditional support.

Dedication

To Yán Dì (炎帝) and Huáng Dì (黄帝), who inspired me to explore the unknown universe.

To my mother, who taught me forbearance and to be proactive.

To my father, who brought me responsibility.

To my brother, who showed me cooperation.

To Meiyue, who loves, understands, and supports me.

To the giants, whose shoulders I stand upon.

To the future, what I am looking forward to.

天地与我并生，而万物与我为一。

庄周 (~369 – ~286 B.C.)

*“Heaven and the earth were born together with me, and the myriad things
and I are one universe.”*

Zhuang Zhou (~369 – ~286 B.C.)

Publications

Zhang, X., Schuhmachers, P., Mourão, A., Giansanti, P., Murer, A., Thumann, S., Kuklik-Roos, C., Beer, S., Hauck, S.M., Hammerschmidt, W., Küppers, R., Kuster, B., Raab, M., Strebhardt, K., Sattler, M., Münz, C., Kempkes, B. (2021). PLK1-dependent EBNA2 phosphorylation restrains EBNA2 activity and lymphomagenesis in EBV-infected mice. *EMBO Rep.* (*Revision*)

1. Introduction

In 1961, Antony Epstein, a young pathologist attended a lecture presented by Denis Burkitt, a surgeon working in Uganda. Denis Burkitt reported a novel sarcoma found in African children in 1958 (Burkitt, 1958). The two set up a collaboration to discover a transmissible vector-borne agent in Denis Burkitt's biopsy specimens of the tumor, which was subsequently termed "Burkitt's Lymphoma" (BL). In December 1963, with the help of Yvonne Barr (Antony's Ph.D. student) and Bert Achong (Antony's colleague), Antony established a suspension cell line from a BL mass, fortunately (now called EB1 cell line), which is the first cell line established from a human lymphoma, and sequentially in early 1964, he observed unequivocal herpes-like virus particles in these BL cells examined by electron microscopy (Epstein et al., 1964). So the first human tumor virus was discovered.

The virus was confirmed to be a novel member of the herpesvirus family at that time and the term "Epstein-Barr virus (EBV)" was coined for convenience hereafter (Henle et al., 1968; Hummeler et al., 1966). In tissue culture, EBV has the potential to transform B cells, a process which is termed B cell immortalization (Pope et al., 1968).

Since its initial discovery in BL, EBV is associated with a diverse range of malignancies of both lymphoid and epithelial origin. In 1968, EBV was shown to play an important role in infectious mononucleosis in a seroepidemiological study (Henle et al., 1968). In 1970, Lars Santesson's lab could detect the EBV genome in nasopharyngeal carcinoma (NPC) using DNA-DNA hybridization (zur Hausen et al., 1970). In 1988, EBV was identified in T-cell lymphoma (Jones et al., 1988) and Hodgkin lymphoma (Donhuijsen-Ant et al., 1988). In addition, EBV is speculated, to some extent, to be associated with autoimmune illnesses such as multiple sclerosis (Bar-Or et al., 2020) and systemic lupus erythematosus (Draborg et al., 2012).

Considering the vast majority of the adult population (over 95%) worldwide is asymptotically and persistently infected with EBV (Münz, 2019), progress in the molecular mechanisms of EBV carcinogenesis will lead to better prevention, diagnosis, staging, and treatment strategies for EBV-associated diseases.

1.1. Epstein-Barr virus

Epstein-Barr virus (EBV), taxonomically designated human herpesvirus 4 (HHV4), belongs to Lymphocryptovirus (LCV) (or gamma 1) genus of the *γ -herpesviridae* (Cho et al., 1999). Like other herpesviruses, the EBV virion is about 200 nm in diameter and has a toroid-shaped DNA core in a nucleocapsid consisting of 162 capsomeres, an outer envelope with external glycoprotein spikes which are important for binding and subsequent fusion of the virion envelope with cellular

membranes, and a tegument which consists of viral and cellular proteins between the nucleocapsid and envelope (Figure 1).

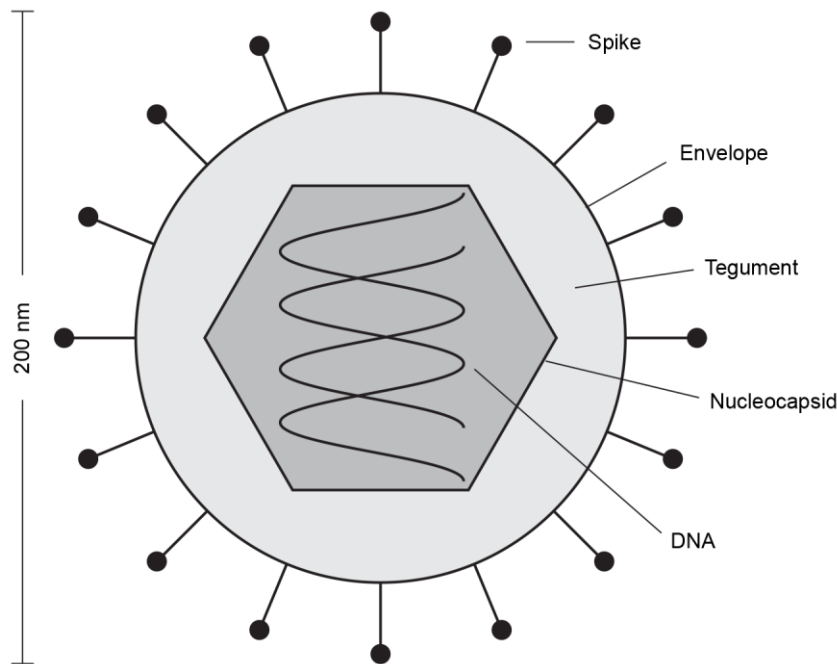


Figure 1. Diagram of EBV virion.

The major structural components of the virion include the spikes, the virion envelope, the tegument; the capsid; and the viral genomic DNA.

1.1.1. EBV genome

The genome of EBV is a linear double-stranded DNA (~172 kb) in the nucleocapsid while it circularizes to replicate as an episome in latently infected cells (Figure 2). There are more than 100 potential open reading frames (ORFs) encoded by the viral genome. The nomenclature of these ORFs is based on their position (1st ORF, 2nd ORF, 3rd ORF, and so on) and direction (rightward or leftward) within BamH I digested fragments (A, B, C, and so on in decreasing size) of the viral genome (Baer et al., 1984). For example, BYRF1 (also known as EBNA2) is the first rightward ORF in the BamH I Y fragment (BamH I Y fragment rightward open reading frame 1). There are two EBV types (type 1 and 2) circulating worldwide. The two types differ mainly on EBNA2 by 54 % identity in the protein sequence (Farrell, 2015). The major biological discrepancy between the two viral types is that type 1 EBV is much more efficient in the immortalization of B cells *in vitro* than type 2 EBV (Rickinson et al., 1987). In this thesis, only type 1 EBNA2 (UniProtKB: P12978) was studied.

The EBV infection *in vitro* leads to the outgrowth of immortalized B cells, termed lymphoblastoid cell lines (LCLs), which exhibit a specific latent transcription program. They are considered as a model to study the early infection by EBV. The function of all latent genes has been extensively studied. The current understanding of these genes is briefly summarized below.

Epstein-Barr virus nuclear antigen 2 (EBNA2) is one of the first expressed viral genes upon EBV infection (Schlee et al., 2004). EBNA2 is required for the immortalization of EBV-infected B cells (Cohen et al., 1989; Hammerschmidt and Sugden, 1989; Pich et al., 2019). It functions as a transactivator protein that is involved in the regulation of latent viral and cellular transcription (Henkel et al., 1994). Since EBNA2 cannot bind to its responsive element directly, it uses cellular adaptor proteins (e.g. CBF1 or PU.1) to target the cis-regulatory regions of its target genes and indirectly confers sequence-specific DNA contact. The large EBNA transcript is first initiated from Wp in primary infected cells while after the expression EBNA2 and LP Cp promoter dominates EBNA transcription driven by EBNA2 (Kempkes and Ling, 2015).

Epstein-Barr virus nuclear antigen leader protein (EBNA-LP) is one of the first expressed viral genes upon EBV infection along with EBNA2 (Harada and Kieff, 1997). EBNA-LP cooperates with EBNA2 in transcriptional regulation and increases the activation of viral target genes (Kempkes and Ling, 2015). However, EBNA-LP only coactivates EBNA2 on a subset of EBNA2-responsive genes (Peng et al., 2005).

Epstein-Barr virus nuclear antigen 1 (EBNA1) is expressed in all forms of EBV latency in dividing cells. EBNA1 binds to the latent origin of plasmid DNA replication (*OriP*) of the EBV genome and tethers the viral episome to the human chromosomes during cell division. In EBV infected B cell exhibiting a non-latency III program EBNA1 is transcribed from Qp promoter, and not from the EBNA2 driven Cp promoter (Frappier, 2015).

Epstein-Barr virus nuclear antigen 3 (EBNA3) protein family includes 3 proteins called EBNA3A, EBNA3B, and EBNA3C. EBNA3A is critical for maintaining lymphoblastoid cell line growth (Maruo et al., 2003). EBNA3B is a viral tumor suppressor whose inactivation promotes immune evasion and virus-driven lymphomagenesis (White et al., 2012). EBNA3C contributes to EBV-induced lymphomagenesis *in vivo* (Romero-Masters et al., 2018).

Epstein-Barr virus latent membrane protein 1 (LMP1) is a transmembrane protein that triggers a series of signal transduction pathways. LMP1 mimics a constitutively active tumor necrosis factor (TNF) receptor, is a principal activator of the nuclear factor- κ B (NF- κ B) pathway in LCLs (Le Clorennec et al., 2006), and mimics CD40 signaling which is essential for the differentiation of B cells (Uchida et al., 1999).

Epstein-Barr virus latent membrane protein 2A (LMP2A) and **2B (LMP2B)** are transmembrane proteins. LMP2A constitutively mimics a B cell receptor (BCR) signal which provides a survival signal for EBV infected cells in the absence of antigen (Cen and Longnecker, 2015). LMP2B is related to LMP2A but lacks the domain required for LMP2A tyrosine kinase signaling, and modulates LMP2A activity (Le Clorennec et al., 2006).

Epstein-Barr virus-encoded small RNAs (EBERs, including EBER1 and EBER2) are by far the most abundant EBV viral transcript in latently infected cells. EBERs are expected to form a

double-stranded RNA-like structure. EBERs contribute to oncogenesis by modulating innate immunity in patients with nasopharyngeal carcinoma (NPC) and Burkitt's lymphoma (Takada, 2012).

BamHI-A Rightward Transcripts (BARTs) represent another abundant, stable viral RNA species present in all infected cell types. They are indisputably abundant in EBV-associated epithelial tumors, e.g. NPC, and are therefore thought to be a contributing factor in NPC pathogenesis (Skalsky and Cullen, 2015).

Amongst these genes, EBNA2 is required for B cell immortalization. However, how EBNA2 regulates B cell immortalization is unclear so far. Since EBNA2 is one of the major subjects in this thesis, more detail about it will be depicted in chapter 1.2.

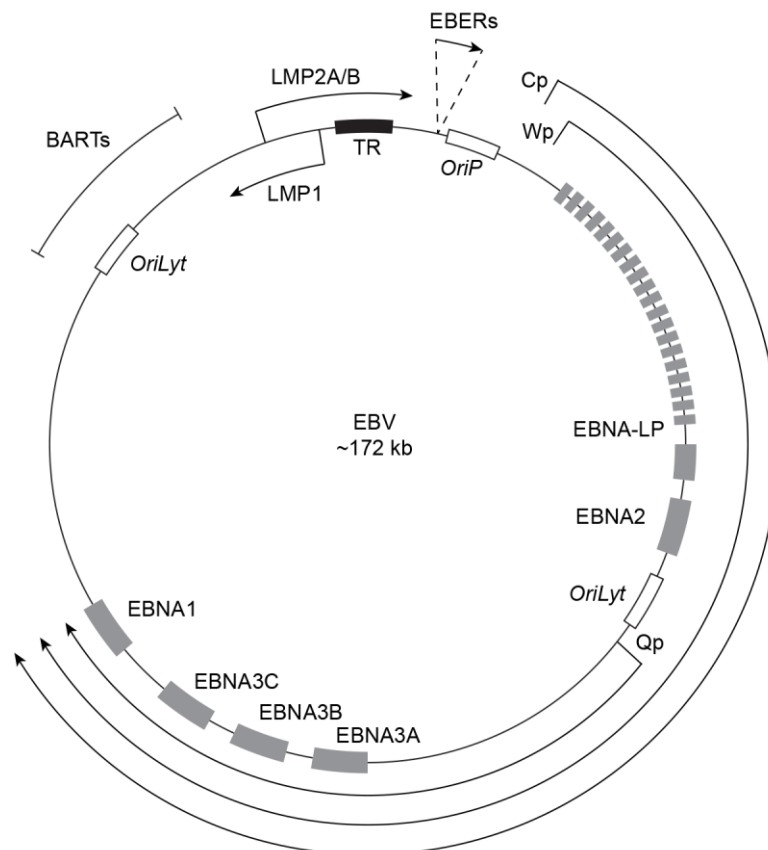


Figure 2. Schematic representation of the EBV genome.

Shown are the transcripts of BARTs and EBERs, messenger RNAs (mRNAs) from different promoters, Wp, Cp, and Qp, and major proteins, EBNA 1, 2, 3A, 3B, 3C, and LP, and LMP1 and 2A/B (grey boxes). The terminal repeats (TR) for EBV episome circularization, the origin of DNA replication (*OriP*), and lytic origins of replication (*OriLyt*) are indicated.

1.1.2. The life cycle of EBV

EBV has a tropism for human B lymphocytes and epithelial cells (Hochberg et al., 2004; Möhl et al., 2016). Like other herpesviruses, EBV possesses the capacity to switch between the latency and lytic cycle. David Thorley-Lawson and his colleagues contributed lots of wisdom in the characterization and modeling of EBV viral latent and lytic cycles (Thorley-Lawson, 2001, 2005,

2015; Thorley-Lawson and Allday, 2008; Thorley-Lawson and Gross, 2004). Their stunning germinal center (GC) model provides a historical perspective of EBV's life cycle. There are also other models to explain EBV's life cycle, e.g. the direct infection model suggesting that EBV directly infects memory B cells. This section will describe the GC model only.

In the GC model, EBV is considered to use the normal pathways of B cell biology in Waldeyer's ring, a lymphoid tissue including tonsils and adenoids to initiate infection, differentiation, persistence, replication, and reactivation (Figure 3).

Initially, EBV is transmitted through saliva contact, like kissing, and crosses the epithelial barrier of Waldeyer's ring to infect naïve B cells. Upon infection, it drives the infected cell to become a proliferating B blast using the **latency III** program.

Next, EBV-infected naïve blasts migrate into the follicle to initiate a GC reaction and they switch latency III program to **latency II** program which provides surrogate antigens and helper T cell signals by expressing latent membrane protein 1 (LMP1) and latent membrane protein 2A/B (LMP2A/B).

Subsequently, the latently infected GC B cells leave the follicle as resting memory B cells circulating in the periphery. There is no EBV viral protein expressed in the infected cells, which are designated as **latency 0**.

In the infected memory B cells, these cells occasionally divide in the periphery to maintain memory B cell homeostasis. At this time, termed **latency I**, the virus expresses EBNA1 to tether the viral episomes onto the B cell genome, which allows the viral genome to replicate along with the cells.

In EBV infected humans, latently infected memory B lymphocytes (latency 0 and I) circulate systemically and serve as lifelong viral reservoirs (Luzuriaga and Sullivan, 2010).

If an EBV latently infected resting memory B cell returns to Waldeyer's ring and receives signals that initiate terminal differentiation into a plasma cell, the plasma cell will activate the lytic cycle of EBV in which a large amount of infectious progeny virus is produced *de novo* (Laichalk and Thorley-Lawson, 2005).

The released virions can initiate a new round of naïve B cell infection or infect the epithelial cells. The infection of epithelial cells leads to the lytic cycle of the virus, which remarkably amplifies the amount of infectious progeny virus. Ultimately the progeny virus is shed into saliva for infectious transmission to new hosts.

In the GC model, EBV gene expression is tightly regulated in a tissue-specific manner. Dysregulation of the viral or cellular genes can lead to lymphomas or carcinoma which arise from each stage of EBV infection predicted by the model.

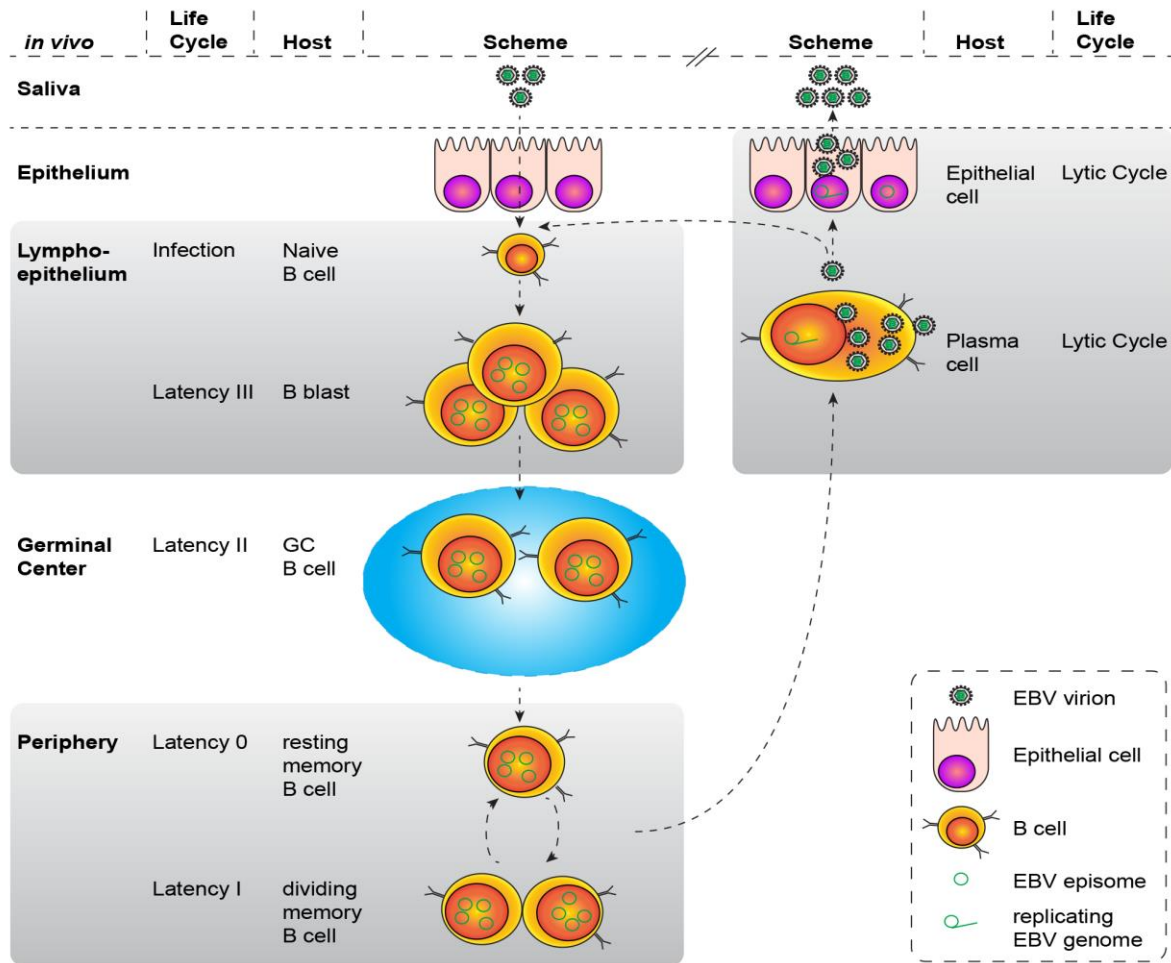


Figure 3. Schematic representation of the EBV life cycle.

EBV crosses the epithelial barrier, infects naïve B cells, and drives them to become proliferating B lymphoblasts. The B lymphoblasts migrate to the germinal center (GC) and undergo a GC reaction to differentiate into memory B cells. The memory B cells further differentiate into plasma cells, the lytic cycle is activated, and large amounts of EBV progeny are produced. The released virial particles can either be further amplified by infection of the epithelial cells or initiate a new round of naïve B cell infection. Each position *in vivo*, life cycle stage, and host of the EBV are indicated.

1.1.3. EBV-associated diseases

EBV has been classified in group 1 carcinogenic viruses including another human γ -herpesvirus, Kaposi's Sarcoma Herpesvirus (KSHV, also called Human Herpesvirus 8 (HHV8)), by the International Agency for Research on Cancer (IARC) since 1997. It is estimated that more than 200,000 cancer cases worldwide could be attributed to EBV each year (Khan and Hashim, 2014) and that EBV-attributable malignancies lead to 1.8% of all cancer deaths (de Martel et al., 2020). The most common EBV-associated diseases are shortly described below.

Infectious mononucleosis (IM) is a clinical syndrome characterized by sore throat, cervical lymph node enlargement, fatigue, and fever, which is most commonly seen in adolescents and young adults and lasting several weeks (Luzuriaga and Sullivan, 2010). IM is usually caused by

EBV primary infection. The EBV primary infection is established by saliva contacts, such as kissing, sharing contagious food, or utensils among adolescents and young adults.

Post-transplantation lymphoproliferative disease (PTLD) is characterized by abnormal proliferation of lymphoid cells (~90% B cell origin) occurring after transplantation (Dharnidharka et al., 2016). Recipients of solid organ or allogeneic hematopoietic stem cell transplants have an increased risk of lymphomas largely related to immunosuppression and EBV infection (Dierickx and Habermann, 2018). The clinical symptoms of PTLDs can be highly variable (fever, night sweats, weight loss, or allograft dysfunction) or related to problems at the site of the lymphoid mass (lymph node enlargement or symptoms in the gastrointestinal tract, brain, liver, lungs, or kidneys (Dharnidharka et al., 2016). The pathogenesis of EBV-positive PTLDs is obvious in recipients. An immunosuppression-related decrease in T cell immunosurveillance can lead to the proliferation and transformation of the EBV-infected B cells.

Hodgkin's lymphoma (HL) is a lymphoid malignancy characterized by the presence of pathognomonic Hodgkin/Reed-Sternberg (HRS) cells. EBV is found in HRS cells in about 40% of classical HL in the Western world. In EBV positive HRS cells, three viral proteins (EBNA1, LMP1, and LMP2A) and two non-coding RNAs (BARTs and EBERs) are expressed (Küppers, 2008).

Nasopharyngeal carcinoma (NPC) is cancer arising from the nasopharynx epithelium (Chua et al., 2016). Undifferentiated NPC is constantly associated with EBV, displays a latency II expression pattern (see Table 1), and is endemic in specific areas, e.g. southern China, Mediterranean Africa, and some regions of the Middle East (Raab-Traub, 2015). Since the geographical distribution of NPC is unbalanced, host genetics (e.g. HLA genotype), environmental factors (e.g. nitrosamine-containing food), and EBV infection as well are considered as contributors to the development of NPC (Chen et al., 2019).

Burkitt's lymphoma (BL) is a cancer characterized by the translocation of chromosomes 8 and 14 (2 or 22 as well). The translocation places the proto-oncogene *C-MYC* originally from chromosome 8 under the transcriptional control of an immunoglobulin locus, which leads to constitutive upregulation of *C-MYC*. The high level of *C-MYC* drives the expression of many genes involved in cell proliferation, which contributes to tumor formation. EBV-positive BL cells express a small fraction of viral latent genes, like EBNA1 and EBERs, which are not fully understood to date (Rochford and Moormann, 2015).

EBV is also associated with other malignancies, such as NK/T cell lymphoma, Gastric cancer, and so on. Even though the EBV-associated diseases differ in their clinical symptoms, the EBV-positive cells might show similar latent or lytic transcriptional programs. A summary of the viral transcription programs in the latent or lytic state is provided in Table 1.

Table 1. The transcription programs of EBV.

Program	Protein	Noncoding RNA	Clinical relevance
Latency III	EBNA1, 2, 3A, 3B, 3C, and -LP, and LMP1 and 2A/B	EBER1 and 2, BART miRNAs, BHRF1 miRNAs	IM, PTLD, immunosuppressed or immunodeficient patients
Latency II	EBNA1 and LMP1 and 2A/B	EBER1 and 2, BART miRNAs	HL, NPC, NK/T cell lymphoma, and Gastric cancer
Latency I	EBNA1	EBER1 and 2, BART miRNAs	BL
Latency 0		EBER1 and 2, BART miRNAs	
Lytic cycle	BZLF1, BRLF1, and p350.....		

The infection of B cells with EBV *in vitro* results in the outgrowth of immortalized lymphoblastoid cell lines (LCLs) which show a latency III transcription program. The process of LCL formation in culture is considered as a research model to investigate the early infection and diseases exhibiting a latency III program, e.g. IM and PTLD.

1.2. EBNA2

EBNA2 is one of the first expressed genes upon EBV infection and functions as the major transcriptional activator in latency III. As EBNA2 plays an important role in EBV pathogenesis, this section will summarize the current knowledge of EBNA2.

1.2.1. EBNA2 features and its binding proteins

As depicted in Figure 4, EBNA2 comprises multiple functional features. The EBNA2 N-terminal dimerization domain (END) (1-58 aa) mediates multiple molecular functions including self-association (Harada et al., 2001), transactivation (Gordadze et al., 2004), and functional cooperation with EBNA-LP (Peng et al., 2005). END binds to early B cell factor 1 (EBF1) to promote the assembly of the EBNA2/chromatin complexes in EBV-infected B cells (Glaser et al., 2017). The three-dimensional structure of the END domain was solved by heteronuclear nuclear magnetic resonance (NMR) spectroscopy. The END monomer consists of four β -strands and a single α -helix and two END monomers form a homodimer by the interaction of two β -strands from each monomer (Friberg et al., 2015). The poly-proline (polyP) stretch bridges the END and the other dimerization domain (DIM) which mediates homodimerization (Harada et al., 2001). The central adaptor region (WW) of EBNA2 (318-327 aa) targets C-promoter binding protein (CBF1), also known as recombination signal binding protein for immunoglobulin kappa J region (RBPJ) (Ling and Hayward, 1995). CBF1/RBPJ is a sequence-specific DNA binding protein, is ubiquitously expressed in all

human cells, and is also an important downstream element of the cellular Notch signal transduction pathway (Hsieh et al., 1996). EBNA2 assembles to the responsive elements of its cellular and viral target genes, like *C-MYC* and *LMP1*, respectively, through interaction with CBF1/RBPJ (Kaiser et al., 1999; Wang et al., 1990). The C-terminal transcriptional activation domain (TAD) (440-469 aa) is flanked by the poly-arginine-glycine (polyRG) repeat and a C-terminal canonical nuclear localization signal (NLS) (478-485 aa). The TAD domain recruits components of the basic transcriptional machinery, like TFIIE, to the TFB1/p62 subunit of the TFIIH complex, through interaction with p100, TFIIB, and TAF40 (Cohen et al., 1991; Tong et al., 1995c, 1995a, 1995b). It recruits histone acetyltransferase activity through interaction with p300, CBP, and PCAF (Wang et al., 2000). The TAD domain is intrinsically unstructured alone but forms a 9-residue α -helix in complex with the TFB1/p62 (Chabot et al., 2014). A second internal NLS (341-355 aa) encompassing the RG repeat can substitute for the canonical NLS to ensure appropriate nuclear localization to exert EBNA2's transactivation (Cohen and Kieff, 1991; Ling et al., 1993).



Figure 4. Schematic illustration of selected features of EBNA2.

The poly-proline (polyP) and the poly-arginine-glycine (RG) stretches, EBNA2 N-terminal dimerization domain (END), the second dimerization domain (DIM), the central adaptor region (WW), the C-terminal transcriptional activation domain (TAD), and the two nuclear localization signals (NLS) are indicated.

1.2.2. Posttranscriptional modification of EBNA2 and its function

EBNA2 functions as a major transactivator in latency III. It is localized in the nucleus, docks to the responsive elements through interaction with DNA binding adaptor, e.g. CBF1 and PU.1, and works as a scaffold protein recruiting co-activators, chromatin remodelers, and the transcription machinery to drive its target viral and cellular gene expression. The post-transcriptional modification (e.g. phosphorylation, methylation, and ubiquitination) of EBNA2 by specific catalytic enzymes modulates its biochemical properties, might further regulate its transactivation, substrate recognition, subcellular localization, signaling transduction pathway, and conformational changes.

EBNA2 proteins isolated from distinct nuclear components display differential phosphorylation patterns in a cell cycle-dependent fashion and the hyperphosphorylation of EBNA2 suppresses its transactivation of the *LMP1* promoter (Grässer et al., 1991; Petti et al., 1990; Yue et al., 2004). The phosphorylation of S243 of EBNA2 by either a viral serine/threonine-protein kinase (PK) encoded by the BGLF4 gene or cellular Cyclin B1/CDK1 contributes to the repression of EBNA2's transactivation (Yue et al., 2005, 2006). In addition, the phosphorylation of S469 by casein kinase 2 (CK2) regulates EBNA2's interaction with hSNF5/Ini1 and EBNA2-driven proliferation (Grässer et al., 1992; Kwiatkowski et al., 2004). Interestingly, it was reported that S457 of the EBNA2 TAD domain is not phosphorylated by casein kinase 1 (CK1) (Grässer et al., 1992).

EBNA2 is supposed to be methylated on the arginines of the RG repeat. The methylation of EBNA2 is a prerequisite for binding to SMN to facilitate B cell immortalization (Barth et al., 2003). Even though Lysine residues of EBNA2 do not confer ubiquitination or SUMOylation, they modulate EBNA2's transactivation (Hille et al., 2002).

1.3. Polo-like kinase family

Polo-like kinase (PLK) family comprises five serine/threonine-protein kinases: PLK1, 2, 3, 4, and 5 in mammalian cells so far (Joukov and Nicolo, 2018). In 1988, PLK was first found to be essential for undergoing normal mitosis in *Drosophila melanogaster* (named Polo, not PLK here) by David M. Glover's laboratory (Sunkel and Glover, 1988). In the next year, polo was characterized as a homolog to a serine/threonine kinase (Llamazares et al., 1991). The PLKs are highly conserved from budding yeast (*Cdc5*) to *Drosophila* (Polo), *Xenopus* (Plxs), and mammals (PLKs). As depicted in Figure 5, the PLKs are characterized by a well-conserved N-terminal catalytic kinase domain (KD) and C-terminal domain with one or more polo-box domains (PBD) (Li et al., 2014).

PLKs are key regulators in mitosis, cytokinesis, and even meiosis in eukaryotes (Barr et al., 2004). PLK1 is the most well-studied one in the PLK family and is a multifunctional kinase implicated in various aspects of mitosis and cytokinesis. PLK2 (also named SNK) localizes at the centrosomes and plays a role in the S phase entry (de Cárcer et al., 2011). PLK3 (also known as FNK or PRK) is required at the G1-S phase transition and for DNA replication (Zimmerman and Erikson, 2007b, 2007a). PLK4 (also named SAK or STK18) functions as a critical regulator of centriole duplication both in *Drosophila* and mammals (Kleylein-Sohn et al., 2007). The human PLK5 encloses only a small portion of the kinase domain along with one PBD and acts as a tumor suppressor in brain cancer (de Cárcer et al., 2011; Goroshchuk et al., 2019).

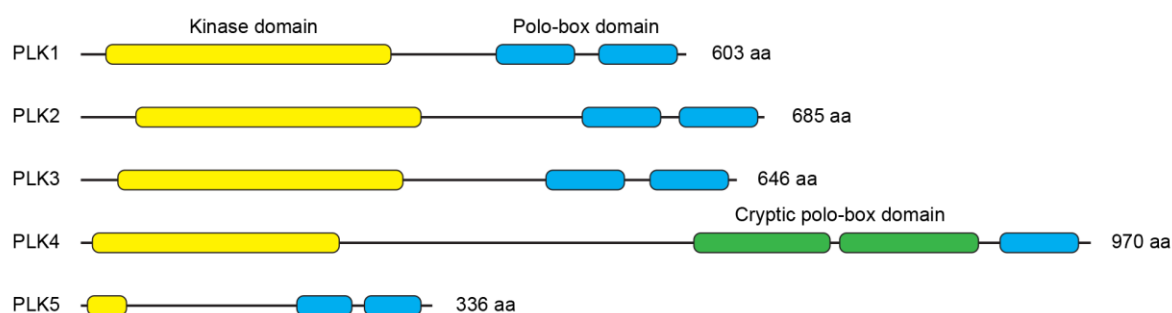


Figure 5. The general structure of the PLK family.

The structure includes an N-terminal serine/threonine kinase domain (truncated in PLK5, without the T-loop) and a C-terminal polo-box domain (PBD). PLK1, 2, 3, and 5 have two PBDs. PLK4 has one PBD and one cryptic PBD. PLK5 has a truncated and inactive kinase domain. The figure is adapted from Goroshchuk et al., 2019.

1.3.1. PLK1 function

PLK1 phosphorylates multiple proteins, e.g. Cyclin B1, involved in mitosis. In mitosis and cytokinesis, PLK1 plays versatile roles including mitotic entry, centrosome separation and maturation, chromosome arm segregation, microtubule-kinetochore attachment, and spindle assembly checkpoint silencing. Inhibition of either PBD or KD or depletion of PLK1 is sufficient for abolishing PLK1 function *in vivo*, resulting in the arrest of cells in a prometaphase-like state, with unseparated centrosomes and monopolar spindles and defects in microtubule-kinetochore attachment and chromosome alignment (Archambault et al., 2015; Schmucker and Sumara, 2014).

1.3.2. Substrate phosphorylation by PLK1

PLK1 is characterized by an N-terminal KD and a C-terminal PBD. PLK1 alone is autoinhibitory since the PBD binds and rigidifies the hinge region of the KD intramolecularly (Xu et al., 2013). As illustrated in Figure 6, Phosphorylation of Ser137 within KD or PBD docking to a binding partner interrupts the intramolecular interaction and releases the mutual inhibition (Jang et al., 2002). Through its PBD which recognizes specific phosphorylated motifs, PLK1 docks onto its substrates to perform critical mitotic functions (Schmucker and Sumara, 2014). The PBD docking causes conformational changes in PLK1, which exposes the KD to partially activate the kinase. Full activation of PLK1 requires its phosphorylation in the activation loop or T-loop (T210) of KD by Aurora kinases (Asteriti et al., 2015; Seki et al., 2008). The phosphorylation of the docking site of the PBD binding motif is a prerequisite for binding to PBD. The priming phosphorylation is mediated either by PLK1 itself, a process called self-priming or by a proline-directed kinase, such as CDK1 or MAPK, a process called non-self-priming (Elia et al., 2003a, 2003b; Neef et al., 2007). However, the interaction between PLK1 and its substrate Bora does not require priming phosphorylation (Seki et al., 2008). Activated PLK1 can either phosphorylate additional sites on the same substrate or residues on proteins in close proximity in multiprotein complexes (Lee et al., 2014; Zitouni et al., 2014).

Although the amino acid sequence of PLK1 shows a high identity with closely related PLK2 and PLK3, *in vitro* biochemical analyses have shown that the three PLKs have different substrate specificities (Park et al., 2009). Furthermore, the PBDs of each PLK interact with specific motifs on their binding partners (Elia et al., 2003b; Reindl et al., 2009).

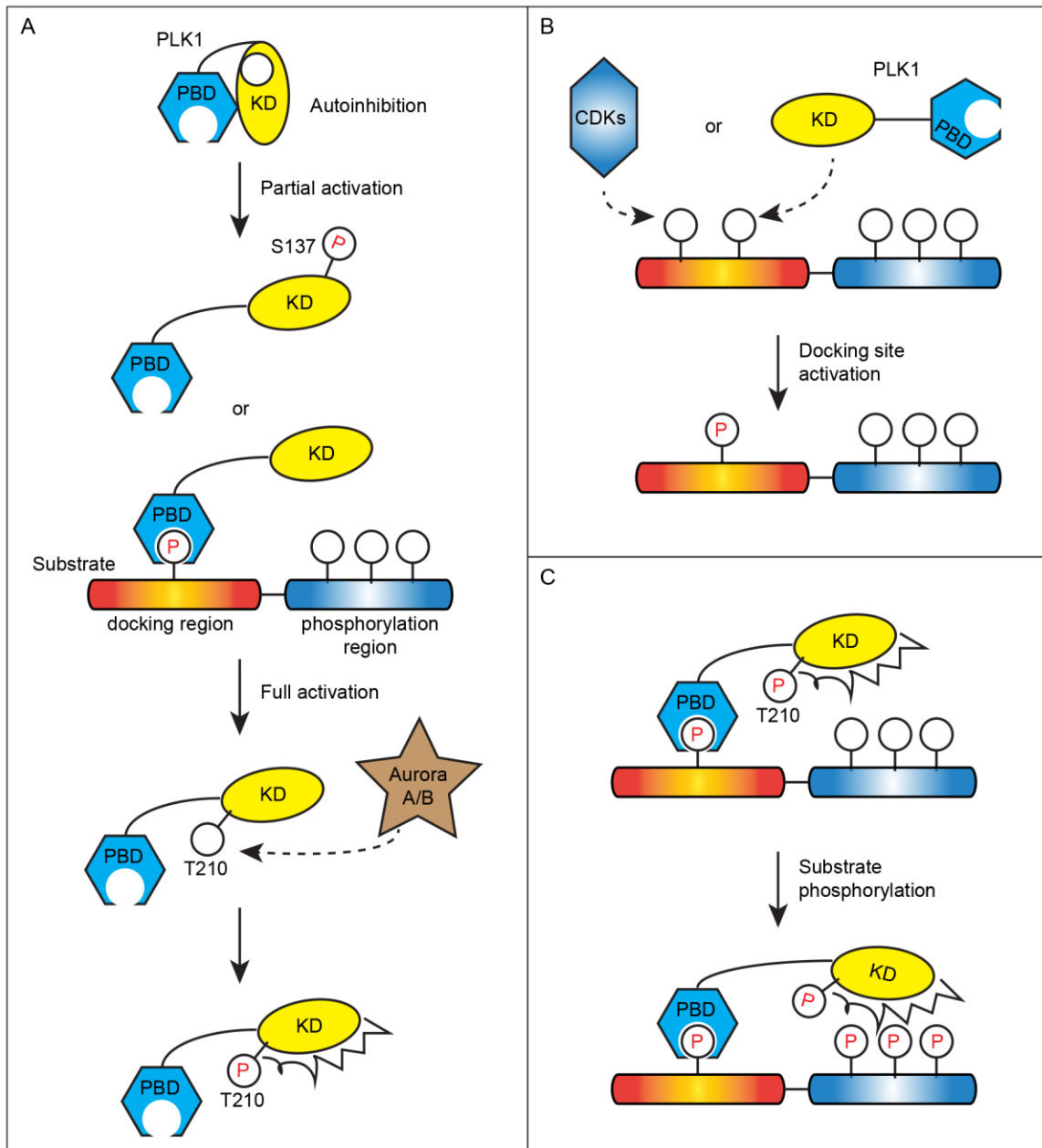


Figure 6. Schematic diagram of the mechanism of PLK1 phosphorylation.

(A) PLK1 is autoinhibited through the interaction of PBD with KD. PLK1 is partially activated through either phosphorylation of S137 within KD or PBD docking to its substrate. Phosphorylation of T210 (for example, by Aurora A/B) fully activates PLK1. (B) PBD1-binding target is generated either by a Pro-directed kinase such as CDK1 (nonself-priming) or by PLK1 itself (self-priming). (C) Once activated PLK1 binds to a phosphorylated target, it phosphorylates its substrate.

1.3.3. PLK1: an oncogene or tumor suppressor gene?

Interestingly, extensive studies have shown that PLK1 expression is upregulated in most tumor entities including non-small-cell lung cancer, head and neck cancer, esophageal cancer, B-cell acute lymphoblastic leukemia, gastric cancer, melanomas, breast cancer, ovarian cancer, endometrial cancer, colorectal cancer, gliomas, and thyroid cancer (Goroshchuk et al., 2020; Takai

et al., 2005). The PLK1 overexpression is also associated with poor prognosis and chemotherapy resistance (Liu et al., 2017). PLK1 is considered as an attractive anti-cancer target (Rosenblum et al., 2020), which gives rise to the development of numerous either KD-specific small-molecule inhibitors including volasertib (BI6727) or PBD-specific small-molecule inhibitors, e.g. Poloxin. Volasertib is highly active across a variety of carcinoma cell lines and induces tumor regression in several xenograft models (Van den Bossche et al., 2016). Unfortunately, most so-called PBD-specific small-molecule inhibitors are non-specific protein alkylators (Archambault and Normandin, 2017). Therefore, further efforts are still needed to develop PBD-specific inhibitors.

Increasing pieces of evidence *in vivo* show that PLK1 has a tumor-suppressive potential. PLK1 homozygous null mice were embryonic lethal, and early PLK1^{-/-} embryos failed to survive after the eight-cell stage, while PLK1 heterozygotes were healthy at birth and the incidence of tumors in these mice was 3-fold higher than that in their wild-type counterparts, suggesting that PLK1 functions as a haploinsufficient tumor suppressor (Lu et al., 2008). In Apc^{Min/+} mice, PLK1 inhibition promotes the development of adenomatous polyps, and overexpression of PLK1 significantly increases the survival rate of colon cancer patients exhibiting a truncated APC (Raab et al., 2018). Furthermore, in an inducible knock-in mouse model, PLK1 overexpression prevents the development of Kras-induced and Her2-induced mammary gland tumors and PLK1 overexpression correlates with improved survival in patients with specific breast cancer subtypes (de Cárcer et al., 2018). Therefore, whether PLK1 is an oncogene or tumor suppressor is still under hot debate.

1.4. Association of EBV pathogenesis with PLK1

Evidence showed that PLK1 is upregulated in EBV positive (or EBNA2-expressing) cells even though EBV-related studies focused on PLK1 are very rare. PLK1 gene was overexpressed in many BL cell lines compared to normal lymphocytes (Syed et al., 2006). Cells with exogenously expressing EBNA2 showed upregulated PLK1 in mRNA and protein levels (Pan et al., 2009). PLK1, along with Aurora A/B and CDK1, was upregulated in EBV-transformed LCLs (Dai et al., 2012). Interestingly, in 2016, Dr. Sybille Thumann (AG Kempkes) and Dr. Stefanie Hauck (HMGU) identified polo-like kinase 1 (PLK1) enriched in EBNA2 co-immunoprecipitates by liquid chromatography with tandem mass spectrometry (LC-MS/MS), indicating EBNA2 and PLK1 interact with each other. However, the role of PLK1 played in EBV-associated tumorigenesis is still unclear.

1.5. Objective

Even though EBNA2 and PLK1 have attracted much attention since their first discoveries, studies focusing on the regulation of EBNA2's transactivation and the contribution of PLK1's

phosphorylation to EBV-induced carcinogenesis have been lagging, and our knowledge about how EBNA2 and PLK1 interact at the molecular level remains quite rudimentary.

Considering the importance of EBNA2's transactivation in B cell immortalization and PLK1's phosphorylation in the cell cycle, I want to characterize the interaction of EBNA2 and PLK1 and the function of the EBNA2/PLK1 complex *in vitro* and *in vivo* in my thesis. Based on my goal, the following four working packages were defined in this thesis:

- (1) Characterization of the interaction of EBNA2 and PLK1
- (2) Identification of phosphorylation sites of EBNA2 by PLK1
- (3) Characterization of the function of EBV expressing EBNA2 deficient on PLK1 docking or phosphorylation *in vitro*
- (4) Characterization of the function of EBV expressing EBNA2 deficient on PLK1 docking or phosphorylation *in vivo*

2. Material

2.1. Human donor samples

Anonymous human adenoid samples from routine adenoidectomy were collected from the Department of Otorhinolaryngology, Klinikum Grosshadern, Ludwig Maximilians University of Munich, Germany. The local ethics committee (Ethikkommission bei der LMU Muenchen) approved the use of this human material.

2.2. Mouse models

The humanized mice which are the immunodeficient mice (NOD-*scid* γ_c^{null}) engrafted with human fetal liver CD34⁺ hematopoietic progenitor cells were generated and maintained in Prof. Dr. Christian Münz's lab.

2.3. Human primary B cells

The human primary B cells were isolated from human donor adenoids. The local ethics committee (Ethikkommission bei der LMU Muenchen) approved the use of this human material.

2.4. Cell lines

Table 2. General and commercially available cell lines.

Cell line	Description	Source	Reference
DG75	Human EBV negative Burkitt's lymphoma cell line	AG Kempkes	(Ben-Bassat et al., 1977)
DG75 ^{Dox HA-EBNA2}	Doxycycline inducible N-terminal HA-tagged EBNA2 expressing DG75 cell line	AG Kempkes	(Glaser et al., 2017)
HEK 293	Human embryonic kidney epithelial cell line transformed by DNA fragments of adenovirus type 5	DSMZ	ACC 305
Raji	Human EBV positive Burkitt's lymphoma cell line	AG Kempkes	(Pulvertaft, 1964)

2. Material

Sf21	An ovarian cell line isolated from <i>Spodoptera frugiperda</i>	Sigma-Aldrich	05022801
------	---	---------------	----------

Table 3. Recombinant EBV producer cell lines.

Cell line	BACmid	Recombinant EBV
XZ156.7		
XZ156.12	pXZ143	EBNA2-HA WT
XZ156.13		
XZ227.17	pXZ203	EBNA2-HA S379A
XZ227.18		
XZ219.1	pXZ146	EBNA2-HA S457A T465V
XZ239.4		

Table 4. Lymphoblastoid cell lines.

Donor	Recombinant EBV	Clone	Cell line
D6	EBNA2-HA WT	1	XZ454.1
		2	XZ454.2
		3	XZ454.3
	EBNA2-HA S379A	1	XZ455.1
		2	XZ455.2
		3	XZ455.3
	EBNA2-HA S457A/T465V	1	XZ456.1
		2	XZ456.2
		3	XZ456.3
D8	EBNA2-HA WT	1	XZ471.1
		2	XZ471.2
		3	XZ471.3
	EBNA2-HA S379A	1	XZ472.1
		2	XZ472.2
		3	XZ472.3
	EBNA2-HA S457A/T465V	1	XZ473.1
		2	XZ473.2
		3	XZ473.3
D9	EBNA2-HA WT	1	XZ481.1

2. Material

		2	XZ481.2
		3	XZ481.3
	EBNA2-HA S379A	1	XZ482.1
		2	XZ482.2
		3	XZ482.3
	EBNA2-HA S457A/T465V	1	XZ483.1
		2	XZ483.2
		3	XZ483.3
	EBNA2-HA WT	1	XZ494.1
		2	XZ494.2
		3	XZ494.3
D10	EBNA2-HA S379A	1	XZ495.1
		2	XZ495.2
		3	XZ495.3
	EBNA2-HA S457A/T465V	1	XZ496.1
		2	XZ496.2
		3	XZ496.3

2.5. Bacterial strains

Table 5. Bacterial strains.

Strain	Genotype	Source	Application
DH5 α	<i>F⁻ endA1 glnV44 thi-1 recA1 relA1 gyrA96 deoR nupG purB20 ϕ80lacZΔM15 Δ(lacZYA-argF) U169 hsdR17(<i>r_k⁺m_k⁺</i>) λ⁻</i>	AG Kempkes	Cloning
Rosetta 2 (DE3)	<i>F⁻ ompT hsdS_B(<i>r_B⁻m_B⁻) gal dcm(DE3) pRARE2 (Cam^R)</i></i>	Merk Millipore	Protein expression
SW105	DH10B [<i>λc1857 (cro-bioA)<>Tet</i>] <i>gal490 (cro-bioA)<>araC-P_{BAD}Flpe gal⁺ ΔgalK</i>	(Warming et al., 2005)	BAC recombineering
GM2163	<i>F⁻ ara-14 leuB6 thi 1 fhuA31 lacY1 tsx78 galK2 galT22 supE44 rpsL136(Str^R) xyl5 mtf1 dam13:Tn9 (Cam^R) dcm:6 mcrB1 hsdR2(<i>r_k⁺m_k⁺</i>) mcrA</i>	AG Kempkes	Cloning

2.6. Recombinant DNA

Table 6. Plasmids used in mammalian cells

Plasmid	Description	Source
pSG5	A eukaryotic expression vector	Agilent Technologies
pAG155	A C-terminal HA-tagged EBNA2 gene inserted in the backbone of pSG5	AG Kempkes
pCKR656	A truncation of 342-487aa in C-terminus of EBNA2 gene in the backbone of pAG155	This thesis
pCKR657	A truncation of 475-487aa in C-terminus of EBNA2 gene in the backbone of pAG155	This thesis
pEGFP/NLS	A eukaryotic expression vector encoding enhanced green fluorescence protein (<i>eGFP</i>) and nucleus localization signal (<i>NLS</i>)	AG Kempkes
pXZ150	An EBNA2 327-487aa integrated into the frame and C-terminus of the <i>eGFP</i> gene between BamH I and Xba I in the backbone of pEGFP/NLS	This thesis
pXZ151	An EBNA2 327-407aa integrated into the frame and C-terminus of the <i>eGFP</i> gene between BamH I and Xba I in the backbone of pEGFP/NLS	This thesis
pXZ152	An EBNA2 408-487aa integrated into the frame and C-terminus of the <i>eGFP</i> gene between BamH I and Xba I in the backbone of pEGFP/NLS	This thesis
pCKR672	An EBNA2 342-474aa integrated into the frame and C-terminus of the <i>eGFP</i> gene between BamH I and Xba I in the backbone of pEGFP/NLS	This thesis
pXZ229	An EBNA2 342-422aa integrated into the frame and C-terminus of the <i>eGFP</i> gene between BamH I and Xba I in the backbone of pEGFP/NLS	This thesis
pCKR661	An EBNA2 423-474aa integrated into the frame and C-terminus of the <i>eGFP</i> gene between BamH I and Xba I in the backbone of pEGFP/NLS	This thesis
pXZ153	Substitutions of ST266AV within EBNA2 gene in the backbone of pAG155	This thesis
pXZ154	Substitutions of TSS377VAA within EBNA2 gene in the backbone of pAG155	This thesis
pXZ155	Substitutions of SPSS467APAA within EBNA2 gene in the backbone of pAG155	This thesis
pXZ179	A substitution of S379A within EBNA2 gene in the backbone of pAG155	This thesis
pXZ288	Substitutions of F400A/WY444AA/YIF460AAA within EBNA2 gene in the backbone of pAG155	This thesis

2. Material

pXZ289	Substitutions of S379A/F400A/WY444AA/YIF460AAA within EBNA2 gene in the backbone of pAG155	This thesis
pCKR675	A substitution of S184A within EBNA2 gene in the backbone of pAG155	This thesis
pCKR676	A substitution of S258A within EBNA2 gene in the backbone of pAG155	This thesis
pXZ140	A substitution of S457A within EBNA2 gene in the backbone of pAG155	This thesis
pXZ141	A substitution of T465V within EBNA2 gene in the backbone of pAG155	This thesis
pCKR677	A substitution of S479A within EBNA2 gene in the backbone of pAG155	This thesis
pXZ142	Substitutions of S457A/T465V within EBNA2 gene in the backbone of pAG155	This thesis
pCKR678	Substitutions of S457A/T465V/S479A within EBNA2 gene in the backbone of pAG155	This thesis
pCKR679	Substitutions of S258A/S457A/T465V/S479A within EBNA2 gene in the backbone of pAG155	This thesis
pCKR680	Substitutions of S184A/S258A/S457A/T465V/S479A within EBNA2 gene in the backbone of pAG155	This thesis
pGa981-6	A reporter construct encoding <i>firefly</i> luciferase upstreamed by hexamerized 50 bp EBNA2 response element of the TP-1 promoter	(Minoguchi et al., 1997)
pPGK	<i>Renilla</i> luciferase expression plasmid	Promega
pcDNA3.1 Hygro	A eukaryotic expression vector	AG Strebhardt
3x Flag-tagged PLK1	A PLK1 integrated into C-terminus of Flag tag between EcoR I and Hind III in the backbone of pcDNA3.1 Hygro	AG Strebhardt
3x Flag-tagged PLK1 K82M	A substitution of K82M within PLK1 gene in the backbone of 3x Flag-tagged PLK1	AG Strebhardt
p509	A prokaryotic expression plasmid encoding BZLF1	AG Hammerschmidt
p2670	A prokaryotic expression plasmid encoding BALF4	AG Hammerschmidt

Table 7. Plasmids used in protein expression from *E.coli* or Sf21 insect cells.

Plasmid	Description	Source
pGEX 4T2	A prokaryotic expression vector encoding Glutathione S-transferase (GST) and a Thrombin recognition site	GE Healthcare

2. Material

pAH362	An EBNA2 246-487aa integrated into the frame and C-terminus of GST gene in the backbone of pGEX 4T2	AG Kempkes
pXZ92	An EBNA2 342-487aa integrated into the frame and C-terminus of GST gene in the backbone of pGEX 4T2	This thesis
pXZ93	An EBNA2 342-422aa integrated into the frame and C-terminus of GST gene in the backbone of pGEX 4T2	This thesis
pXZ94	An EBNA2 423-487aa integrated into the frame and C-terminus of GST gene in the backbone of pGEX 4T2	This thesis
pXZ109	An EBNA2 423-474aa integrated into the frame and C-terminus of GST gene in the backbone of pGEX 4T2	This thesis
pXZ110	An EBNA2 423-445aa integrated into the frame and C-terminus of GST gene in the backbone of pGEX 4T2	This thesis
pXZ111	An EBNA2 446-474aa integrated into the frame and C-terminus of GST gene in the backbone of pGEX 4T2	This thesis
pXZ112	An EBNA2 475-487aa integrated into the frame and C-terminus of GST gene in the backbone of pGEX 4T2	This thesis
pXZ113	An EBNA2 446-487aa integrated into the frame and C-terminus of GST gene in the backbone of pGEX 4T2	This thesis
pXZ198	Substitutions of S457A/T465V within EBNA2 gene in the backbone of pAH362	This thesis
pGEX 6P1	A prokaryotic expression vector encoding GST and a PreScission protease recognition site	AG Sattler
pXZ162	An EBNA2 423-474aa integrated into the frame and C-terminus of GST gene between in the backbone of pGEX 6P1	This thesis
pXZ299	An EBNA2 453-474aa flanked by Arginines and integrated into the frame and C-terminus of GST gene between in the backbone of pGEX 6P1	This thesis
pXZ190	An EBNA2 342-422aa integrated into the frame and C-terminus of GST gene between BamH I and Not I in the backbone of pGEX 6P1	This thesis
pXZ261	Substitutions of F400A/WY444AA within EBNA2 gene in the backbone of pXZ162	This thesis
pXZ262	Substitutions of SID448AAA within EBNA2 gene in the backbone of pXZ162	This thesis
pXZ263	Substitutions of YIF460AAA within EBNA2 gene in the backbone of pXZ162	This thesis
pXZ264	Substitutions of F400A/WY444AA/SID448AAA within EBNA2 gene in the backbone of pXZ162	This thesis
pXZ265	Substitutions of F400A/WY444AA/YIF460AAA within EBNA2 gene in the backbone of pXZ162	This thesis
pXZ266	Substitutions of F400A/WY444AA/SID448AAA, YIF460AAA within EBNA2 gene in the backbone of pXZ162	This thesis

2. Material

pGEX 5X1-CRS	A Cyclin B1 fragment 104-159aa integrated into the frame and C-terminus of GST gene between EcoR I and Xho I in the backbone of pGEX 5X1	AG Strebhardt
pETM-11	A prokaryotic expression vector encoding a TEV protease recognition site	AG Sattler
pXZ164	A PLK1 13-345aa integrated into C-terminus of hexahistidine (6x His) tag gene between Afl III and Hind III in the backbone of pETM-11	This thesis
pXZ165	A PLK1 345-603aa integrated into C-terminus of hexahistidine (6x His) tag gene in the backbone of pETM-11	This thesis
pXZ304	An EBNA2 upstream of an Arginine and integrated into the frame of C-terminus of 6x His tag gene in the backbone of pETM-11	This thesis
pFastBac HT A	A donor vector used in the baculovirus protein expression system	AG Sattler
pXZ161	A PLK1 integrated into C-terminus of 6x His tag gene in the backbone of pFastBac HT A	This thesis
pXZ191	A substitution of S379A within the EBNA2 gene in the backbone of pXZ190	This thesis

Table 8. Plasmids used for other purposes

Plasmid	Description	Source
pXZ132	A synthetic DNA included in pUC57, to insert HA tag in C-terminus of EBNA2 gene in a BACmid, p6008	This thesis
p6012	A plasmid used as a template in PCR to amplify <i>rpsL/aph</i> cassette in BAC recombineering	AG Hammerschmidt

Table 9. BACmids used in this thesis.

BACmid	Description	Source
p6008	An EBV BACmid of B95.8 genome inserted the 12 kb deletion with the autologous sequences of the M-ABA EBV isolate to restore right-handed <i>OriLyt</i> and to express all 25 EBV-encoded pre-miRNAs from their endogenous viral promoters as well as the LF1, LF2, and LF3 genes with eukaryotic expression of eGFP and puromycin N-acetyl-transferase.	AG Hammerschmidt
pXZ135	An insertion of <i>rpsL/aph</i> cassette into C-terminus of EBNA2 gene in the backbone of p6008	This thesis
pXZ143	An HA tag integrated into the C-terminus of the EBNA2 gene in the backbone of p6008	This thesis

2. Material

pXZ201	An insertion of <i>rpsL/aph</i> cassette at position 1392 in EBNA2 gene locus in the backbone of pXZ143	This thesis
pXZ146	Substitutions of S457A/T465V within EBNA2 gene in the backbone of pXZ143	This thesis
pXZ202	An insertion of <i>rpsL/aph</i> cassette at position 1134 in EBNA2 gene locus in the backbone of pXZ143	This thesis
pXZ203	A substitution of S379A within the EBNA2 gene in the backbone of pXZ143	This thesis

2.7. Oligonucleotides

All oligonucleotides used in this thesis were designed through Primer3 web-based software (<http://bioinfo.ut.ee/primer3/>) and ordered at Metabion, Germany. All oligonucleotides are described and listed in Table S1, Table S2, and Table S3.

2.8. Peptides

The EBNA2 fragment 376-382aa derived peptide (NH₂-NTSSPSM-COOH) with phosphorylated or unphosphorylated serine 379 was synthesized by Peptide Specialty Laboratories, Germany.

2.9. Antibodies

Table 10. Antibodies used in immunoprecipitation and primary antibodies used in western blotting.

Name	Form	Host	Subtype	IP	WB	Source
α -N-His (2F12)	monoclonal	Mouse	IgG 2b		1:50	MAB, HMGU
α -EBNA2 (R3)	monoclonal	Rat	IgG 2a kappa		1:50	MAB, HMGU
α -EBNA2 (1E6)	monoclonal	Rat	IgG 2a kappa	100 μ l		MAB, HMGU
α -GST (6G9)	monoclonal	Rat	IgG 2a kappa	100 μ l	1:50	MAB, HMGU
α -HA (3F10)	monoclonal	Rat	IgG 1	100 μ l	1:50	MAB, HMGU
α -GFP (3E5)	monoclonal	Rat	IgG 1	100 μ l		MAB, HMGU
α -BSA (3C5)	monoclonal	Mouse	IgG 2b	100 μ l		MAB, HMGU
α -LMP1 (1G6)	monoclonal	Rat	IgG 2a		1:5	MAB, HMGU
α -C-MYC (9E10)	monoclonal	Mouse	IgG 1		1:10	MAB, HMGU
α -GAPDH (Mab374)	monoclonal	Mouse	IgG 1		1:1000	Merck Millipore

2. Material

α -Flag M2 (F3165)	monoclonal	Mouse	IgG 1	1 μ g	1:1000	Sigma-Aldrich
α -PLK1 [35-206] (ab17056)	monoclonal	Mouse	IgG 2b	1 μ g	1:1000	Abcam, UK
α -GFP (7.1 and 13.1)	bi-monoclonal	Mouse	IgG 1 kappa		1:1000	Roche, Switzerland
α -p300 (C-20) (sc-585)	polyclonal	Rabbit	IgG		1:1000	Santa Cruz, USA

IP, immunoprecipitation. WB, western blotting.

Table 11. Secondary antibodies used in western blotting.

Name	Host	Addition	WB	Source
α -Rat-IgG-HRP (sc-2006)	Goat	HRP	1:5000	Santa Cruz, USA
α -Mouse-IgG-HRP (sc-2005)	Goat	HRP	1:4000	Santa Cruz, USA
α -Rabbit-IgG-HRP (sc-2004)	Goat	HRP	1:5000	Santa Cruz, USA
α -Mouse-IgG k-BP-HRP (sc-516102)	Goat	HRP	1:4000	Santa Cruz, USA
α -Mouse-IgG-HRP (7076S)	Horse	HRP	1:4000	Cell Signaling Technology

Table 12. Antibodies used in flow cytometry.

Name	Host	Subtype	Addition	FACS	Source	Identifier
α -Human CD19 (HIB19)	Mouse	IgG1 kappa	APC	1:50	BD Pharmingen	555415
isotype control (MCA928APC)	Mouse	IgG1 kappa	APC	1:50	Bio-Rad	MCA928APC
α -Human CD3 (UCHT1)	Mouse BALB/c	IgG1 kappa	PE	1:50	BD Pharmingen	555335
isotype control (MCA928PE)	Mouse	IgG1 kappa	PE	1:50	Bio-Rad	MCA928PE

FACS, fluorescence-activated cell sorting.

2.10. Cell culture materials

Name	Source
RPMI 1640	GIBCO, UK
OptiMEM	GIBCO, UK

2. Material

Fetal Bovine Serum (FBS)	PAA Laboratories, Austria
L-Glutamine (200 mM)	GIBCO, UK
Penicillin-Streptomycin (10,000 U/mL)	GIBCO, UK
Sodium pyruvate (100 mM)	Thermo Fisher Scientific, USA
Sodium selenite	Sigma-Aldrich, USA
Thiols	Sigma-Aldrich, USA
Doxycycline	Sigma-Aldrich, USA
Puromycin	Merck (Calbiochem), Germany
Trypsin-EDTA (0.05%)	GIBCO, UK
Dimethyl sulfoxide (DMSO)	Merck, Germany
BSA	MP Biomedicals, Germany
Ficoll-Paque Plus	GE Healthcare, UK
Trypan blue	GIBCO, UK
Cyclosporin A	Sigma-Aldrich

2.11. Bacterial culture materials

Name	Source
Agar	Bacto™, BD, USA
Tryptone	Bacto™, BD, USA
Yeast Extract	Bacto™, BD, USA
Ampicillin	Sigma-Aldrich, USA
Chloramphenicol	Sigma-Aldrich, USA
Streptomycin	Sigma-Aldrich, USA
Kanamycin	Sigma-Aldrich, USA
IPTG (Isopropylthio- β -galactoside)	Biotium, USA

2.12. Chemicals and reagents

Name	Source
cOmplete Protease Inhibitor	Roche Diagnostics, Germany
PhosSTOP Phosphatase Inhibitor Cocktail Tablets	Sigma-Aldrich, USA
L-Glutathione reduced	Sigma-Aldrich, USA
PLK1, Active	SignalChem, Canada

2. Material

Cyclin B1/CDK1, active	Merk Millipore, UK
Lambda phosphatase (λ PPase)	Santa Cruz Biotechnology
Protein Kinases (PK) buffer	New England Biolabs, USA
[γ - ³² P] ATP (3000 Ci/mmol, 50 mCi/ml)	Hartmann analytic, Germany
Benzonase Nuclease	Millipore, Germany
Glutathione Sepharose 4B	GE Healthcare, UK
Protein G-Sepharose	GE Healthcare, UK
PerfectPro Ni-NTA Agarose	5 Prime, Germany
Acrylamide/Bis-acrylamide, 30%	Roth, Germany
APS	MP Biomedicals, Germany
Isopropanol	Roth, Germany
TEMED	GE Healthcare, UK
Triton X-100	Sigma-Aldrich, USA
Tween 20	AppliChem, Germany
Nonfat dried milk powder	AppliChem, Germany
Page Ruler Prestained Protein Ladder	Thermo Fisher Scientific, USA
Page Ruler Prestained Protein Ladder, Plus	Thermo Fisher Scientific, USA
ECL	GE Healthcare (Amersham), UK
Volasertib (BI 6727)	Selleck Chemicals, USA
Agarose	Invitrogen, USA
Ethidium bromide	Merck, Germany
Proteinase K (PCR grade)	Roche Diagnostics, Germany
RNase A	Merck, Germany
Alkaline Phosphatase, Calf Intestinal (CIP)	New England Biolabs, USA
T4 DNA Ligase	New England Biolabs, USA
T4 polynucleotide kinase (T4 PNK)	Thermo Fisher Scientific, USA
All restriction endonucleases	New England Biolabs, USA or Thermo Fisher Scientific, USA
Polyethylenimine (PEI)	Sigma-Aldrich, USA
dNTP mix (10 mM each)	Thermo Fisher Scientific, USA
λ DNA-Hind III Digest	New England Biolabs, USA
λ DNA-BstE II Digest	New England Biolabs, USA
Phusion High-Fidelity PCR Kit	Thermo Fisher Scientific, USA
peqGold Taq Polymerase, all inclusive	PEQLAB, Germany

All chemicals and reagents which are not listed in the table were purchased at Merck, AppliChem, Roth, and Sigma-Aldrich.

2.13. Kits

Name	Source
QIAamp DNA Blood Mini Kit	QIAGEN, Germany
NucleoSpin Gel and PCR Clean-up	Macherey-Nagel, Germany
NucleoSpin Plasmid	Macherey-Nagel, Germany
PureLink™ HiPure Plasmid Maxiprep Kit	Thermo Fisher Scientific, USA
NucleoBond Xtra BAC kit	Macherey-Nagel, Germany
Qubit™ dsDNA BR Assay Kit	Invitrogen, USA
Dual-Luciferase® Reporter Assay System	Promega, USA
Immobilon-P PVDF Membrane	Merk Millipore, Germany
Fuji Medical X-Ray Film	FUJIFILM Corporation, Japan
CellTrace™ Violet cell proliferation kit	Invitrogen, USA

2.14. Laboratory equipment

Name	Source
Gene Pulser II Electroporation System	Bio-Rad Laboratories
1 mm-gap Gene Pulser Electroporation Cuvette	Bio-Rad Laboratories
2 mm-gap Gene Pulser Electroporation Cuvette	Bio-Rad Laboratories
BD FACS Canto	Becton, Dickinson and Company, USA
BD LSR Fortessa	Becton, Dickinson and Company, USA
REAX2000	Heidolph, Germany
Centrifuge 5415D	Eppendorf, Germany
BioPhotometer D30	Eppendorf, Germany
Thermomixer compact	Eppendorf, Germany
Vacumat 100	Helmut Saur Laborbedarf, Germany
Qubit 2.0 Fluorometer	Invitrogen, USA
Orion Microplate Luminometer MPL4	Berthold, Germany
Mark III Refractometer	Reichert, USA
Hemocytometer	Carl Roth, Germany
Gravity and Spin Chromatography Columns	Bio-Rad Laboratories

2.15. Bioinformatics tools

Name	Source	Identifier
FlowJo v10	Becton, Dickinson and Company, USA	https://www.flowjo.com/
Clone Manager Basic 9	Scientific & Educational Software, USA	https://scied.com/
BLAST	National Center for Biotechnology Information, USA	https://blast.ncbi.nlm.nih.gov/Blast.cgi
UCSC Genome Browser	University of California, USA	https://genome.ucsc.edu/
Primer3	Whitehead Institute for Biomedical Research, USA	http://bioinfo.ut.ee/primer3/
GraphPad Prism 8	GraphPad Software, USA	https://www.graphpad.com/
MEGA X	Pennsylvania State University, USA	https://www.megasoftware.net/
ImageJ	Schneider et al., 2012	https://www.flowjo.com/
PyMOL v1.7.4	Schrödinger, USA	https://pymol.org/2/

3. Methods

3.1. Mammalian cell culture methods

3.1.1. Cell culture

3.1.1.1. Suspension cell lines

All EBV transformed lymphoblastoid cell lines (LCLs) were maintained in RPMI 1640 supplemented with 10% fetal bovine serum (FBS), 1% non-essential amino acids, 2 mM L-glutamine, 1 mM sodium pyruvate, 50 U/ml penicillin, and 50 µg/ml streptomycin at 37°C in 6% CO₂ atmosphere. DG75 cells (Ben-bassats et al., 1977) were cultivated in RPMI 1640 supplemented with 10% FBS, 4 mM L-glutamine, 100 U/ml penicillin, and 100 µg/ml streptomycin at 37°C in 6% CO₂ atmosphere. EBNA2 inducible DG75^{Dox HA-EBNA2} cells (Glaser et al., 2017) were maintained in the same condition as DG75 cells with the addition of 1 µg/ml puromycin for pRTR plasmid selection. Raji (Pulvertaft, 1964) cells were maintained RPMI 1640 supplemented with 10% FBS, 1 mM sodium pyruvate, 100 nM sodium selenite, 50 µM thiols, 100 U/ml penicillin, and 100 µg/ml streptomycin at 37°C in 6% CO₂ atmosphere. Sf21 insect cells were maintained in Lonza Insect-Xpress media at 27°C with shaking in Prof. Michael Sattler's lab. Cells were maintained at $2 - 5 \times 10^5$ cells/ml and subcultured with fresh medium every 3 – 4 days.

3.1.1.2. Adherent cell lines

HEK 293 cells were maintained in the same condition as Raji cells were. All recombinant EBV producer cells were cultivated under the same condition as HEK 293 cells in the presence of 1 µg/ml puromycin for BACmid selection. To detach adherent cells from the culture dishes, cells were washed briefly with PBS, subsequently digested with trypsin-EDTA (0.05%), and incubated at 37°C for approx. 1 min until cell detachment was observed under a microscope. Cells were diluted by 1:2 – 1:10 with fresh medium and subcultured every 3 – 4 days.

PBS (pH 7.4)137 M NaCl, 2.7 M KCl, 7.3 M Na₂HPO₄, 1.5 M KH₂PO₄

3.1.1.3. Human primary B cells

Human primary B cells freshly isolated from donor adenoids were maintained in RPMI 1640 supplemented with 10% fetal bovine serum (FBS), 1% non-essential amino acids, 2 mM L-glutamine, 1 mM sodium pyruvate, 50 U/ml penicillin, and 50 µg/ml streptomycin in a 50 ml Falcon tube at 4°C with rolling for no more than 24 h before infection.

3.1.2. Long term cell storage

To store cells for a longer period, cells were frozen in liquid nitrogen. In brief, 1×10^7 cells were pelleted by centrifugation (300 g, 10min), resuspended in 1 ml freezing medium, and transferred to a 1.8 ml Cryotube (NUNC). Cells were slowly cooled down to -80°C using an isopropanol-filled freezing container and stored there for no more than half of a year. Subsequently, tubes were transferred to liquid nitrogen. To re-cultivate frozen cells, the frozen cells were thawed rapidly in a 37°C water bath, optionally washed with 10 ml medium to remove DMSO, and then resuspended in fresh medium. Selection additions were added to the medium on the day after if required.

Freezing medium 90% (v/v) FBS and 10% (v/v) DMSO

3.1.3. Generation of clonal recombinant EBV producer cell lines

3.1.3.1. Transfection of BACmid DNA into HEK 293 cells

HEK293 cells were plated in a 6-well-plate on the day before transfection (~50% density). For the transfection two reaction batches were pre-mixed: i) 500 μl OptiMEM with 1 μg of the desired BACmid (tips were cut to enlarge the opening to avoid damaging the BACmid DNA) and ii) 500 μl OptiMEM with 4.5 μg PEI (1 mg/ml). Subsequently, the BACmid solution was mixed with the PEI solution and incubated for 15 min at room temperature (RT). For transfection, the culture medium was replaced by 1 ml OptiMEM and the BACmid/PEI mixture was added to the cells dropwise. Optionally, the reaction solution was replaced by 2 ml fresh medium without selection 4 hours post-transfection. The transfected cells were incubated at 37°C in 6% CO_2 atmosphere. Ideally, many cells should be green after 24 h if checked under a fluorescence microscope.

3.1.3.2. Selection of the single clones

One day post-transfection, the infected cells were trypsinized and subcultured in a high dilution in five 15 cm in diameter culture dishes with fresh medium containing 1 $\mu\text{g}/\text{ml}$ puromycin for the selection of cells containing the desired BACmid. Around 2 weeks later eGFP-expressing single clonal colonies derived from single cells grew out. These colonies were identified under a fluorescence microscope. To pick colonies the culture medium was removed, the cells were washed carefully with PBS, and small pieces of filter paper, sterilized by autoclaving and soaked by trypsin, were carefully put onto the desired colonies using tweezers. After 1 min incubation, the filter piece was immediately transferred in a well of a 6-well-plate pre-filled with 3 ml fresh medium supplemented with 1 $\mu\text{g}/\text{ml}$ puromycin. Clonal transfected cell lines were checked daily under a microscope for cell density and subcultured accordingly. For each recombinant EBV genome, several clones were picked, cultivated, and induced to check virus titers (see chapter 3.1.5) of recombinant EBVs. Potent clones were stored, maintained, and used for further recombinant EBV production (see chapter 3.1.4).

3.1.4. Production and concentration of recombinant EBV

To produce a large scale of recombinant EBV, clonal recombinant EBV producer cells described above (see chapter 3.1.3), were transiently transfected with BZLF1 (p509) and BALF4 (p2670) expression plasmids which induce the lytic cycle of EBV to produce large amounts of viral particles. In brief, EBV producer cells were seeded on 15 cm diameter culture dishes with approx. 20 – 30% confluency one day before transfection. For the transfection, the culture medium was replaced by 30 ml of fresh medium without puromycin selection. 6 µg p509 and 6 µg p2670 were diluted by 2.5 ml RPMI1640 for each transfection. 72 µl PEI (1 mg/ml) was added to the DNA solution and mixed well. Subsequently, the reaction was incubated for 15 min at RT. Then 2.5 ml DNA/PEI mixture was added per dish dropwise and the cells incubated for 3 days at 37°C in 6% CO₂ atmosphere. After 3 days of incubation, the recombinant EBV containing supernatants were harvested, centrifuged twice (1,200 rpm and 4,000 rpm for 10 min each) to remove all cells and cell debris, and stored at 4°C.

For small-scale production to check the virus titers, a similar protocol was applied. In brief, The clonal cells were seeded in 2 ml culture medium without puromycin selection in a well of a 6-well-plate. 0.5 µg p509, 0.5 µg p2670, and 6 µl PEI (1 mg/ml) were mixed in 200 µl RPMI 1640 and transfected in the clonal cells. 3 days after transfection, the recombinant EBV containing supernatants were harvested, filtrated (0.8 µm) to remove all cells and cell debris, and stored at 4°C.

For the infection of humanized mice through intraperitoneal injection (i.p) of recombinant EBV, the recombinant EBV supernatant was concentrated to reduce the infection volume. In brief, 30 ml virus supernatant was ultracentrifuged at 24,000 g for 4 h in a Beckman SW28 rotor. Approx. 200 µl was left after discarding most of the supernatant. White viral particles could be observed at that time. The virus was added with 200 – 300 µl PBS containing a cOmplete protease inhibitor, dissolved with slow shaking at 4°C overnight, and stored at 4°C.

3.1.5. Titration of recombinant EBV

For quantification of viral titers, 1×10^5 Raji cells were infected with 100 µl virus supernatant (small-scale production), or with 5, 10, 20, 50, 100, and 500 µl virus supernatant (large-scale production), respectively, or with 0.5, 1, 2, 5, 10 and 20 µl virus concentrate, respectively, and further cultivated in 2 ml fresh medium in a well of a 24-well-plate. 3 days after infection the cells were harvested by centrifugation (500 g, 5 min), washed twice in 1 ml PBS/5% FBS. Subsequently, GFP-positive cells were quantified by FACS analysis. The infection volumes along with 10 – 20% of GFP⁺ cells were used to plot and apply linear regression. Viral titers were termed as green Raji units (GRUs) per ml and calculated as follows: GRUs/ml = the slope of the graph $\times 10^6$.

3.1.6. Preparation of human primary B cells from adenoids

Anonymous adenoids from routine adenoidectomy were collected from the Department of Otorhinolaryngology, Klinikum Grosshadern, Ludwig Maximilians University of Munich, Germany. Human primary B cells were isolated from adenoids by Ficoll density gradient centrifugation. In brief, an adenoid was disrupted mechanically using scalpels and ground on a cell strainer (100 μm) with a syringe plunger to generate cell mash. The cell mash went through another cell strainer (100 μm) and diluted in fresh cell culture medium to generate approx. 30 ml single-cell suspension in a 50 ml Falcon tube. 0.5 ml sheep red blood cells were mixed in the cell suspension to deplete T cells by erythrocyte rosette following centrifugation. The cell suspension was carefully overlaid onto 20 ml Ficoll-Paque Plus to form two phases. The two phases were centrifugated at 1,800 rpm for 30 min with the lowest acceleration and deceleration at 4°C. The lymphocytes from the interphase were transferred to a new 50 ml Falcon tube and washed in 50 ml PBS three times (1,600 rpm, 1,400 rpm, 1,200 rpm for 10 min each). The remaining erythrocytes were lysed in 5 ml red blood cell lysis buffer for 2 min followed by centrifugation (1,200 rpm for 10 min). The lymphocytes were resuspended in 10 – 30 ml cell culture medium, counted, analyzed by FACS.

To quantify the percentage of human primary B cells in the cell suspension, the cells were analyzed by FACS as follows. 4 reactions of 1×10^6 cells were prepared, washed with 1 ml PBS/5% FBS, and resuspended in 50 μl PBS/5% FBS. For each reaction, 1 μl of the following specific antibodies were added: i) APC-conjugated mouse anti-human CD19 (BD Pharmingen, 555415), for B cell identification, ii) APC-conjugated mouse IgG1 isotype control (BioRad, MCA928APC), as an isotype control for i), iii) PE-conjugated mouse anti-human CD3 (BD Pharmingen, 555333), for B cell identification, and vi) PE-conjugated mouse IgG1 isotype control (BioRad, MCA928PE) as an isotype control for iii). The reactions were incubated for 30 min on ice in the dark, subsequently washed twice with 1 ml PBS/5% FBS and finally resuspended in 500 μl PBS/5% FBS. The percentage of APC or PE positive cells was quantified via FACS analysis. Flow cytometry data were analyzed using the FlowJo software.

Red blood cell lysis buffer 155 mM NH_4Cl , 10 mM KHCO_3 , 0.1 mM EDTA (pH 8)

3.1.7. Establishment of LCLs by recombinant EBV

To establish LCLs human primary B cells were infected with recombinant EBV to initiate and maintain cell proliferation, which leads to B cell immortalization or LCL establishment. In brief, 1.5×10^5 human primary B cells were infected with 1.5×10^4 GRUs of a recombinant EBV to make the multiplicity of infection (m.o.i.) as 0.1 in 200 μl cell culture medium in a well of a 96-well-plate. For each recombinant EBV and B cells from each donor triplicates were applied. 2 days post-infection 150 μl culture medium were carefully replaced by fresh culture medium containing 1 $\mu\text{g}/\text{ml}$

Cyclosporin A to suppress T cells proliferation. The cells were subcultured by 1:2 in a well of a multi-well plate with a bigger surface but should be never split too harshly, like the cell density below 1×10^5 cells/ml. After the cells were transferred into tissue flasks, no Cyclosporin A was added to the culture medium anymore.

3.1.8. Cell proliferation assays

In this study, I applied several different assays to check cell proliferation. Assays for cell proliferation can monitor the number of cells over time, e.g. Trypan Blue viability assay, the number of cellular divisions, e.g. CellTrace Violet assay. A detailed description is given below.

3.1.8.1. Trypan Blue viability assay

To monitor the proliferation of LCLs established by recombinant EBVs, 8×10^5 cells were seeded in a well of a 6-well-plate in 2 ml cell culture medium. Cell numbers were monitored daily from day 0 to day 6. In brief, cells were diluted by 1:2 with trypan blue, added to a hemacytometer and unstained living cells were counted under a light microscope. The cell concentration was calculated as follows: cells/ml = mean of cell numbers of four big squares $\times 2$ (the dilution factor) $\times 10^4$. For each LCL triplicates were performed.

3.1.8.2. CellTrace Violet assay

Fresh human primary B cells were pelleted by centrifugation (300 g, 10 min, 4°C), incubated in CellTrace Violet (5 μ M) for 20 minutes in a 37°C water bath in dark, washed with RPMI 1640/2% FBS to remove the unbound dye, and resuspended in cell culture medium. 1×10^6 B cells were infected with 1×10^5 GRUs of recombinant EBV (m.o.i. = 0.1) in 1,200 μ l cell culture medium in a well of a 24-well-plate. From 0 to 6 days post-infection, cells were pelleted by centrifugation (500 g, 5 min, 4°C), washed with PBS/5% FBS, and stained with an APC-conjugated mouse anti-human CD19 antibody (BD Pharmingen, 555415) for B cell identification as described previously. Subsequently, the cells were analyzed on a BD FACS Fortessa machine.

3.2. Bacterial culture methods

3.2.1. Propagation and storage of bacteria

Bacteria were cultured in LB medium at 37°C with shaking (200 rpm) or for isolation of colonies streaked on LB agar plates at 37°C. All mediums and reagents were sterilized by autoclaving or filtering (0.22 μ m) if heat-sensitive. Bacteria transformants were selected by the addition of appropriate antibiotics according to the resistance gene. Bacteria were store at 4°C for no more than 2 days. For short-term storage, bacteria were frozen -20°C with 20% glycerol, and for long-term storage frozen -80°C with 20% glycerol.

LB medium (pH 7.4)

1% Tryptone, 0.5% Yeast Extract, 1% NaCl

saltfree LB medium (pH 7.4)	1% Tryptone, 0.5% Yeast Extract
LB agar	LB medium supplemented with 1.5% (w/v) Agar
Antibiotics	100 µg/ml Ampicillin, 50 µg/ml kanamycin, 1 mg/ml streptomycin, and/or 12.5 µg/ml chloramphenicol, respectively

3.2.2. Preparation of chemically competent bacteria

500 ml LB medium containing 20 mM KCl and 20 mM MgSO₄ were inoculated with 5 ml overnight culture of single clonal *E. coli* (e.g. DH5α, Rosetta 2 (DE3), GM2163, and so on) and incubated at 37°C with shaking (200 rpm) for 2 – 3 h until an OD₅₉₅ of 0.4 – 0.55 was reached. Subsequently, the culture was divided into precooled 50 ml Falcon tubes, incubated on ice for 10 min, and pelleted by centrifugation (4,000 rpm, 10 min, 4°C). Each pellet was resuspended in 15 ml ice-cold TFB1 solution, incubated for 5 min on ice, and pelleted by centrifugation (4,000 rpm, 10 min, 4°C) again. Finally, each pellet was resuspended in 2 ml ice-cold TFB2 solution, aliquoted in 200 µl per precooled 1.5 ml Eppendorf tube, shock frozen on dry ice, and stored at -80°C.

TFB1 solution (pH 5.8, HAc)	30 mM KAc, 50 mM MnCl ₂ , 100 mM RbCl, 10 mM CaCl ₂ , and 15 % (w/v) Glycerol, sterile filtrated (0.22 µm) and stored at 4°C
TFB2 solution	10 mM MOPS (pH 7, NaOH), 75 mM CaCl ₂ , 10 mM RbCl, 15 % (w/v) Glycerol, sterile filtrated (0.22 µm) and stored at 4°C

3.2.3. Preparation of electro-competent bacteria SW105

The *E. coli* strain SW105 optionally with the BACmid of interest was streaked on an LB agar plate containing chloramphenicol incubated at 32°C overnight, and a fresh single colony was cultured into 40 ml saltfree LB agar medium containing chloramphenicol at 32°C overnight with shaking (200 rpm). The overnight culture was inoculated into 50 ml salt-free LB medium containing chloramphenicol and cultured for 2 h at 32°C overnight with shaking (200 rpm) until an OD₅₉₅ of 0.6 was reached. Subsequently, the bacteria culture was immediately put in a 42°C water bath for 15 min with shaking (200 rpm) to induce the expression of the recombinases. Then the bacteria culture was incubated on ice for 20 min and divided into precooled 50 ml Falcon tubes (20 ml bacteria per tube). The bacteria were pelleted by centrifugation (4,000 rpm, 10 min, 4°C). Each pellet was suspended in 10 ml precooled ddH₂O without stirring and pelleted by centrifugation (4,000 rpm, 10 min, 4°C) again. Each pellet was resuspended in 10 ml precooled ddH₂O again and pelleted by centrifugation (4,000 rpm, 10 min, 4°C) again. Each bacteria pellet was resuspended in 1.5 ml precooled ddH₂O. The bacteria were read to transform immediately if you like or could be long-term stored as follows. The bacteria were pelleted by centrifugation (15,000 rpm, 15 sec, 4°C),

resuspended in 160 μ l 20% glycerol, aliquoted by 40 μ l per pre-cooled 1.5 ml Eppendorf tube, shock frozen on dry ice, and stored at -80°C.

3.2.4. Heat shock transformation of *E.coli*

50 μ l of chemically competent *E. coli* were thawed on ice and 50 ng of the DNA of interest, e.g. a plasmid, were added, mixed, and incubated for 10 min on ice. Then the bacteria were heat-shocked for 1 min at 42°C, immediately incubated on ice for 2 min, and then cultured in 600 μ l LB medium for 1 h at 37°C with vigorous shaking. Optionally, bacteria were pelleted by centrifugation (2,000 rpm, 2 min, RT) and suspended in 100 μ l LB medium containing the appropriate antibiotic. To select the transformant, the bacteria were streaked on LB agar plates containing the appropriate antibiotic by serial dilutions and incubated at 37°C overnight.

3.2.5. Electroporation of *E.coli*

40 μ l electro-competent *E. coli* SW105 were mixed with 100 – 500 ng of target DNA (less than 5 μ l in ddH₂O). The bacteria/DNA mixture was transferred into a precooled cuvette (1 mm gap) and electroporated (1,700 V, 200 Ω , 25 μ F) using a BioRad GenePulser II device. The electroporated bacteria were transferred in 1 ml LB medium and incubated for 1 h at 32°C with vigorous shaking. To select the transformant, the bacteria were streaked on LB agar plates containing the appropriate antibiotic by serial dilutions and incubated at 32°C for 24 h.

3.2.6. Cloning and mutagenesis of plasmids

All the plasmid used in the study were cloned based on conventional PCR, restriction digestion, and ligation. Mutated alleles were generated by overlap PCR adapted from the previous protocol (Francis et al., 2017). The essence of overlap PCR is based on four strategically designed primers. Internally positioned primers must contain complementary sequences to each other, and both of them must contain the mutation of interest, like a substitution, a deletion, or an insertion. The flanking primers might contain restriction enzyme recognition sites to facilitate the cloning of the amplified fragment. Two steps were performed, in the first round of PCR reactions using the forward primer of the flanking primers with the reverse primer of the internally positioned primers and vice versa, respectively. The resulting amplified short fragments worked as templates when mixed with the flanking primer pairs, which results in amplification of the final long fragment with the desired mutation in the second round of PCR.

The sequence of EBNA2 fragment 1-341aa was amplified from pAG155 using the following forward: xz54-F, 5'- ACGACCAACAATTACATCATCTACCCT-3' and reverse: xz317-R, 5'- ATTAGCTAGCGTAATCTGGAACATCGTATGGGTATCCCCGGCTCTGGCCTTG-3' primers. The PCR product was purified from agarose gel using a NucleoSpin Gel and PCR Clean-up kit and cloned into pAG155 between *Ava* I and *Nhe* I restriction sites to yield the plasmid termed pCKR656.

3. Methods

The sequence of 1-474aa was amplified from pAG155 using the following forward: xz54-F, 5'- ACGACCAACAATTACATCATCTACCCT-3' and reverse: xz318-R, 5'- ATTAGCTAGCGTAATCTGGAACATCGTATGGGTAATAATCTTCATCTGAGCTAGGAGATTCTG T-3' primers. The PCR product was purified from agarose gel using a NucleoSpin Gel and PCR Clean-up kit and cloned into pAG155 between Ava I and Nhe I restriction sites to yield the plasmid termed pCKR657.

The sequence of EBNA2 S457A was amplified from pAG155 by 2 step PCR reactions. In the first PCR reactions the following forward: xz72-F, 5'- ATATGAATTCCATCATGCCAGAGCCAAACACCTCCAGTCC -3' and reverse: xz129-R, 5'- CAAAATGTAATCCCAAGCTTCGTCTAAGTCTG-3' primers and forward: xz129-F, 5'- CAGACTTAGACGAAGCTTGGGATTACATTTTTG-3' and reverse: xz53-R2, 5'- ATCTTTAGCTAGCGTAATCTGGAAC-3' primers were used. The resulting PCR products were purified from agarose gel using a NucleoSpin Gel and PCR Clean-up kit and used as templates in the second PCR reaction with the following forward: xz72-F, 5'- ATATGAATTCCATCATGCCAGAGCCAAACACCTCCAGTCC -3' and reverse: xz53-R2, 5'- ATCTTTAGCTAGCGTAATCTGGAAC-3' primers. The PCR product was purified from agarose gel using a NucleoSpin Gel and PCR Clean-up kit and cloned into pAG155 between Bbs I and Nhe I restriction sites to yield the plasmid termed pXZ140.

The sequence of EBNA2 T465V was amplified from pAG155 by 2 step PCR reactions. In the first PCR reactions the following forward: xz72-F, 5'- ATATGAATTCCATCATGCCAGAGCCAAACACCTCCAGTCC -3' and reverse: xz130-R, 5'- GAGCTAGGAGATTCTACTGTCTCAAAAATG-3' primers and forward: xz130-F, 5'- CATTTTTGAGACAGTAGAATCTCCTAGCTC-3' and reverse: xz53-R2, 5'- ATCTTTAGCTAGCGTAATCTGGAAC-3' primers were used. The resulting PCR products were purified from agarose gel using a NucleoSpin Gel and PCR Clean-up kit and used as templates in the second PCR reaction with the following forward: xz72-F, 5'- ATATGAATTCCATCATGCCAGAGCCAAACACCTCCAGTCC -3' and reverse: xz53-R2, 5'- ATCTTTAGCTAGCGTAATCTGGAAC-3' primers. The PCR product was purified from agarose gel using a NucleoSpin Gel and PCR Clean-up kit and cloned into pAG155 between Bbs I and Nhe I restriction sites to yield the plasmid termed pXZ141.

The sequence of EBNA2 S457A/T465V was amplified by 2 step PCR reactions. In the first PCR reactions the template pXZ140 with the forward: xz72-F, 5'- ATATGAATTCCATCATGCCAGAGCCAAACACCTCCAGTCC-3' and reverse: xz130-R, 5'- GAGCTAGGAGATTCTACTGTCTCAAAAATG-3' primers and the template pXZ141 with the forward: xz129-F, 5'- CAGACTTAGACGAAGCTTGGGATTACATTTTTG-3' and reverse: xz53-R2, 5'-ATCTTTAGCTAGCGTAATCTGGAAC-3' primers were used respectively. The resulting PCR products were purified from agarose gel using a NucleoSpin Gel and PCR Clean-up kit and used as templates in the second PCR reaction with the following forward: xz72-F, 5'-

3. Methods

ATATGAATTCCATCATGCCAGAGCCAAACACCTCCAGTCC -3' and reverse: xz53-R2, 5'-ATCTTTAGCTAGCGTAATCTGGAAC-3' primers. The PCR product was purified from agarose gel using a NucleoSpin Gel and PCR Clean-up kit and cloned into pAG155 between Bbs I and Nhe I restriction sites to yield the plasmid termed pXZ142.

The sequence of EBNA2 ST266AV was amplified from pAG155 by 2 step PCR reactions. In the first PCR reactions the following forward: xz53-F1, 5'-AGCCCCTCAGGCCAGGTTGGTCCAG-3' and reverse: xz153-R1, 5'-CTGGATCATTTGGGACGGCTTGATGAGTAAG-3' primers and forward: xz153-F2, 5'-CTTACTCATCAAGCCGTCCCAAATGATCCAG-3' and reverse: xz52-R, 5'-CTCTGGTCTCCAAGTCCACCG-3' primers were used. The resulting PCR products were purified from agarose gel using a NucleoSpin Gel and PCR Clean-up kit and used as templates in the second PCR reaction with the following forward: xz53-F1, 5'-AGCCCCTCAGGCCAGGTTGGTCCAG-3' and reverse: xz52-R, 5'-CTCTGGTCTCCAAGTCCACCG-3' primers. The PCR product was purified from agarose gel using a NucleoSpin Gel and PCR Clean-up kit and cloned into pAG155 between Bsu36 I and Ava I restriction sites to yield the plasmid termed pXZ153.

The sequence of EBNA2 TSS377VAA was amplified from pAG155 by 2 step PCR reactions. In the first PCR reactions the following forward: xz54-F, 5'-ACGACCAACAATTACATCATCTACCCT-3' and reverse: xz154-R1, 5'-AGGCATGCTAGGAGCGGCGACGTTTGGCTCTGG-3' primers and forward: xz154-F2, 5'-CCAGAGCCAAACGTCGCCGCTCCTAGCATGCCT-3' and reverse: xz53-R2, 5'-ATCTTTAGCTAGCGTAATCTGGAAC-3' primers were used. The resulting PCR products were purified from agarose gel using a NucleoSpin Gel and PCR Clean-up kit and used as templates in the second PCR reaction with the following forward: xz54-F, 5'-ACGACCAACAATTACATCATCTACCCT-3' and reverse: xz53-R2, 5'-ATCTTTAGCTAGCGTAATCTGGAAC-3' primers. The PCR product was purified from agarose gel using a NucleoSpin Gel and PCR Clean-up kit and cloned into pAG155 between Ava I and Nhe I restriction sites to yield the plasmid termed pXZ154.

The sequence of EBNA2 SPSS467APAA was amplified from pAG155 by 2 step PCR reactions. In the first PCR reactions the following forward: xz54-F, 5'-ACGACCAACAATTACATCATCTACCCT-3' and reverse: xz155-R1, 5'-CATAATCTTCATCTGCGGCAGGAGCTTCTGTTGTCTC-3' primers and forward: xz155-F2, 5'-GAGACAACAGAAGCTCCTGCCGAGATGAAGATTATG-3' and reverse: xz53-R2, 5'-ATCTTTAGCTAGCGTAATCTGGAAC-3' primers were used. The resulting PCR products were purified from agarose gel using a NucleoSpin Gel and PCR Clean-up kit and used as templates in the second PCR reaction with the following forward: xz54-F, 5'-ACGACCAACAATTACATCATCTACCCT-3' and reverse: xz53-R2, 5'-ATCTTTAGCTAGCGTAATCTGGAAC-3' primers. The PCR product was purified from agarose gel

3. Methods

using a NucleoSpin Gel and PCR Clean-up kit and cloned into pAG155 between Ava I and Nhe I restriction sites to yield the plasmid termed pXZ155.

The sequence of EBNA2 S379A was amplified from pAG155 by 2 step PCR reactions. In the first PCR reactions the following forward: xz54-F, 5'-AGGCATGCTAGGACTGGCGGTGTTTGGCTCTGG-3' and reverse: xz179-R1, 5'-AGGCATGCTAGGAGCGGAGGTGTTTGGCTCTGG-3' primers and forward: xz179-F2, 5'-CCAGAGCCAAACACCTCCGCTCCTAGCATGCCT-3' and reverse: xz53-R2, 5'-ATCTTTAGCTAGCGTAATCTGGAAC-3' primers were used. The resulting PCR products were purified from agarose gel using a NucleoSpin Gel and PCR Clean-up kit and used as templates in the second PCR reaction with the following forward: xz54-F, 5'-ACGACCAACAATTACATCATCTACCCT-3' and reverse: xz53-R2, 5'-ATCTTTAGCTAGCGTAATCTGGAAC-3' primers. The PCR product was purified from agarose gel using a NucleoSpin Gel and PCR Clean-up kit and cloned into pAG155 between Ava I and Nhe I restriction sites to yield the plasmid termed pXZ179.

The sequence of EBNA2 S184A was amplified from pAG155 by 2 step PCR reactions. In the first PCR reactions the following forward: xz51-F, 5'-ATTAGAATTCCATCATGGGGCATGGACCTCTAGCATCTG-3' and reverse: xz346-R, 5'-TAAGCCTCGGTTGTGcCAGAGGTGACAAAATGGTGGG-3' primers and forward: xz346-F, 5'-TTGTACCTCTGgCACAACCGAGGCTTACCCCTC-3' and reverse: xz53-R1.1, 5'-ATTAggtctcaggCATGCGTGGTGGTGGTGGT-3' primers were used. The resulting PCR products were purified from agarose gel using a NucleoSpin Gel and PCR Clean-up kit and used as templates in the second PCR reaction with the following forward: xz54-F, 5'-ACGACCAACAATTACATCATCTACCCT-3' and reverse: xz53-R2, 5'-ATCTTTAGCTAGCGTAATCTGGAAC-3' primers. The PCR product was purified from agarose gel using a NucleoSpin Gel and PCR Clean-up kit and cloned into pAG155 between BstE II and Aar I restriction sites to yield the plasmid termed pCKR675.

The sequence of EBNA2 S258A was amplified from pAG155 by 2 step PCR reactions. In the first PCR reactions the following forward: xz203-Fwd Seq, 5'-CTCCTACCCCTCTGCCACCTGCAAC-3' and reverse: xz347-R, 5'-TAAGAGGGTGCATTGcTTGGTCTGGCACATGCAAGACA-3' primers and forward: xz347-F, 5'-CATGTGCCAGACCAAgCAATGCACCCTCTTACTCATCAAAG-3' and reverse: xz317-R, 5'-attaGCTAGCGTAATCTGGAACATCGTATGGGTATCCCCGGCTCTGGCCTTG-3' primers were used. The resulting PCR products were purified from agarose gel using a NucleoSpin Gel and PCR Clean-up kit and used as templates in the second PCR reaction with the following forward: xz203-Fwd Seq, 5'-CTCCTACCCCTCTGCCACCTGCAAC-3' and reverse: xz317-R, 5'-ATTAGCTAGCGTAATCTGGAACATCGTATGGGTATCCCCGGCTCTGGCCTTG-3' primers. The PCR product was purified from agarose gel using a NucleoSpin Gel and PCR Clean-up kit and cloned into pAG155 between Aar I and Ava I restriction sites to yield the plasmid termed pCKR676.

3. Methods

The sequence of EBNA2 S479A was amplified from pAG155 by 2 step PCR reactions. In the first PCR reactions the following forward: xz53-F2.2, 5'-ATTAGGTCTCATGCCAGAGCCAAACACCTCCA-3' and reverse: xz348-R, 5'-GGGCGAGGTCTTTTAGCGGGTCCCTCCACATAATCTTCA-3' primers and forward: xz348-F, 5'-TATGTGGAGGGACCCgcTAAAAGACCTCGCCCCT-3' and reverse: xz53-R2, 5'-ATCTTTAGCTAGCGTAATCTGGAAC-3' primers were used. The resulting PCR products were purified from agarose gel using a NucleoSpin Gel and PCR Clean-up kit and used as templates in the second PCR reaction with the following forward: xz53-F2.2, 5'-ATTAGGTCTCATGCCAGAGCCAAACACCTCCA-3' and reverse: xz53-R2, 5'-ATCTTTAGCTAGCGTAATCTGGAAC-3' primers. The PCR product was purified from agarose gel using a NucleoSpin Gel and PCR Clean-up kit and cloned into pAG155 between Bbs I and Nhe I restriction sites to yield the plasmid termed pCKR677.

The sequence of EBNA2 S457A/T465V/S479A was amplified from pXZ142 by 2 step PCR reactions. In the first PCR reactions the following forward: xz53-F2.2, 5'-ATTAGGTCTCATGCCAGAGCCAAACACCTCCA-3' and reverse: xz348-R, 5'-GGGCGAGGTCTTTTAGCGGGTCCCTCCACATAATCTTCA-3' primers and forward: xz348-F, 5'-TATGTGGAGGGACCCgcTAAAAGACCTCGCCCCT-3' and reverse: xz53-R2, 5'-ATCTTTAGCTAGCGTAATCTGGAAC-3' primers were used. The resulting PCR products were purified from agarose gel using a NucleoSpin Gel and PCR Clean-up kit and used as templates in the second PCR reaction with the following forward: xz53-F2.2, 5'-ATTAGGTCTCATGCCAGAGCCAAACACCTCCA-3' and reverse: xz53-R2, 5'-ATCTTTAGCTAGCGTAATCTGGAAC-3' primers. The PCR product was purified from agarose gel using a NucleoSpin Gel and PCR Clean-up kit and cloned into pXZ142 between Bbs I and Nhe I restriction sites to yield the plasmid termed pCKR678.

The sequence of EBNA2 S258A/S457A/T465V/S479A was generated by subcloning. The insert of pCKR676 between Aar I and Ava I sites was digested, purified from agarose gel using a NucleoSpin Gel and PCR Clean-up kit and cloned into pCKR678 between the same sites to yield the plasmid termed pCKR679.

The sequence of EBNA2 S184A/S258A/S457A/T465V/S479A was generated by subcloning. The insert of pCKR676 between BstE II and Aar I sites was digested, purified from agarose gel using a NucleoSpin Gel and PCR Clean-up kit and cloned into pCKR679 between the same sites to yield the plasmid termed pCKR680.

The sequence of EBNA2 F400A/WY444AA/YIF460AAA was amplified from pAG155 by 2 step PCR reactions. In the first PCR reactions the following forward: xz72-F, 5'-ATATGAATTCCATCATGCCAGAGCCAAACACCTCCAGTCC-3' and reverse: xz261-R, 5'-AGCCGCATCATCGGGGGCGAGAATGGGAGCCTCT-3' primers, forward: xz261-F, 5'-GCCCCCGATGATGCGGCTCCTCCATCTATAGACCCC-3' and reverse: xz263-R, 5'-

3. Methods

AGCAGCGGCATCCCAACTTTTCGTCTAAGTCT-3' primers and forward: xz263-F, 5'-GCCGCTGCTGAGACAACAGAATCTC-3' and reverse: xz53-R2, 5'-ATCTTTAGCTAGCGTAATCTGGAAC-3' primers were used, respectively. The resulting PCR products were purified from agarose gel using a NucleoSpin Gel and PCR Clean-up kit and used as templates in the second PCR reaction with the following forward: xz72-F, 5'-ATATGAATTCCATCATGCCAGAGCCAAACACCTCCAGTCC-3' and reverse: xz53-R2, 5'-ATCTTTAGCTAGCGTAATCTGGAAC-3' primers. The PCR product was purified from agarose gel using a NucleoSpin Gel and PCR Clean-up kit and cloned into pAG155 between Bbs I and Nhe I restriction sites to yield the plasmid termed pXZ288.

The sequence of EBNA2 S379A/F400A/WY444AA/YIF460AAA was generated by subcloning. The insert of pXZ288 between Bbs I and Nhe I sites was digested, purified from agarose gel using a NucleoSpin Gel and PCR Clean-up kit and cloned into pXZ179 between the same sites to yield the plasmid termed pXZ289.

The sequence of EBNA2 327-487aa was amplified from pAG155 using the following forward: xz150-F, 5'-TATAGGATCCATCTGCGACCCCCCGCAAC-3' and reverse: xz150-R, 5'-ATTATCTAGATCACTGGATGGAGGGGCGAGGT-3' primers. The PCR product was purified from agarose gel using a NucleoSpin Gel and PCR Clean-up kit and cloned into pEGFP/NLS between BamH I and Xba I restriction sites to yield the plasmid termed pXZ150.

The sequence of EBNA2 327-407aa was amplified from pAG155 using the following forward: xz150-F, 5'-TATAGGATCCATCTGCGACCCCCCGCAAC-3' and reverse: xz151-R, 5'-attatctagatcaATTGGATGGGCCAGGAGTTGG-3' primers. The PCR product was purified from agarose gel using a NucleoSpin Gel and PCR Clean-up kit and cloned into pEGFP/NLS between BamH I and Xba I restriction sites to yield the plasmid termed pXZ151.

The sequence of EBNA2 408-487aa was amplified from pAG155 using the following forward: xz152-F, 5'-TATAGGATCCAATGCCGCCCCCGTTTGTA-3' and reverse: xz150-R, 5'-ATTATCTAGATCACTGGATGGAGGGGCGAGGT-3' primers. The PCR product was purified from agarose gel using a NucleoSpin Gel and PCR Clean-up kit and cloned into pEGFP/NLS between BamH I and Xba I restriction sites to yield the plasmid termed pXZ152.

The sequence of EBNA2 342-474aa was amplified from pAG155 using the following forward: xz190-F, 5'-ATTAGGATCCGGACAGAGCAGG-3' and reverse: xz331-R, 5'-AATTTCTAGACTAATAATCTTCATC-3' primers. The PCR product was purified from agarose gel using a NucleoSpin Gel and PCR Clean-up kit and cloned into pEGFP/NLS between BamH I and Xba I restriction sites to yield the plasmid termed pCKR672.

The sequence of EBNA2 342-422aa was amplified from pAG155 using the following forward: xz190-F, 5'-ATTAGGATCCGGACAGAGCAGG-3' and reverse: xz229-R, 5'-ATTATCTAGACGTTAGGGG-3' primers. The PCR product was purified from agarose gel using a

3. Methods

NucleoSpin Gel and PCR Clean-up kit and cloned into pEGFP/NLS between BamH I and Xba I restriction sites to yield the plasmid termed pXZ229.

The sequence of EBNA2 423-474aa was amplified from pAG155 using the following forward: xz162-F, 5'-ATTAGGATCCCCAATACATGAACCG-3' and reverse: xz331-R, 5'-AATTTCTAGACTAATAATCTTCATC-3' primers. The PCR product was purified from agarose gel using a NucleoSpin Gel and PCR Clean-up kit and cloned into pEGFP/NLS between BamH I and Xba I restriction sites to yield the plasmid termed pCKR661.

The sequence of EBNA2 342-487aa was amplified from pAG155 using the following forward: xz92-F, 5'-ATTAGTCGACTGGACAGAGCAGG-3' and reverse: xz92-R, 5'-ATTAGCGGCCGCTACTGGATGGA-3' primers. The PCR product was purified from agarose gel using a NucleoSpin Gel and PCR Clean-up kit and cloned into pGEX 4T2 between Sal I and Not I restriction sites to yield the plasmid termed pXZ92.

The sequence of EBNA2 342-422aa was amplified from pAG155 using the following forward: xz92-F, 5'-ATTAGTCGACTGGACAGAGCAGG-3' and reverse: xz93-R, 5'-ATTAGCGGCCGCTAAACGTTAGG-3' primers. The PCR product was purified from agarose gel using a NucleoSpin Gel and PCR Clean-up kit and cloned into pGEX 4T2 between Sal I and Not I restriction sites to yield the plasmid termed pXZ93.

The sequence of EBNA2 423-487aa was amplified from pAG155 using the following forward: xz94-F, 5'-ATTAGTCGACTTCACCAATACATGAAC-3' and reverse: xz92-R, 5'-ATTAGCGGCCGCTACTGGATGGA-3' primers. The PCR product was purified from agarose gel using a NucleoSpin Gel and PCR Clean-up kit and cloned into pGEX 4T2 between Sal I and Not I restriction sites to yield the plasmid termed pXZ94.

The sequence of EBNA2 342-422aa was amplified from pAG155 using the following forward: xz190-F, 5'-ATTAGGATCCGGACAGAGCAGG-3' and reverse: xz93-R, 5'-ATTAGCGGCCGCTAAACGTTAGG-3' primers. The PCR product was purified from agarose gel using a NucleoSpin Gel and PCR Clean-up kit and cloned into pGEX 6P1 between BamH I and Not I restriction sites to yield the plasmid termed pXZ190.

The sequence of EBNA2 423-474aa was amplified from pAG155 using the following forward: xz162-F, 5'-ATTAGGATCCCCAATACATGAACCG-3' and reverse: xz111-R, 5'-AATTGCGGCCGCTAATAATCTTCATC-3' primers. The PCR product was purified from agarose gel using a NucleoSpin Gel and PCR Clean-up kit and cloned into pGEX 6P1 between BamH I and Not I restriction sites to yield the plasmid termed pXZ162.

The sequence of EBNA2 423-474aa was amplified from pAG155 using the following forward: xz94-F, 5'-ATTAGTCGACTTCACCAATACATGAAC-3' and reverse: xz111-R, 5'-AATTGCGGCCGCTAATAATCTTCATC-3' primers. The PCR product was purified from agarose

3. Methods

gel using a NucleoSpin Gel and PCR Clean-up kit and cloned into pGEX 4T2 between Sal I and Not I restriction sites to yield the plasmid termed pXZ109.

The sequence of EBNA2 423-445aa was amplified from pAG155 using the following forward: xz94-F, 5'-ATTAGTCGACTTCACCAATACATGAAC-3' and reverse: xz110-R, 5'-AATTGCGGCCGCTAATACCAATCA-3' primers. The PCR product was purified from agarose gel using a NucleoSpin Gel and PCR Clean-up kit and cloned into pGEX 4T2 between Sal I and Not I restriction sites to yield the plasmid termed pXZ110.

The sequence of EBNA2 446-474aa was amplified from pAG155 using the following forward: xz111-F, 5'-ATTAGTCGACTCCTCCATCTATAGACC-3' and reverse: xz111-R, 5'-AATTGCGGCCGCTAATAATCTTCATC-3' primers. The PCR product was purified from agarose gel using a NucleoSpin Gel and PCR Clean-up kit and cloned into pGEX 4T2 between Sal I and Not I restriction sites to yield the plasmid termed pXZ111.

The sequence of EBNA2 475-487aa was amplified from pAG155 using the following forward: xz112-F, 5'-ATTAGTCGACTGTGGAGGGACCCAG-3' and reverse: xz92-R, 5'-ATTAGCGGCCGCTACTGGATGGA-3' primers. The PCR product was purified from agarose gel using a NucleoSpin Gel and PCR Clean-up kit and cloned into pGEX 4T2 between Sal I and Not I restriction sites to yield the plasmid termed pXZ112.

The sequence of EBNA2 446-487aa was amplified from pAG155 using the following forward: xz111-F, 5'-ATTAGTCGACTCCTCCATCTATAGACC-3' and reverse: xz92-R, 5'-ATTAGCGGCCGCTACTGGATGGA-3' primers. The PCR product was purified from agarose gel using a NucleoSpin Gel and PCR Clean-up kit and cloned into pGEX 4T2 between Sal I and Not I restriction sites to yield the plasmid termed pXZ113.

The sequence of EBNA2 246-487aa S457A/T465V was amplified from pXZ142 using the following forward: xz198-F, 5'-ATTAGTCGACTCGCATGCATCTCCCTGTCTTG-3' and reverse: xz92-R, 5'-ATTAGCGGCCGCTACTGGATGGA-3' primers. The PCR product was purified from agarose gel using a NucleoSpin Gel and PCR Clean-up kit and cloned into pGEX 6P1 between Sal I and Xba I restriction sites to yield the plasmid termed pXZ198.

The sequence of EBNA2 423-474aa F400A/WY444AA was amplified from pAG155 by 2 step PCR reactions. In the first PCR reactions the following forward: xz162-F, 5'-ATTAGGATCCCCAATACATGAACCG-3' and reverse: xz261-R, 5'-AGCCGCATCATCGGGGGCGAGAATGGGAGCCTCT-3' primers and forward: xz261-F, 5'-GCCCCGATGATGCGGCTCCTCCATCTATAGACCCC-3' and reverse: xz111-R, 5'-AATTGCGGCCGCTAATAATCTTCATC-3' primers were used, respectively. The resulting PCR products were purified from agarose gel using a NucleoSpin Gel and PCR Clean-up kit and used as templates in the second PCR reaction with the following forward: xz162-F, 5'-ATTAGGATCCCCAATACATGAACCG-3' and reverse: xz111-R, 5'-AATTGCGGCCGCTAATAATCTTCATC-3' primers. The PCR product was purified from agarose

3. Methods

gel using a NucleoSpin Gel and PCR Clean-up kit and cloned into pGEX 6P1 between BamH I and Not I restriction sites to yield the plasmid termed pXZ261.

The sequence of EBNA2 423-474aa SID448AAA was amplified from pAG155 by 2 step PCR reactions. In the first PCR reactions the following forward: xz162-F, 5'-ATTAGGATCCCCAATACATGAACCG-3' and reverse: xz262-R, 5'-GGCTGCAGCTGGAGGATACCAATCATCG-3' primers and forward: xz262-F, 5'-GCTGCAGCCCCCGCAGACTTAGACGA-3' and reverse: xz111-R, 5'-AATTGCGGCCGCTAATAATCTTCATC-3' primers were used, respectively. The resulting PCR products were purified from agarose gel using a NucleoSpin Gel and PCR Clean-up kit and used as templates in the second PCR reaction with the following forward: xz162-F, 5'-ATTAGGATCCCCAATACATGAACCG-3' and reverse: xz111-R, 5'-AATTGCGGCCGCTAATAATCTTCATC-3' primers. The PCR product was purified from agarose gel using a NucleoSpin Gel and PCR Clean-up kit and cloned into pGEX 6P1 between BamH I and Not I restriction sites to yield the plasmid termed pXZ262.

The sequence of EBNA2 423-474aa YIF460AAA was amplified from pAG155 by 2 step PCR reactions. In the first PCR reactions the following forward: xz162-F, 5'-ATTAGGATCCCCAATACATGAACCG-3' and reverse: xz263-R, 5'-AGCAGCGGCATCCCAACTTTCTGCTAAGTCT-3' primers and forward: xz263-F, 5'-GCCGCTGCTGAGACAACAGAATCTC-3' and reverse: xz111-R, 5'-AATTGCGGCCGCTAATAATCTTCATC-3' primers were used, respectively. The resulting PCR products were purified from agarose gel using a NucleoSpin Gel and PCR Clean-up kit and used as templates in the second PCR reaction with the following forward: xz162-F, 5'-ATTAGGATCCCCAATACATGAACCG-3' and reverse: xz111-R, 5'-AATTGCGGCCGCTAATAATCTTCATC-3' primers. The PCR product was purified from agarose gel using a NucleoSpin Gel and PCR Clean-up kit and cloned into pGEX 6P1 between BamH I and Not I restriction sites to yield the plasmid termed pXZ263.

The sequence of EBNA2 423-474aa F400A/WY444AA/SID448AAA was amplified by 2 step PCR reactions. In the first PCR reactions the template pXZ261 with the following forward: xz162-F, 5'-ATTAGGATCCCCAATACATGAACCG-3' and reverse: xz264-R, 5'-GGCTGCAGCTGGAGGAGCCGCATC -3' primers and template pXZ262 with the following forward: xz262-F, 5'-GCTGCAGCCCCCGCAGACTTAGACGA-3' and reverse: xz111-R, 5'-AATTGCGGCCGCTAATAATCTTCATC-3' primers were used, respectively. The resulting PCR products were purified from agarose gel using a NucleoSpin Gel and PCR Clean-up kit and used as templates in the second PCR reaction with the following forward: xz162-F, 5'-ATTAGGATCCCCAATACATGAACCG-3' and reverse: xz111-R, 5'-AATTGCGGCCGCTAATAATCTTCATC-3' primers. The PCR product was purified from agarose gel using a NucleoSpin Gel and PCR Clean-up kit and cloned into pGEX 6P1 between BamH I and Not I restriction sites to yield the plasmid termed pXZ264.

3. Methods

The sequence of EBNA2 423-474aa F400A/WY444AA/YIF460AAA was amplified from pXZ261 by 2 step PCR reactions. In the first PCR reactions the following forward: xz162-F, 5'-ATTAGGATCCCCAATACATGAACCG-3' and reverse: xz263-R, 5'-AGCAGCGGCATCCCAACTTTTCGTCTAAGTCT-3' primers and forward: xz263-F, 5'-GCCGCTGCTGAGACAACAGAATCTC-3' and reverse: xz111-R, 5'-AATTGCGGCCGCTAATAATCTTCATC-3' primers were used, respectively. The resulting PCR products were purified from agarose gel using a NucleoSpin Gel and PCR Clean-up kit and used as templates in the second PCR reaction with the following forward: xz162-F, 5'-ATTAGGATCCCCAATACATGAACCG-3' and reverse: xz111-R, 5'-AATTGCGGCCGCTAATAATCTTCATC-3' primers. The PCR product was purified from agarose gel using a NucleoSpin Gel and PCR Clean-up kit and cloned into pGEX 6P1 between BamH I and Not I restriction sites to yield the plasmid termed pXZ265.

The sequence of EBNA2 423-474aa F400A/WY444AA/SID448AAA/YIF460AAA was amplified by 2 step PCR reactions. In the first PCR reactions the template pXZ265 with the following forward: xz162-F, 5'-ATTAGGATCCCCAATACATGAACCG-3' and reverse: xz264-R, 5'-GGCTGCAGCTGGAGGAGCCGCATC-3' primers and the template pXZ264 with the following forward: xz262-F, 5'-GCTGCAGCCCCCGCAGACTTAGACGA-3' and reverse: xz111-R, 5'-AATTGCGGCCGCTAATAATCTTCATC-3' primers were used, respectively. The resulting PCR products were purified from agarose gel using a NucleoSpin Gel and PCR Clean-up kit and used as templates in the second PCR reaction with the following forward: xz162-F, 5'-ATTAGGATCCCCAATACATGAACCG-3' and reverse: xz111-R, 5'-AATTGCGGCCGCTAATAATCTTCATC-3' primers. The PCR product was purified from agarose gel using a NucleoSpin Gel and PCR Clean-up kit and cloned into pGEX 6P1 between BamH I and Not I restriction sites to yield the plasmid termed pXZ266.

The sequence of EBNA2 342-422aa S379A was amplified from pXZ179 with the following forward: xz190-F, 5'-ATTAGGATCCGGACAGAGCAGG-3' and reverse: xz93-R, 5'-ATTAGCGGCCGCTAAACGTTAGG-3' primers. The resulting PCR product was purified from agarose gel using a NucleoSpin Gel and PCR Clean-up kit and cloned into pGEX 6P1 between BamH I and Not I restriction sites to yield the plasmid termed pXZ191.

The sequence of EBNA2 453-474aa flanked by arginines was amplified from pAG155 with the following forward: xz299-F, 5'-ATTAggatcccgtGACTTAGACGAAAGTTGG -3' and reverse: xz299-R, 5'-TATAGCGGCCGCTAATAATCacgTTCATCTGAGCTAGGAG -3' primers. The resulting PCR product was purified from agarose gel using a NucleoSpin Gel and PCR Clean-up kit and cloned into pGEX 6P1 between BamH I and Not I restriction sites to yield the plasmid termed pXZ299.

The polyR region sequence of EBNA2 was amplified from pAG155 using peqGold Taq Polymerase with the following forward: xz302-F, 5'-ATTACGTCTCACATGAGGATGCCTACATTCTATCTTGCG-3' and reverse: xz51-R, 5'-

GCAAATAAGGCCCGGTCA-3' primers. The PCR product was digested by BsmB I and BamH I, purified from agarose gel using a NucleoSpin Gel and PCR Clean-up kit and cloned into pETM-11 between Nco I and BamH I restriction sites to yield the plasmid termed pXZ302mdt. The rest sequence of EBNA2 was amplified from pAG155 using Phusion High-Fidelity DNA Polymerase with the following forward: xz302-F, 5'-ATTACGTCTCACATGAGGATGCCTACATTCTATCTTGCG-3' and reverse: xz213-R, 5'-ATTACTCGAGTCACTGGATGGAGGGGCGAG-3' primers. The PCR product was purified from agarose gel using a NucleoSpin Gel and PCR Clean-up kit and cloned into pXZ302mdt between BamH I and Xho I restriction sites to yield the plasmid termed pXZ304.

The sequence of PLK1 was amplified from 3x Flag-tagged PLK1 with the following forward: xz161-F, 5'-ATTAGAATTCATGAGTGCTGCAGTGAAGTGCAGG-3' and reverse: xz213-R, 5'-AATTAAGCTTAGGAGGCCTTGAGACGGTT-3' primers. The PCR product was purified from agarose gel using a NucleoSpin Gel and PCR Clean-up kit and cloned into pFastBac HTA between EcoR I and Xho I restriction sites to yield the plasmid termed pXZ161.

The sequence of PLK1 13-345aa was amplified from 3x Flag-tagged PLK1 with the following forward: xz164-F, 5'-ATTAACATGTTAGCACCGGCCGACCCTG-3' and reverse: xz164-R, 5'-AATTAAGCTTTTTATTGAGGACTGTGAGGGGCTTC-3' primers. The PCR product was digested by Afl III and Hind III, purified from agarose gel using a NucleoSpin Gel and PCR Clean-up kit and cloned into pETM-11 between Nco I and Hind III restriction sites to yield the plasmid termed pXZ164.

The sequence of PLK1 345-603aa was amplified from 3x Flag-tagged PLK1 with the following forward: xz165-F, 5'-ATTACCATGGCGAAAGGCTTGGAGAACCCCTGCCTG-3' and reverse: xz165-R, 5'-AATTAAGCTTAGGAGGCCTTGAGACGGTTGCTGG-3' primers. The PCR product was purified from agarose gel using a NucleoSpin Gel and PCR Clean-up kit and cloned into pETM-11 between Nco I and Hind III restriction sites to yield the plasmid termed pXZ165.

3.2.7. Isolation of plasmids

To isolate a small scale (mini-prep) of plasmid DNA from *E.coli* (e.g. DH5 α and GM2163), bacteria were collected from 5 ml overnight culture ($OD_{595} = 2.5 - 5$) and the plasmid was isolated using the NucleoSpin Plasmid Kit according to the manufacturer's instructions. To isolate a large scale (maxi-prep) of plasmid DNA from *E.coli* (e.g. DH5 α and GM2163), bacteria were collected from 400 ml overnight culture ($OD_{595} = 2.5 - 5$) and the plasmid was isolated using the PureLink HiPure Plasmid Maxiprep Kit according to the manufacturer's instructions.

3.2.8. BAC recombineering

All BAC used to produce recombinant EBV strains used in this study were generated by a two-step selection protocol using the λ prophage-based heat-inducible Red recombination system expressed in a streptomycin-sensitive *E.coli* strain, SW105. For the first step, an *rpsL/aph* expression cassette was flanked by 50 bp EBV sequences of the respective EBNA2 gene locus by

PCR using the template p6012. The resulting PCR product was used to insert the *rpsL/aph* cassette by homologous recombination into the specific EBV/EBNA2 target site by transformation and kanamycin (30 µg/ml) and chloramphenicol (12.5 µg/ml) selection of SW105 pre-transformed with the recombinant target EBV BACmid. As a second step, a synthetic DNA fragment or PCR product carrying the desired mutation flanked by ~300 bp of the genomic viral sequence was used to replace the *rpsL/aph* cassette by homologous recombination to generate the final mutant EBV plasmid by streptomycin (1 mg/ml) and chloramphenicol selection (12.5 µg/ml).

3.2.8.1. BACmid with C-terminal HA-tagged EBNA2

The sequence of the *rpsL/aph* cassette was amplified from p6012 with the following forward: xz135-F, 5'-ATGAAGATTATGTGGAGGGACCCAGTAAAAGACCTCGCCCCTCCATCCAGGGCCTGGTGATGATGGCGGGATCG-3' and reverse: xz135-R, 5'-GTAACATTTATTTGGGATACATTGGTTGCTGGAGAGGGCAAGGGTTTTTATCAGAAGAACTCGTCAAGAAGGCG-3' primers. The resulting PCR product was purified from agarose gel, electroporated into an *E. coli* strain SW105 harboring p6008 and selected by kanamycin (positive) and streptomycin (replica negative) to yield the BACmid termed pXZ135.

Next, the synthetic DNA sequence (GenScript) of HA tag flanked by 300 bp upstream and 300 bp downstream of EBNA2 stop codon was harbored in a plasmid termed pXZ132, pXZ132 was digested by BsmB I. A ~650 bp fragment was purified from agarose gel, electroporated into an *E. coli* strain SW105 harboring pXZ135 and selected by chloramphenicol and streptomycin to yield the BACmid termed pXZ143.

3.2.8.2. BACmid with HA-tagged EBNA2 S457A/T465V

The sequence of the *rpsL/aph* cassette was amplified from p6012 with the following forward: xz201-F, 5'-TATAGACCCCGCAGACTTAGACGAAAGTTGGGATTACATTTTTGAGACAGGGCCTGGTGATGATGGCGGGATCG-3' and reverse: xz201-R, 5'-TCTTTTACTGGGTCCCTCCACATAATCTTCATCTGAGCTAGGAGATTCTATCAGAAGAACTCGTCAAGAAGGCG -3' primers. The resulting PCR product was purified from agarose gel, electroporated into an *E. coli* strain SW105 harboring pXZ143 and selected by kanamycin (positive) and streptomycin (replica negative) to yield the BACmid termed pXZ201.

Next, the DNA sequence of EBNA2 S457A/T465V flanked by 300 bp upstream and 300 bp downstream of EBNA2 S457 was amplified by 2 step of PCR reactions. In the first PCR reactions the template pXZ142 with the following forward: xz146-F, 5'-GGAGACCAGAGCCAAACACC-3' and reverse: xz130-R, 5'-GAGCTAGGAGATTCTACTGTCTCAAAAATG-3' primers and the template pXZ135 with the following forward: xz130-F, 5'-CATTTTTGAGACAGTAGAATCTCCTAGCTC-3' and reverse: xz146-R, 5'-TTGGGACTGGGGTAAAAGTGG-3' primers were used, respectively. The resulting PCR products

were purified from agarose gel and used as templates in the second PCR reaction with the following forward: xz146-F, 5'-GGAGACCAGAGCCAAACACC-3' and reverse: xz146-R, 5'-TTGGGACTGGGGTAAAAGTGG-3' primers. The PCR product was purified from agarose gel, electroporated into an *E. coli* strain SW105 harboring pXZ201 and selected by chloramphenicol and streptomycin to yield the BACmid termed pXZ146.

3.2.8.3. BACmid with C-terminal HA-tagged EBNA2 S379A

The sequence of the *rpsL/aph* cassette was amplified from p6012 with the following forward: xz202-F, 5'-CAAGCAACGCAAGCCCGGTGGACCTTGGAGACCAGAGCCAAACACCTCCAGGCCTGGTGATGATGGCGGGATCG-3' and reverse: xz202-R, 5'-TTGTCCCTGATGAAGACCGAGGACTGGACTTAGTTCAGGCATGCTAGGACTCAGAAGAAGTCTGTCAAGAAGGCG-3' primers. The resulting PCR product was purified from agarose gel, electroporated into an *E. coli* strain SW105 harboring pXZ143 and selected by kanamycin (positive) and streptomycin (replica negative) to yield the BACmid termed pXZ202.

Next, the DNA sequence of EBNA2 S379A flanked by 300 bp upstream and 300 bp downstream of EBNA2 S379 was amplified from pXZ179 with the following forward: xz203-F, 5'-TGCCAGACCAATCAATGCACCCTC-3' and reverse: xz203-R, 5'-GGGCGAGGTCTTTTACTGGGTCCCT-3' primers. The resulting PCR products were purified from agarose gel, electroporated into an *E. coli* strain SW105 harboring pXZ202 and selected by chloramphenicol and streptomycin to yield the BACmid termed pXZ203.

3.2.9. Isolation of BACmids

To isolate a small scale (mini-prep) of BACmid DNA from *E. coli* SW105, bacteria were streaked on half of an LB agar plate containing appropriate antibiotics and incubated at 37°C for one day. The lawn of the fresh bacteria was collected with an American toothpick and resuspend in 200µl of Solution I. 200 µl freshly-prepared solution II was added, the reaction was shocked sharply on a hard surface (no vortexing here!) to mix well, and incubated on ice for 5 minutes to lyse the bacteria. Then 200 µl precooled solution III was added, mixed by inverting gently and then vigorously for a few seconds, and incubated for 5 min on ice to neutralize the reaction. The lysate was cleared by centrifugation (16,000 g, 10 min, 4°C) and the supernatant was transferred to a new 1.5 ml Eppendorf tube. Then 350 µl isopropanol was added and mixed well by inverting. The BACmid DNA was pelleted by centrifugation (16,000 g, 10 min, RT), washed once with 500 µl 80% ethanol, and pelleted again by centrifugation (16,000 g, 10 min, RT). Any traces of supernatant were removed by pipetting. The pellet was shortly airdried and then dissolved in 40 µl TE Buffer.

To isolate a large scale (maxi-prep) of BACmid DNA from *E. coli* SW105, bacteria were collected from 4x 400 ml overnight culture (LB containing 300 mM NaCl) ($OD_{595} = 2.5 - 5$), and the

plasmid was isolated using the NucleoBond Xtra BAC kit according to the manufacturer's instructions.

To further purify the supercoiled BACmid DNA, a mass (g) of CsCl was dissolved in a volume (ml) of maxi-prep of BACmid DNA. The mixture was transferred to an ultracentrifuge tube (~12 ml) and the tube was filled by 1.55 g/ml CsCl solution, followed by adding 200 µl 1% ethidium bromide (EtBr), and sealed firmly. The BACmid DNA was separated by ultracentrifugation (35,000rpm, 20°C) for 3 days and DNA bands were visualized under UV light (350 nm). A hole on the top of the tube and a hole which is 0.5 cm under the lower band (where the supercoiled BACmid DNA are) were punctuated using a large gauge veterinary needle (2.1 mm) and the lower band (~1 ml) was transferred to a 15 ml Falcon tube using a syringe (2 ml) and the large gauge veterinary needle. The EtBr was removed for 4 times of extraction using 2 ml CsCl-saturated isopropanol until the red color was gone. The DNA was concentrated by lyophilization until the volume was approx. 700 µl. The DNA was dialyzed in a close membrane (Spectra/por membrane, MWCO: 6 – 8,000) against 2L TE buffer at 4°C overnight. The supercoiled BACmid DNA was transferred to an Eppendorf tube and stored at 4°C.

Solution I	10 mM Tris-HCl (pH 8.0), 1 mM EDTA (pH 8.0), 200 µg/ml RNase A
Solution II	200 mM NaOH, 1% SDS
Solution III	3.1 M Potassium acetate (KAc) (pH 5.5)
1.55 g/ml CsCl solution	240.8 g CsCl dissolved in 259.2 ml ddH ₂ O, filtered (0.22 µm), and checked with a refractometer
TE Buffer	10 mM Tris-HCl (pH 8.0), 1 mM EDTA (pH 8.0)

3.3. DNA related techniques

3.3.1. Isolation of genomic DNA from mammalian cells

To isolate complete genomic DNA from mammalian cells, 5×10^6 cells were collected and the genomic DNA was isolated using a QIAamp DNA Mini Kit according to the manufacturer's instructions.

3.3.2. Polymerase chain reaction (PCR)

To amplify a specific DNA sequence, a Phusion High-Fidelity PCR Kit was applied according to the manufacturer's instructions. To amplify the ploy proline region of the EBNA2 gene, a peqGold Taq Polymerase was applied according to the manufacturer's instructions.

3.3.3. Restriction endonuclease digestion of DNA

To check the integrity of Plasmid or BACmid DNA or to digest DNA for molecular cloning, 0.5 – 1 µg purified DNA or 40 µl mini-prep of a BACmid was subjected to restriction endonuclease digestion according to the manufacturer's instructions of the respective endonuclease.

3.3.4. 5'-phosphorylation of oligonucleotides

To phosphorylate 5' -termini of oligonucleotides, a T4 Polynucleotide Kinase was applied according to the manufacturer's instructions.

3.3.5. Oligo annealing to form linkers

To generate a linker, forward and reverse Oligos were diluted in annealing buffer (20 µM each), incubated at 95°C for 5 min, and slowly cool down to RT.

Annealing buffer 10 mM Tris-base (pH 7.6), 50 mM NaCl, 1 mM EDTA (pH 8)

3.3.6. DNA gel electrophoresis

DNA fragments were mixed with DNA loading buffer, loaded on 0.7 – 2% agarose gels containing 0.01% (v/v) EtBr, electrophoresed in 1× TAE buffer applying voltage by 4 – 8 V/cm, and visualized under UV light. For BACmid digest, The electrophoresis was done in 1× TBE buffer containing 0.01% (v/v) EtBr with circulation.

TAE buffer (50×) 2 M Tris-base, 1 M Acetic acid, 50 mM EDTA (pH 8)

TBE buffer (10×) 1 M Tris-base 1 M Boric acid, 20 mM EDTA (pH 8)

3.3.7. Purification of DNA fragments

To purify DNA from a gel or a reaction, a NucleoSpin Gel and PCR Clean-up Kit was applied according to the manufacturer's instructions.

3.3.8. Determining the concentration of DNA

To determine the concentration of PCR or mini-prep DNA, the measurement was done on an Eppendorf photometer according to the manufacturer's instructions. To determine the concentration of supercoiled BACmid or maxi-prep DNA, a Qubit dsDNA BR Assay Kit was applied and the measurement was done on a Qubit fluorometer according to the manufacturer's instructions.

3.3.9. Sanger sequencing of DNA

For plasmid or PCR DNA, Sanger sequencing was conducted at Eurofins Genomics GmbH, Germany. For BACmid DNA, Sanger sequencing was conducted at Sequiserve GmbH, Germany. The trace files were analyzed using Chromas Lite software.

3.3.10. EBV diagnosis by PCR

200 ng genomic DNA isolated from human primary B cells used as a template to amplify 296 bp of the EBV BamH I W fragment by PCR with the following forward: BamHI W-F, 5'-TCGCGTTGCTAGGCCACCTT-3' and reverse: BamHI W-R, pXZ5'-CTTGGATGGCGGAGTCAGCG-3' primers (Wagner et al., 1992). Genomic DNA isolated from DG75 and Raji cells used as a negative and positive control, respectively, in the PCR. The amplified DNA was analyzed by DNA gel electrophoresis.

3.4. Protein biochemistry related techniques

3.4.1. Recombinant protein expression

3.4.1.1. In *E.coli* Rosetta 2 (DE3)

N-terminal GST-fused EBNA2 mutants, 6x His-tagged EBNA2 mutants or 6x His-tagged PLK1 mutants were expressed in *E.coli* Rosetta 2 (DE3). In brief, A starter culture of *E.coli* Rosetta 2 (DE3) transformed with the corresponding plasmid was inoculated into 400 ml LB medium supplemented with appropriate antibiotics and cultured at 37°C with shaking (200 rpm). Upon the OD₅₉₅ reached 0.5 – 0.7, the bacteria culture was induced with 1 mM isopropyl β- d-1-thiogalactopyranoside (IPTG) at 37°C for 3 – 6 h or at 18°C overnight.

3.4.1.2. In Sf21 insect cells

To express 6x His-tagged full-length EBNA2 or PLK1 in Sf21 insect cells, I established a collaboration with Prof. Michael Sattler, Helmholtz Zentrum München (HMGU). I constructed all the plasmids used for protein expression. Prof. Sattler's postdoc Dr. André Mourão expressed the protein in Sf21 insect cells using a baculovirus expression system.

3.4.2. Recombinant protein purification

3.4.2.1. GST-fused protein purification

For GST-fused protein purification, the bacteria were resuspended in 20 ml fresh ice-cold binding buffer, lysed by sonication (10% intensity, 10 sec on and 1 sec off for 1 min) on ice. The bacterial lysate was cleared by centrifugation (25,000 g, 20 min, 4°C) and then incubated with Glutathione Sepharose 4B beads at 4°C for 1 h with rolling. The beads were pelleted by centrifugation (500 g,

5 min, 4°C), wash several times with washing buffer, and transferred to a new 1.5 ml Eppendorf tube. The beads were eluted by three times incubation (10 min, RT) with elution buffer. The GST-fused proteins in the eluates were pooled together.

Binding buffer	25 mM HEPES (pH 7.6, KOH), 0.1 mM EDTA (pH 8) 12.5 mM MgCl ₂ , 10% Glycerol, 0.1% NP-40, 100 mM KCl, 1 mM PMSF, 1 mM DTT
Washing buffer	25 mM HEPES (pH 7.6, KOH), 10% Glycerol, 1 mM PMSF, 1 mM DTT
Elution buffer	100 mM Tris-HCl (pH 8), 10 mM L-Glutathione reduced, 1 mM DTT

3.4.2.2. 6x His-tagged protein purification

For 6x His-tagged proteins purification, the bacteria or insect cells were resuspended in 10 ml fresh ice-cold binding buffer, lysed by sonication (10% intensity, 10 sec on and 1 sec off for 1 min) on ice. If the lysate was very viscous after sonication then it was incubated with 1.7 U/ml Benzonase nuclease for 15 min on ice to break down nucleic acids. The lysate was cleared by centrifugation (25,000 g, 20 min, 4°C) and then incubated with PerfectPro Ni-NTA Agarose beads at 4°C for 1 h with rolling. The beads were pelleted by centrifugation (500 g, 5 min, 4°C), wash several times with washing buffer, and transferred to a chromatography column. The His-tagged proteins were eluted with elution buffer.

Binding buffer (pH 7.4)	4.3 mM NaH ₂ PO ₄ , 300 mM NaCl, 1.4 mM KH ₂ PO ₄ , 2.7 mM KCl, 1 mM PMSF, 20 mM imidazole
Washing buffer (pH 7.4)	4.3 mM NaH ₂ PO ₄ , 300 mM NaCl, 1.4 mM KH ₂ PO ₄ , 2.7 mM KCl, 1 mM PMSF, 50 – 100 mM imidazole
Elution buffer (pH 7.4)	4.3 mM NaH ₂ PO ₄ , 300 mM NaCl, 1.4 mM KH ₂ PO ₄ , 2.7 mM KCl, 1 mM PMSF, 200 – 500 mM imidazole

3.4.3. Generation of whole mammalian cell extracts

To generate the whole-cell lysates, 1×10^7 cells were harvested by centrifugation (500 g, 5 min), washed once with PBS, resuspended in 520 µl fresh NP-40 lysis buffer, and lysed for 1 h (30min at 4°C with rolling and 30min on ice). The cell extract was cleared by centrifugation (16,000 g, 15 min, 4°C), transferred to a new 1.5 ml Eppendorf tube, and optionally stored at -80°C.

NP-40 lysis buffer	1% NP-40, 150 mM NaCl, 10 mM Tris-HCl (pH 7.4), 1 mM EDTA (pH 8), 3% Glycerol, supplemental with cOmplete protease inhibitor and PhoStop phosphatase inhibitor
---------------------------	--

3.4.4. Bradford assay

The protein concentration was quantified by Bradford assay using a serial dilution (0 – 12 µg) of BSA as reference. In brief, 2 µl protein was diluted in 1 ml Bradford Solution (1x, diluted from 5x) in a cuvette and mixed well by inverting the cuvette. The absorbance of OD₅₉₅ was measured using an Eppendorf photometer. The protein concentration was calculated according to the calibration curve of BSA.

Bradford Solution (5x) 100 mg Coomassie Brilliant Blue G-250, 47% methanol, 42.5% phosphoric acid

3.4.5. Dual-luciferase assay

To evaluate the transactivation activity of EBNA2, a reporter construct, pGa981-6 which consists of a *firefly* luciferase gene and its upstream of the hexamerized 50 bp of the EBNA2 responsive element of the TP-1 promoter (reviewed in Minoguchi et al., 1997), and an internal control construct, pPGK consecutively expressing *renilla* luciferase, were used, along with a Dual-Luciferase Reporter Assay System applied according to the manufacturer's instruction. In brief, 5×10^6 DG75 cells were electroporated with 5 µg pGa981-6, 0.2 µg pPGK, and 1.5 µg EBNA2 construct using a BioRad GenePulser II device (2 mm gap cuvette, 250 V, 950 µF). 40 ng PLK1 construct was electroporated at the same time if needed. Cells were harvested 24 h post-transfection by centrifugation at 300 g for 10 min at 4°C, washed once with ice-cold PBS, and pelleted by centrifugation (300 g, 10 min, 4°C) again. The cell pellet was resuspended, lysed with 100 µl passive lysis buffer, incubated on ice for 15 min, and frozen at -80°C. The cell extract was cleared by centrifugation (15,300 rpm, 15 min, 4°C) immediately upon thawing. 10 µl cell extract was transferred into a well of a white 96-well-plate. The dual-luciferase activities of the cell extract were measured by a Berthold Orion Microplate Luminometer according to an automatic program: the addition of 50 µl Luciferase assay reagent II (LARII) followed by the first measurement and then the addition of 50 µl Stop&Glo reagent followed by the second measurement.

3.4.6. Co-immunoprecipitation

1×10^7 LCL cells, DG75 cells transfected with 5 µg plasmids for 48 h, or EBNA2 inducible DG75^{Dox} HA-EBNA2 cells induced with doxycycline for 24 h, were harvested by centrifugation (500 g, 5 min). The whole-cell extract was generated as described before (see chapter 3.4.3). 450 µl whole-cell extract was incubated with an EBNA2-, PLK1-, HA-, or GFP-specific or their isotype control antibodies immobilized on Protein G-Sepharose beads at 4°C overnight. The beads were pelleted by centrifugation (2,000 g, 2 min), washed 5 times with 500 µL NP-40 lysis buffer, and boiled at 95°C for 5 min in 60 µl 2x Laemmli buffer. Subsequently, the beads were pelleted by centrifugation (8,000 g, 2 min). The immunoprecipitate in the supernatant was transferred into a 1.5 ml Eppendorf tube

and optionally stored at -80°C. The immunoprecipitate was separated by SDS-PAGE and proteins of interest were visualized by WB using specific antibodies.

3.4.7. GST pull-down assay

GST-fused EBNA2 mutant was expressed in *E.coli* Rosetta 2 (DE3) and immobilized on Glutathione Sepharose 4B beads as described before (see chapter 3.4.2.1). Optionally, the protein immobilized on beads was subjected to kinase assay *in vitro* (see chapter 3.4.8) before the pull-down assay. The beads were incubated at 4°C for 3 h with 500 µl whole-cell extract from DG75 cells (see chapter 3.4.3) or 50 pmol 6× His-tagged PLK1 purified from Sf21 insect cells, KD, or PBD both purified from *E.coli* Rosetta 2 (DE3) (see chapter 3.4.2.2). Subsequently, the beads were pelleted by centrifugation (8,000 g, 2 min). The proteins in the supernatant were transferred in a 1.5 ml Eppendorf tube and optionally stored at -80°C. The proteins were separated by SDS-PAGE and proteins of interest were visualized by WB using specific antibodies.

3.4.8. Kinase assay *in vitro*

The purified protein or protein immobilized on Glutathione Sepharose 4B beads was incubated for 30 min at 37°C with recombinant Cyclin B1/CDK1 (100 ng) or PLK1 (50 ng) at the presence of 1 mM nonradioactive ATP or plus 0.5 µl γ -³²P labeled ATP (10 mCi/ml) in PK buffer in a total reaction volume of 20 µl.

3.4.9. Dephosphorylation of protein

Purified protein was treated with λ Protein Phosphatase (200 U) in NEBuffer Pack for Protein Metallo Phosphatases (PMP) supplemented with 1mM MnCl₂, 30°C for 30min after PLK1 kinase assay.

3.4.10. Sodium dodecyl sulfate-polyacrylamide gel electrophoresis (SDS-PAGE)

Separation gels and stacking gels contained 6 – 15% and 5% polyacrylamide, respectively, and 1% SDS as well. 15 – 30 µg protein was mixed with Lämmli buffer (2 x or 5 x), boiled at 95°C for 5 min, loaded on the gel, and separated by electrophoresis in running buffer for approx. 1 h at 25 mA per gel.

Lämmli buffer (2x)	4% SDS, 20% Glycerol, 5% β -mercaptoethanol, 120 mM Tris-HCl, pH 6.8, 1 spatula tip of bromophenol blue
Lämmli buffer (5x)	10% SDS, 50% Glycerol, 12.5% β -mercaptoethanol, 300 mM Tris-HCl, pH 6.8, 1 spatula tip of bromophenol blue
Running buffer (1x)	25 mM Tris Base, 0.2 M Glycine, 0.1% SDS

3.4.11. Coomassie brilliant blue staining

SDS-PAGE separated proteins were visualized by Coomassie brilliant blue staining. In brief, the gel was incubated in Coomassie staining solution for approx. 1 h with swirling until the entire gel was in dark blue and washed three times in ddH₂O. The gel was incubated in the decoloring solution and the solution was changed occasionally until the band pattern became clear.

Coomassie staining solution 0.1% Coomassie Brilliant Blue G250, 45% ethanol, 10% Acetic acid

Decoloring solution 20% Ethanol, 10% Acetic acid

3.4.12. Gel drying

An SDS-PAGE gel (Coomassie-stained optionally) was equilibrated for 15 min in a gel drying solution. Two cellophane sheets were soaked in dH₂O. The drying sandwich was set up as follows: one gel drying frame, one cellophane sheet, the gel, the other cellophane sheet, and the other gel frame, without any air bubbles. The gel was dried for one day at RT.

Gel drying solution 10% Glycerol, 20% Ethanol

3.4.13. Phosphorimaging

To visualize a dried radioactive (³²P) gel, the β radiation emitted from ³²P nuclei was detected by a Fuji Medical X-Ray Film and visualized by a developer machine. Alternatively, the β radiation was detected by a storage phosphor screen and visualized by a Typhoon FLA 7000 machine.

3.4.14. Western blotting (WB)

SDS-PAGE separated proteins were transferred to PVDF or NC membranes for specific protein detection by antibodies. In brief, a membrane was activated by incubation in 100% methanol for 2 min and washed in ddH₂O for 30 sec (only for PVDF membranes). Subsequently, the membrane was equilibrated, together with Whatman paper, and sponges, in transferring buffer. The blotting sandwich was set up, starting on the cathode side, as follows: One sponge, three layers of Whatman paper, the running gel, PVDF membrane, three layers of Waterman paper, and another sponge. The blotting was conducted at 400 mA for 1 h in transferring buffer with circulation in a cold room. The membrane was incubated in blocking buffer for 30 min with rolling and subsequently incubated with diluted primary antibodies specific for the protein of interest for 1 h at RT or overnight at 4°C. After three times washing steps with PBS/T buffer, the membrane was incubated with the appropriate horseradish peroxidase (HRP)-coupled secondary antibodies, specific for the primary antibodies, diluted in blocking buffer for 1h at RT. The membrane was washed three times with

PBS/T buffer again. Then the secondary antibodies were detected using an Enhanced Chemiluminescence (ECL) system according to the manufacturer's instructions. The emitted light, resulting from the HRP mediated oxidation of luminol, was detected by a Fuji Medical X-Ray Film and visualized by a developer machine. Alternatively, the emitted light was detected and visualized by a Fusion FX spectra machine.

Transferring buffer (1x)	25 mM Tris-base, 192 mM Glycine, 0.1% SDS, 20% Methanol
Blocking buffer	50 mM Tris-HCl, pH 7.5, 150 mM NaCl, 5% (w/v) non-fat milkpowder
PBS/T buffer	PBS plus 0.05% Tween-20

3.5. Protein biophysics related techniques

To decipher the interaction of EBNA2 and PLK1, I established a collaboration with Prof. Michael Sattler (HMGU). I constructed all the plasmids used for protein expression. Prof. Sattler's postdoc Dr. André Mourão expressed and purified the proteins and characterized their interaction using isothermal titration calorimetry (ITC) and nuclear magnetic resonance (NMR) spectroscopy.

3.5.1. Isothermal titration calorimetry (ITC)

Isothermal titration calorimetry (ITC) experiments were performed on an ITC200 instrument in triplicates and analyzed with the Malvern software. For the PLK1 PBD interaction with EBNA2 fragment 342-422aa (PDS1)-derived synthetic heptapeptide (PNTSSPS, wild-type) or phospho-heptapeptide (PNTSpSPS), 100 μ M PBD was provided in the cell and titrated with 1 mM of heptapeptide wild-type or phosphor-heptapeptide with 25 times 1.5 μ l injections at 25°C. ITC experiments for the PLK1 PBD and EBNA2 fragment 423-474aa (PDS2) peptides were performed similarly, using 30 μ M PLK1 PBD and 300 mM EBNA2 PDS2 peptides.

3.5.2. Nuclear magnetic resonance (NMR) spectroscopy

EBNA2 fragment 423-474aa (PDS2) was grown in minimal media supplemented with $^{15}\text{NH}_4\text{Cl}$ and ^{13}C -glucose. Purification was done as reported previously (Mourão et al., 2016). Backbone chemical shift assignments were performed based on HNCA, HNCACB, CBCACONH, HNCO, and CCONH-TOCSY (Sattler et al., 1999) recorded at 600 MHz proton Larmor frequency on a Bruker spectrometer equipped with a cryoprobe using a sample at 250 μ M in aqueous PBS buffer at pH 6.5 supplemented with 5% D_2O . NMR spectra were processed with nmrPipe (Delaglio et al., 1995), and analyzed with CCPNMR (Vranken et al., 2005).

3.6. Animal study

To characterize the recombinant EBV *in vivo*, I collaborated with Prof. Christian Münz, Universität Zürich (UZH) for mouse experiments. I produced, concentrated, and titrated the recombinant EBV. Prof. Münz's postdoc Dr. Anita Murer performed the first mouse experiment in 2019 when I helped in the generation, infection, and sacrifice of the humanized mice. Prof. Münz's Ph.D. student Patrick Schuhmachers performed the rest two mouse experiments. The respective animal protocol ZH008_20 was approved by the veterinary office of the canton of Zurich, Switzerland.

3.6.1. Generation of humanized mice

NOD-*scid* γ_c^{null} (NSG) mice obtained from the Jackson Laboratories were bred and maintained under specific pathogen-free conditions at the Institute of Experimental Immunology, Universität Zürich. CD34⁺ human hematopoietic progenitor cells were isolated from human fetal liver tissue (obtained from Advanced Bioscience Resources) using the CD34 MicroBead Kit (Miltenyi Biotec) following the protocol provided by the manufacturer. Newborn NSG mice (age: 1 to 5 days) were irradiated with 1 Gy by use of an X-ray source. $1 - 3 \times 10^5$ CD34⁺ human hematopoietic progenitor cells were injected intra-hepatically 5 to 7 hours after irradiation. Reconstitution of mice with human immune system components was investigated 10 – 12 weeks after engraftment by flow cytometry for the cell surface expression of huCD45, huCD3, huCD19, huCD4, huCD8, huNKp46, and HLA-DR on PBMCs.

3.6.2. Infection of huNSG mice with recombinant EBV

12 – 16 weeks after engraftment, huNSG mice were infected intraperitoneally with 1×10^5 GRUs of EBV EBNA2 WT, EBV EBNA2 S379A, or EBV EBNA2 S457A/T465V. For each experiment, a different cohort of mice reconstituted with CD34⁺ cells derived from one donor was generated. The animals were ascribed to a distinct experimental group ensuring similar ratios of males to females and similar reconstitution levels and immune cell activation in the peripheral blood. 5 weeks after infection mice were sacrificed, if not necessitated earlier differently by the regulations of our experimental animal license as a consequence of general health conditions or weight loss over 20%. For analysis of the experiments, infected mice that did not present viral loads neither in blood nor in spleen were excluded from analysis since we considered them non-infected.

3.6.3. Liquid chromatography-tandem mass spectrometry (LC-MS/MS)

3.6.3.1. Identification of EBNA2 interactome

To identify EBNA2 interactome, my former colleague Dr. Sybille Thumann collaborated with Dr. Stefanie Hauck, Helmholtz Zentrum München (HMGU). Dr. Thumann overexpressed HA-tagged

EBNA2 in DG75 cells and performed immunoprecipitation with an HA-specific antibody. The immunoprecipitates were eluted and analyzed by Dr. Hauck using liquid chromatography-tandem mass spectrometry (LC-MS/MS). For the detailed method, it can be found in Dr. Sybille Thumann's Ph.D. thesis (Thumann, 2016).

3.6.3.2. Identification of the PLK1-dependent phosphorylation sites of EBNA2

To identify the PLK1-dependent phosphorylation sites of EBNA2, I established a collaboration with Prof. Bernhard Küster, Technische Universität München (TUM). I purified 6× His-tagged EBNA2 and GST-fused EBNA2 453-474aa from *E.coli*, performed PLK1 kinase assay (nonradioactive), and separated the proteins using SDS-PAGE. The protein of interest was extracted from the gel and analyzed by Dr. Piero Giansanti from Prof. Küster's lab using liquid chromatography-tandem mass spectrometry (LC-MS/MS).

6× His-tagged EBNA2 and GST-fused EBNA2 453-474aa were subjected to PLK1 kinase assays. 50 µg 6× His-tagged EBNA2 or 130 µg GST-fused EBNA2 protein were incubated in 1× PK buffer, 1.25 mM ATP in presence or absence of 250 ng active PLK1 at 37°C for 1h. All reactions were carried out in a total volume of 20 µL and then were quenched with 5 µl 5× Lämmli sample buffer.

Proteins were separated by SDS-PAGE and stained with Coomassie Brilliant Blue. Bands corresponding to EBNA2 full length (86 kDa) or GST-EBNA2 C-terminal fragment (28 kDa) were sliced out from the gel lanes, and proteins were then reduced, alkylated, and digested with either Trypsin or GluC (Roche), as previously described (Shevchenko et al., 1996).

Dried peptides were reconstituted in 0.1% FA/2% ACN and subjected to MS analysis using a Dionex Ultimate 3000 UHPLC+ system coupled to a Fusion Lumos Tribrid mass spectrometer (Thermo Fisher). Peptides were delivered to a trap column (75 µm × 2 cm, packed in-house with 5 µm Reprosil C18 resin; Dr. Maisch) and washed using 0.1% FA at a flow rate of 5 µL/min for 10 min. Subsequently, peptides were transferred to an analytical column (75 µm × 45 cm, packed in-house with 3 µm Reprosil C18 resin, Dr. Maisch) applying a flow rate of 0.3 µl/min. Peptides were chromatographically separated using a 50 min linear gradient from 4% to 32% solvent B (0.1% FA, 5% DMSO in ACN) in solvent A (0.1% FA in 5% DMSO). The mass spectrometer was operated in data-dependent mode, automatically switching between MS and MS/MS. Full-scan MS spectra (from 360 to 1500 *m/z*) were acquired in the Orbitrap with a resolution of 60,000 at 200 *m/z*, using an automatic gain control (AGC) target value of 5e5 charges and maximum injection time (maxIT) of 10 ms. The 10 most intense ions within the survey scan were selected for HCD fragmentation with normalized collision energy set to 28%.

The isolation window was set to 1.7 Th, and MS/MS spectra were acquired in the Orbitrap with a resolution of 15,000 at 200 *m/z*, using an AGC target value of 2e5, and a maxIT of 75 ms. Dynamic exclusion was set to 20 s.

Peptide and protein identification was performed using MaxQuant (version 1.5.3.30) with its built-in search engine Andromeda (Shevchenko et al., 1996). Spectra were searched against a SwissProt database, either the *Spodoptera frugiperda* (OX 7108 - 26,502 sequences) or *Escherichia coli* (UP000002032 – 4,156 sequences), supplemented with the EBNA2 protein sequence. Enzyme specificity was set to Trypsin/P or GluC accordingly, and the search included cysteine carbamidomethylation as a fixed modification, protein N-term acetylation, oxidation of methionine, and phosphorylation of serine, threonine, tyrosine residue (STY) as variable modifications. Up to two and three missed cleavage sites were allowed for trypsin and GluC, respectively. The precursor tolerance was set to 4.5 ppm (after MS1 feature re-calibration), and fragment ion tolerance to 20 ppm. The match between runs feature was enabled. Peptides identification were further filtered for a minimum Andromeda score of 20 or 40, for unmodified and modified (phosphorylated) sequences, respectively. A site localization probability of at least 0.75 was used as the threshold for confident localization.

3.6.4. The whole blood and spleen preparations for immunophenotyping

The whole blood of mice was collected from the tail vein and prepared for immunophenotyping by lysing erythrocytes with NH₄Cl. Spleens of mice were mashed, subsequently filtered with a 70 µm cell strainer, and afterward, mononuclear cells were separated using Ficoll-Paque gradients. Total cell counts were determined from purified mononuclear cell suspensions using a DxH500 Hematology Analyzer (Beckman Coulter). Purified cell suspensions were stained for 30 – 40 minutes at 4°C in the dark with a master mix of the respective antibodies followed by a washing step in PBS. The stained cells were analyzed in an LSR Fortessa cytometer (BD Biosciences). Flow cytometry data were analyzed using the FlowJo software.

3.6.5. Viral loads detection in blood and spleen in infected humanized mice

Viral loads in the blood and spleen of mice were determined by TaqMan real-time PCR (Applied Biosystems) of EBV BamH I W fragments. For this purpose, DNA was isolated from whole blood using a NucliSENS EasyMAG System (bioMérieux) and from the spleen with a DNeasy Blood and Tissue kit (Qiagen) following the manufacturers' instructions. TaqMan real-time PCR assays were performed as described previously (Caduff et al., 2020).

3.7. Statistical analyses

The statistical analyses in this thesis were performed using the GraphPad Prism 8 software.

4. Results

The results of this thesis are structured into five main parts. In the first part (chapter 4.1), the interaction of EBNA2 and PLK is described, and the identification of the residues of EBNA2 mediated to PLK1 binding and the characterization of their biological function are shown. In the second part (chapter 4.2), The identification of PLK1-dependent phosphorylation sites of EBNA2 and the characterization of their biological function are depicted. In the third part (chapter 4.3), the construction of EBV BACmid encoding HA-tagged EBNA2 WT, S379A (PLK1 docking mutant), or S457A/T465V (PLK1 phosphorylation mutant) and the production of recombinant EBVs are explained. In the fourth (chapter 4.4) and fifth part (chapter 4.5), the characterization of recombinant EBVs *in vitro* and *in vivo* are shown, respectively.

4.1. Characterization of the interaction of EBNA2 and PLK1

4.1.1. EBNA2 and PLK1 interact with each other in EBV-transformed B cells.

To identify potential EBNA2 interacting cellular proteins, Dr. Sybille Thumann (AG Kempkes) transfected EBV negative DG75 B cells with HA-tagged EBNA2 expression constructs or the corresponding empty vector and performed immunoprecipitations with HA-specific antibodies. In collaboration with Dr. Stefanie Hauck (HMGU), tryptic peptides of these immunoprecipitates were analyzed and quantified by label-free based mass spectrometry. Polo-like kinase 1 (PLK1) was one of 19 candidate proteins that were significantly enriched in EBNA2 co-immunoprecipitates. As expected, the EBNA2 DNA anchor protein CBF1 was one of these proteins, reassuring that the experimental approach was valid (Thumann, 2016).

To further verify the interaction of EBNA2 and PLK1, immunoprecipitation experiments were performed for the whole-cell extracts of EBV-transformed B cells in which both proteins are expressed at endogenous physiological levels. PLK1 was specifically co-immunoprecipitated with EBNA2 and vice versa (Figure 7). In summary, EBNA2 and PLK1 interact with each other in EBV-transformed B cells.

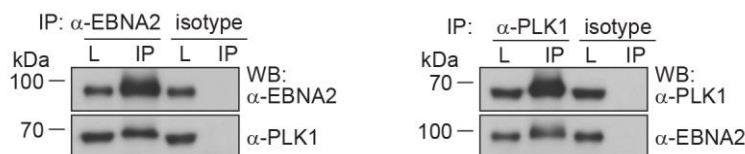


Figure 7. Endogenous EBNA2 and PLK1 interact with each other in EBV-transformed B cells.

Total cell lysates (L) of EBV-immortalized B cells were subjected to reciprocal immunoprecipitations (IP) using EBNA2- (left) (α -EBNA2), PLK1- (right) (α -PLK1) specific, and their isotype-matched control antibodies, visualized by western blotting (WB) using EBNA2- and PLK1- specific antibodies, respectively.

4.1.2. PLK1 binds to two regions of EBNA2

To identify PLK1 docking sites within EBNA2, serial deletion mutants of HA- or GFP-tagged EBNA2 fragments were generated using overlap PCR-based mutagenesis (Figure S1) and tested for their binding to PLK1 by transfection and co-immunoprecipitation in DG75 cells or by GST-pulldown assays using GST-fused EBNA2 fragments. The carboxyl terminus of EBNA2 (342-474aa) was required and sufficient for the EBNA2/PLK1 complex formation (Figure 8A and B). Further deletions retained binding activities, but the binding was much weaker, indicating that two regions, PLK1 docking sites 1 and 2 (PDS1 and PDS2), cooperate in PLK1 binding (Figure 8C). Next, GST-fused EBNA2 fragments produced in *E. coli* were used as baits to pull down PLK1 from DG75 B cell extracts. Surprisingly, fragment 342-422 (PDS1) bound PLK1 with very low efficiency although it was produced well, indicating PDS1 needs a cellular process, e.g. phosphorylation, to activate its binding to PLK1. In contrast, the production of fragment 423-487 was not very efficient but the pulldown of PLK1 was strong (Figure 8D). An even smaller PDS2 fragment (446-474) retained weak but detectable binding capacities (Figure S2). To test if EBNA2 and PLK1 physically interact *in vitro*, purified recombinant PLK1 derived from baculovirus-infected insect cells was mixed with purified GST-EBNA2 fragments immobilized on glutathione beads. GST-fragment 423-474 (PDS2) efficiently bound to PLK1 while the purified 342-422 (PDS1) fragment did not (Figure 8E). In summary, two PLK1 docking sites were identified in EBNA2, PDS1 (342-422) and PDS2 (423-474) which cooperate to build a stable EBNA2/PLK1 complex.

4. Results

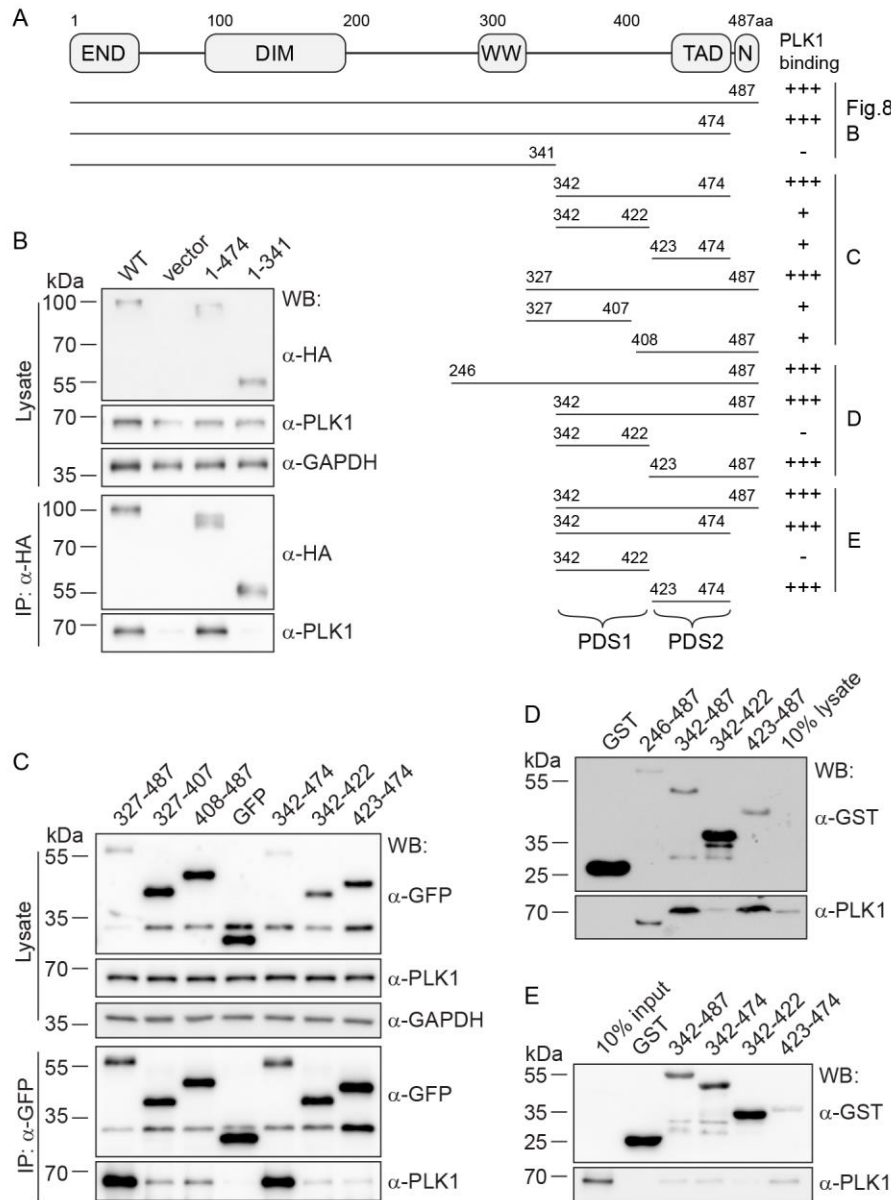


Figure 8. Two C-terminal regions of EBNA2 serve as PLK1 docking sites (PDS1 and PDS2) to confer EBNA2/PLK1 interaction.

(A) Schematic overview of the EBNA2 fragments used to map the PLK1 docking sites (PDS1 and PDS2). The panel on the right summarizes the results shown below. (B) Total cell lysates of DG75 cells exogenously expressing HA-tagged EBNA2 fragments 1-474 and 1-341 were subject to immunoprecipitations (IP) using an HA- (α -HA) specific antibody, visualized by western blotting (WB) using HA-, PLK1- (α -PLK), and GAPDH- (α -GAPDH) specific antibodies, respectively. (C) Total cell lysates of DG75 cells exogenously expressing GFP-fused EBNA2 fragments 327-487, 327-407, 408-487, 342-487, 342-422, and 423-487 were subject to immunoprecipitations using a GFP- (α -GFP) specific antibody, visualized by western blotting using GFP-, PLK1- (α -PLK1), and GAPDH- (α -GAPDH) specific antibodies, respectively. (D) Total cell lysates of DG75 cells were subjected to GST-pulldown using GST-fused EBNA2 C-terminal fragments 246-487, 342-487, 342-422, and 423-487, visualized by western blotting using GST- (α -GST) and PLK1- (α -PLK1) specific antibodies, respectively. (E) Purified recombinant PLK1s were subjected to GST-pulldown using GST-fused EBNA2 C-terminal fragments 342-487, 342-474, 342-422, and 423-474, visualized by western blotting using GST- (α -GST) and PLK1- (α -PLK1) specific antibodies, respectively.

4.1.3. Phosphorylated S379 in EBNA2 PDS1 serves as a canonical PLK1 docking site primed by CDK1.

It is well established that PLK1 PBD frequently docks onto substrates that have been primed for PLK1 binding by CDK1 phosphorylation. These substrates share a consensus motif of [Pro/Phe]-[Φ/Pro]-[Φ]-[Thr/Gln/His/Met]-Ser-[pThr/pSer]-[Pro/X] (Φ represents hydrophobic and X represents any residue) (Elia et al., 2003a). Crystal structures of the PLK1 PBD in complex with peptides show that the positively charged groove of PBD docks in a similar fashion to the negatively charged phosphopeptides (Figure S3A). EBNA2 exhibits three potential CDK1 phosphorylation sites located at residue T267, S379, and S470 (Figure S3A). Interestingly, S379 and S479 are localized in EBNA2 PDS1 and PDS2, respectively. Mutagenesis of S379 located within PDS1 impaired PLK1 binding dramatically while all other EBNA2 mutants were not affected (Figure S3B).

Since PDS1 produced in bacteria had not been able to bind to PLK1 (Figure 8D), GST-fused PDS1 purified from bacterial extracts was speculated lacking this specific phosphorylation of S379. In CDK1 kinase assays, PDS1 WT exhibited ~2-fold stronger phosphorylation by Cyclin B1/CDK1 compared to the S379A mutant (Figure 9A). PLK1 binding of PDS1 was strongly enhanced by CDK1 phosphorylation, while the PDS1 S379A mutant binding was not improved (Figure 9B). To quantify the contribution of PDS1 S379 phosphorylation, PDS1-derived synthetic heptapeptide (PNTSSPS) and phospho-heptapeptide (PNTSpSPS) were tested for PLK1 PBD (aa 345-603) binding by Dr. André Mourão (AG Sattler) using isothermal titration calorimetry (ITC). PNTSpSPS bound to PLK1 PBD in a molar ratio of 1:1 while no interaction was detected between PNTSSPS and PLK1 PBD. The dissociation constant (K_D) for the PNTSpSPS/PLK1 PBD interaction was 8.19 μ M, while the binding of the unphosphorylated peptide was below the threshold and not determined (Figure 9C). In summary, S379 within PDS1 is a PLK1 docking site primed by Cyclin B1/CDK1 phosphorylation.

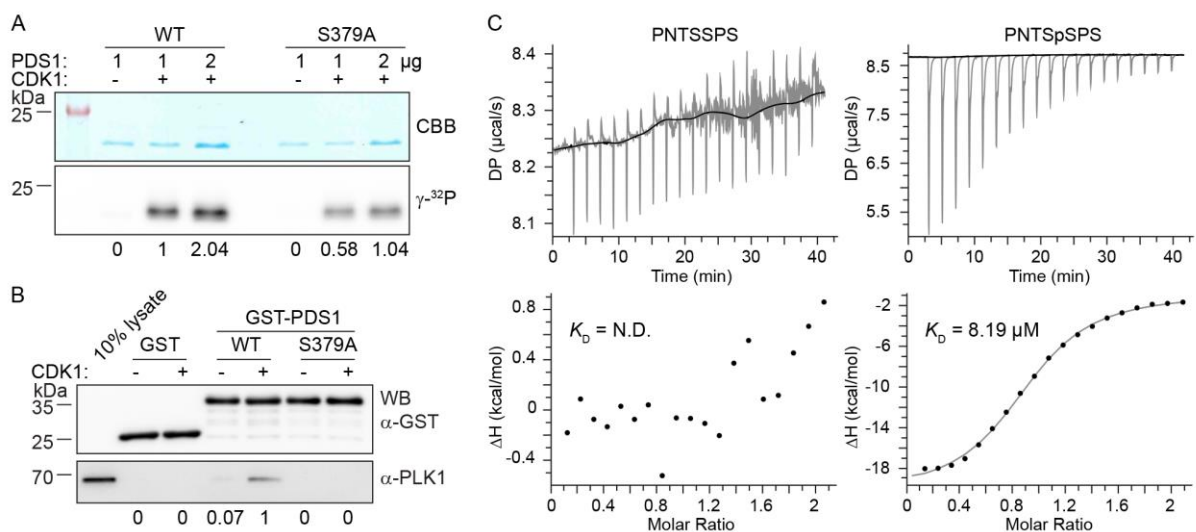


Figure 9. The phosphorylation of S379 by CDK1 activates PDS1 binding to PLK1.

(A) The indicated amounts of PDS1 WT and S379A were kinase assay *in vitro* in the presence of γ -³²P labeled ATP as a phosphate donor before (-) and after (+) recombinant Cyclin B1/CDK1 treatment, visualized by Coomassie Brilliant Blue staining (CBB) and autoradiography, respectively. Normalized phosphorylation intensities are listed below. (B) Total cell lysates of DG75 cells were GST-pulldown using GST-fused PDS1 WT and S379A before (-) and after (+) recombinant Cyclin B1/CDK1 treatment, visualized by western blotting using GST- (α -GST) and PLK1- (α -PLK1) specific antibodies, respectively. Normalized PLK1 binding efficiencies are listed below. (C) ITC thermograms of PLK1-PBD titrated with the peptide PNTSSPS and the phosphopeptide PNTSpSPS of EBNA2, respectively. K_D , dissociation constant. N.D., not determined. Figure 9C was provided by Dr. André Mourão (AG Sattler, HMGU).

4.1.4. PDS2 binding to PLK1 PBD does not require priming by cellular kinases

The PBD of PLK1 preferentially binds to phosphorylated substrates in the majority of reported studies. However, bacterially purified PDS2 bound to PBD directly without any phosphorylation by PLK1 or other kinases (Figure 8C – E). To investigate residues important for this interaction, NMR experiments titrating PLK1 PBD to ¹⁵N-labeled PDS2 were performed by Dr. André Mourão (AG Sattler). NMR spectral changes were observed upon PLK1 PBD addition (Figure 10A). Significant chemical shift perturbations and line broadening (seen by signal intensity reduction) were observed for several residues in PDS2. The backbone chemical shifts of PBD2 were assigned to identify the residues that are affected by PLK1 PBD binding (Figure 10A). Considering that the final molecular weight of the complex is 42 kDa, strong signal intensity reduction is expected for residues involved in the binding interface with PLK1 PBD (Figure 10B and C). Based on this analysis, triple block mutants for three clusters in PDS2 were designed and tested for their binding to PLK1, KD, or PBD in GST-pulldown experiments. Mutagenesis of the individual cluster A or C severely impaired PBD binding while mutagenesis of cluster B did not affect the interaction (Figure S4A). When mutagenesis of clusters A and C were combined (PDS2 mt), PBD binding was abolished (Figure 10D). ITC was performed to confirm these results. The K_D of PDS2 WT, cluster A mt, cluster C mt, or PDS2 mt with PBD is 1.5 μ M, 60 μ M, 35 μ M or not determined, respectively (Figure 10D), indicating that PDS2 might provide an extended surface to contact PBD. In line with these findings, in immunoprecipitation experiments, EBNA2 PDS2 mt (cluster A/C mt) were severely impaired for PLK1 binding, and the combined S379A/PDS2 mt dramatically reduced PLK1 binding (Figure S4B). In summary, the binding of PDS2 to PLK1 PBD is mediated by clusters A and C, but not required priming by cellular kinases.

4. Results

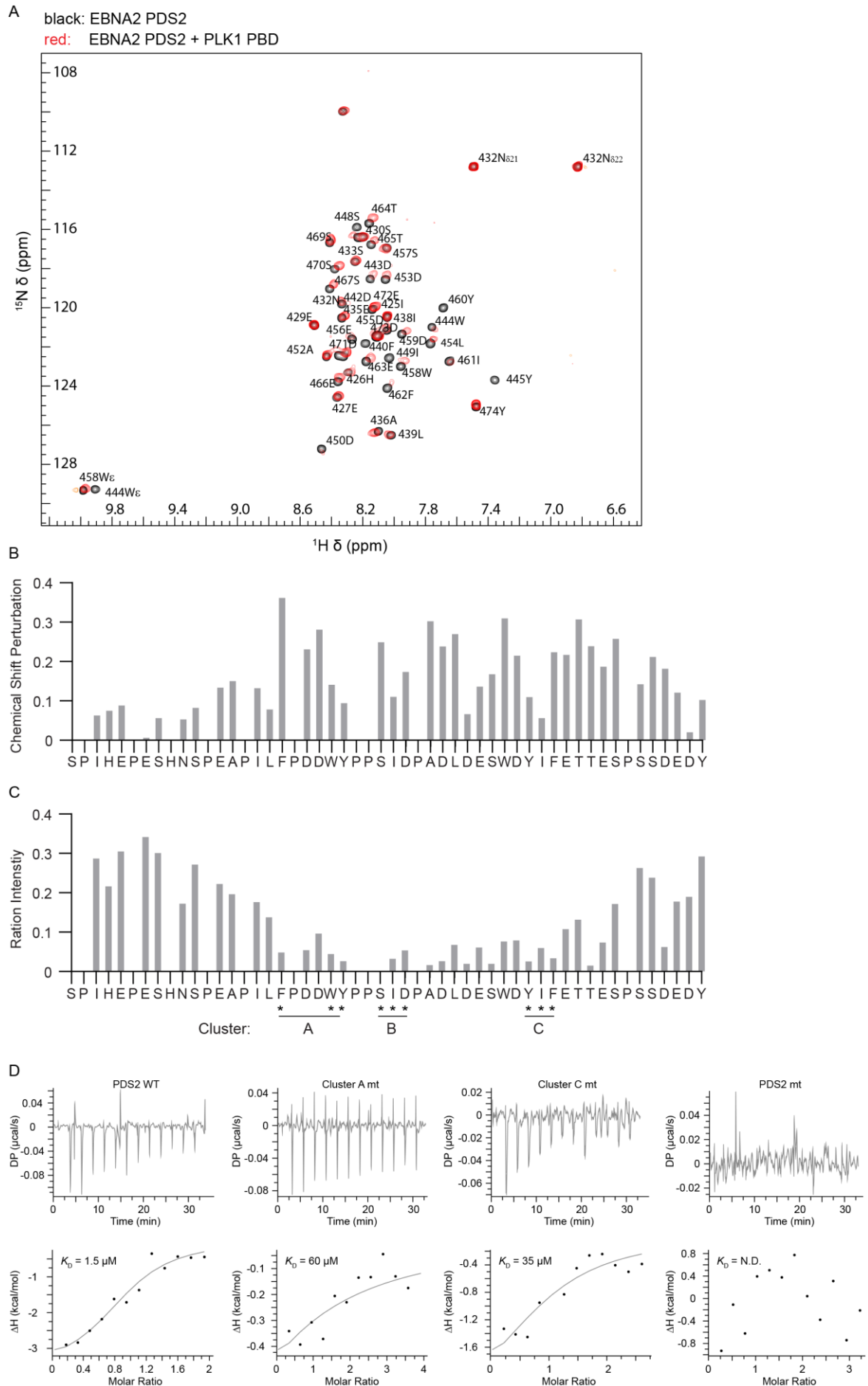
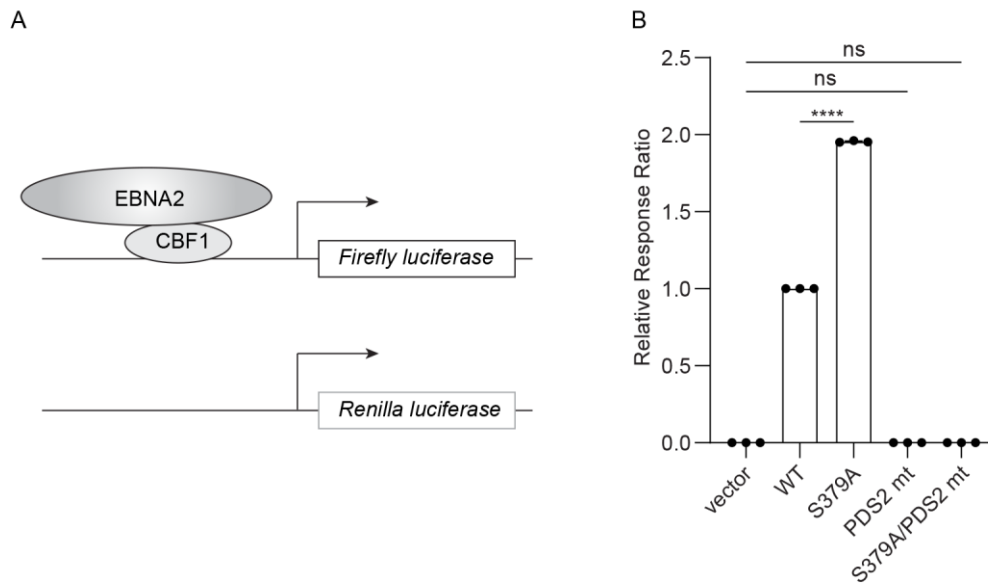


Figure 10. The PDS2/PLK1 PBD binding is mediated by clusters A and C.

(A) NMR spectra of ^{15}N -labeled EBNA2 PDS2 before (black) and after (red) addition of unlabeled PLK1-PBD at 1:1 ratio. (B, C) Bar charts showing (B) chemical shift perturbation and (C) signal intensity ratio of amide signals in the free and PBD-bound state of PDS2. Asterisks (*) indicate residues that were mutated to alanines in triple mutants. (D) ITC thermograms of PLK1-PBD titrated with PDS2 WT, cluster A mt (F440A/WY444AA), cluster C mt (YIF460AAA), and PDS2 mt (cluster A/C mt, F440A/WY444AA/YIF460AAA), respectively. Figure 10 was provided by Dr. André Mourão (AG Sattler, HMGU).

4.1.5. Impact of PLK1 docking sites on EBNA2 transactivation activities

To investigate the biological function of the EBNA2/PLK1 interaction, dual-luciferase assays were performed. In the assay, EBNA2 transactivation activity is reflected by the enzymatic activity of firefly luciferase whose expression is driven by EBNA2. EBNA2 S379A, PDS2 mt, or S379A/PDS2 mt were co-transfected with a firefly luciferase reporter plasmid driven by an EBNA2/CBF1 responsive promoter and a constantly active renilla luciferase plasmid into DG75 cells (Figure 11A). EBNA2 with PDS2 mt had lost all transactivation capacity. Since substitutions in PDS2 mt were located in the TAD of EBNA2, EBNA2 with PDS2 mt were assumed to not only impair PLK1 binding but also directly inactivate the TAD. Surprisingly, the transcriptional activity of the EBNA2 S379A was enhanced, indicating that PLK1 binding to the docking site S379 in PDS1 impairs EBNA2 activity (Figure 11B).

**Figure 11. Inhibition of phosphorylation of the docking site S379 promotes EBNA2 transactivation activity.**

(A) Schematic presentation of the dual-luciferase assay to monitor the transactivation of EBNA2. (B) Luciferase activities of cell extracts of DG75 cells exogenously expressing firefly luciferase driven by EBNA2 WT, S379A, PDS2 mt, and S379A/PDS2 mt were measured by dual-luciferase assay and normalized to renilla luciferase, respectively. Data were presented as the mean \pm S.E.M. of $n = 3$ biological replicates. Statistical significance was tested by one-way ANOVA followed by a Tukey's multiple comparison test (ns: not significant, ****: $P < 0.0001$).

4.2. EBNA2: a novel viral substrate of PLK1.

4.2.1. EBNA2 is a novel substrate of PLK1.

To test if EBNA2 is a substrate of PLK1, an EBNA2-inducible cell line, DG75^{Dox HA-EBNA2} was used in immunoprecipitation assays, followed by kinase assays. In the DG75^{Dox HA-EBNA2} cell, an HA-tagged EBNA2 is under the control of a tetracycline response element (TRE) in a pRTR vector (Bornkamm et al., 2005; Jackstadt et al., 2013), and its expression is induced by the presence of doxycycline, a tetracycline analog (Figure 12A) (Glaser et al., 2017). In the immunoprecipitation experiments, EBNA2/PLK1 complexes were co-precipitated from the cellular extracts (Figure 12B). Parallely, the immunoprecipitates were submitted to kinase assays in the presence or absence of either exogenous recombinant PLK1 or volasertib, a PLK1-specific inhibitor. Phosphorylation of EBNA2 was readily detected, and enhanced or inhibited by the addition of exogenous recombinant PLK1 or volasertib, respectively, suggesting that the endogenous PLK1 trapped in the precipitate is the active kinase (Figure 12C).

To further specify the finding, an N-terminal 6x His-tagged EBNA2 was expressed and purified in *E.coli* and incubated with recombinant PLK1 or lambda protein phosphatase (λ PPase) *in vitro*. In line with the previous result, EBNA2 was phosphorylated by PLK1. Interestingly, PLK1-dependent phosphorylation of EBNA2 could be removed by λ PPase (Figure 12D). In summary, EBNA2 is a novel substrate of PLK1.

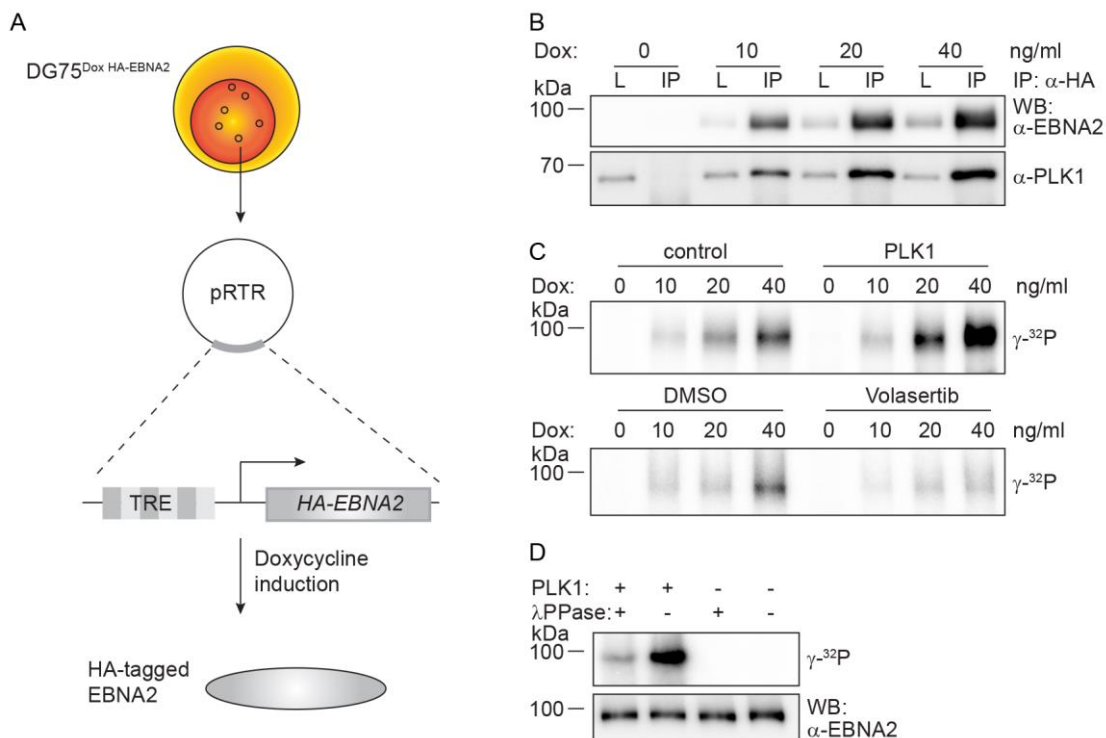


Figure 12. PLK1 phosphorylates EBNA2.

(A) Schematic presentation of an EBNA2-inducible cell line, DG75^{Dox HA-EBNA2}. DG75 cells were stably transfected with a pRTR vector encoding an N-terminal HA-tagged EBNA2 (HA-EBNA2) under control of a tetracycline response

element (TRE). EBNA2 expression was induced by the presence of doxycycline (Dox). (B) Total cell extracts of DG75^{Dox} HA-EBNA2 cells treated with the indicated concentrations of Dox were immunoprecipitation using an HA- (α -HA) specific antibody, visualized by western blotting using EBNA2- (α -EBNA2) and PLK1- (α -PLK1) specific antibodies, respectively. (C) Immunoprecipitates described in B were kinase assay at the presence of γ -³²P labeled ATP before (control) and after recombinant PLK1 (upper) and Volasertib (lower) treatments, visualized by autoradiography, respectively. (D) Bacterially purified 6x His-tagged EBNA2 was kinase assay *in vitro* at the presence of γ -³²P labeled ATP before (-) and after (+) treatment combination of recombinant PLK1 and λ PPase, visualized by autoradiography. Western blotting showing loading control using an EBNA2- (α -EBNA2) specific antibody.

4.2.2. Identification of phosphorylation sites of EBNA2 by PLK1 using LC-MS/MS

To identify the amino acid residues phosphorylated by PLK1, bacterially expressed EBNA2 was treated with recombinant PLK1 or left untreated, separated using SDS-PAGE, and send to Dr. Piero Giansanti (AG Küster, TUM) to perform LC-MS/MS (Figure S5). The protein of interest was extracted from the SDS-PAGE gel, digested by trypsin and endoproteinase Glu-C (V8 Protease) in parallel. Tryptic- or V8 Protease-digested peptides and phospho-peptides were identified by mass spectrometry (Figure S6). Since neither tryptic nor V8 derived peptides covered the C-terminus of EBNA2 sufficiently, a GST-fused EBNA2 subfragment 453-474 flanked by arginine residues and as protein was expressed in *E.coli* and used for further tryptic digest and phosphopeptides mapping (Figure S5). Eleven candidate phosphorylation sites were found. Of these, 5 phosphorylation sites (S184, 258, 457, 479, and T465) were confidently localized (Figure 13A – E) and 6 additional sites (T175, 178, 263, 267, 464, and S266) were ambiguously mapped (Figure S6 and Figure S7).

4. Results

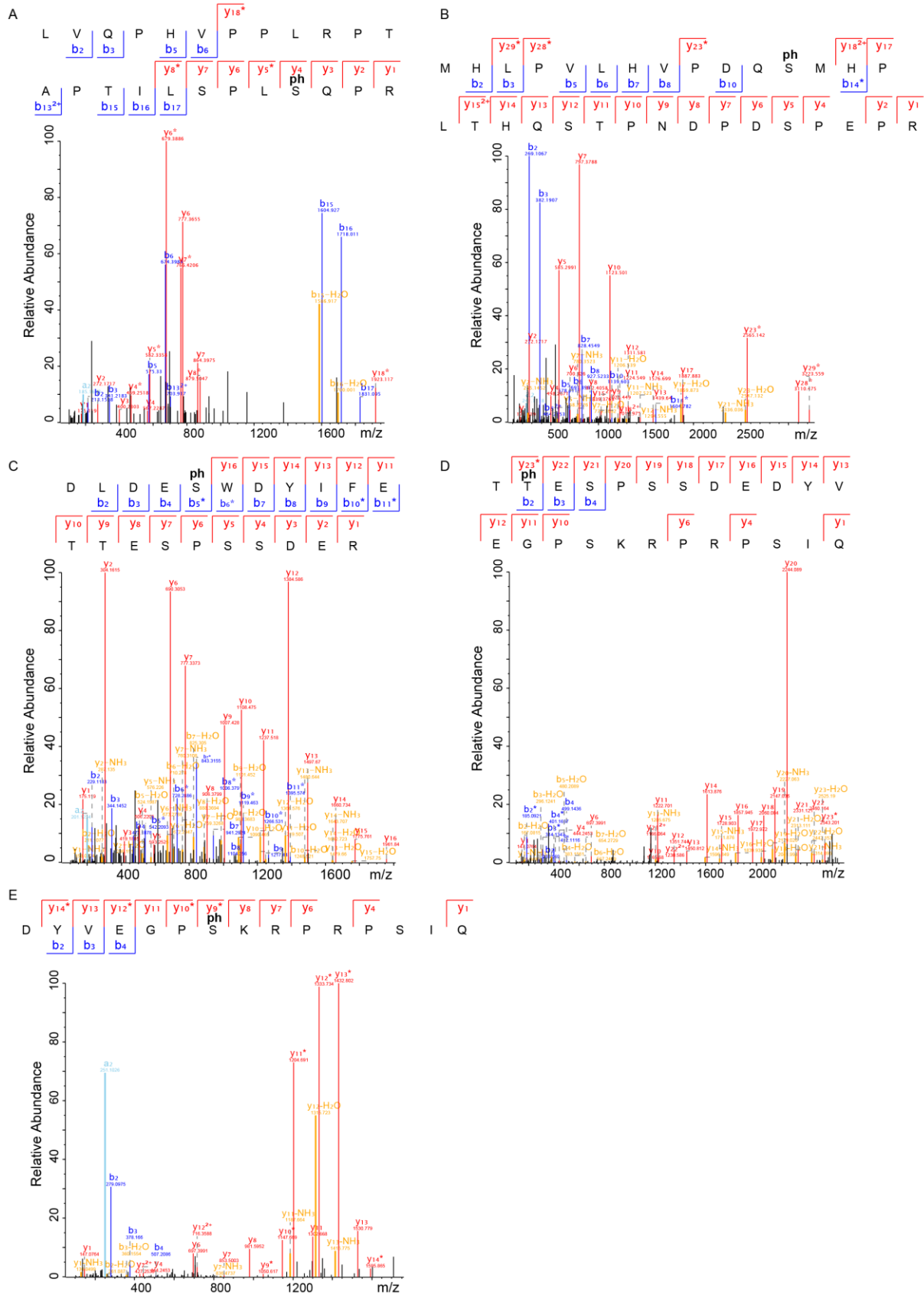


Figure 13. Identification of PLK1-dependent phosphorylation sites of EBNA2.

(A – E) Annotated HCD MS/MS spectra of the phosphopeptides, (A) LVQPHVPLRPTAPTILSPLSQPR, (B) MHLPLVLPDQSMHPLTHQSTPNPDPSPEPR, (C) DLDESWDYIFETTESPSSDER, (D) TTESPSSDEDYVEGPSKRPRPSIQ, and (E) DYVEGPSKRPRPSIQ, bearing 5 confidentially localized

4. Results

phosphorylation sites, S184, 258, 457, T465, and S479, respectively. The “ph” denotes phosphosites localized. The a-, b-, and γ - ions are in pale blue, dark blue, and red, respectively. Ions with neutral losses are in orange, internal fragment ions in purple, ammonium ion in green, and side-chain loss in turquoise. The asterisk (*) denotes loss of H_3O_4P with a delta mass of 97.9768 from the phosphorylated fragment ion. Figure 13 was provided by Dr. Piero Giansanti (AG Küster, TUM).

4.2.3. S457 and T465 are the major phosphorylation sites of EBNA2 by PLK1

To further test, if these 5 phosphorylation sites confidently mapped *in vitro* were also modified by endogenous PLK1 in cells, EBNA2 mutants that inactivated the respective sites as singular or combined mutations were generated and expressed in DG75 cells. Immunoprecipitations and subsequent kinase assays were performed. Phosphorylation of the EBNA2 mutants S457A and T465V was impaired, while the combination of both mutations abolished phosphorylation (Figure 14A and B). Since phosphorylation of the entire EBNA2 protein was blocked by volasertib, we conclude that PLK1 was the major EBNA2 associated kinase that phosphorylates these two residues.

GST-fused EBNA2 fragment 246-487 WT and S457A/T465V were expressed and purified in *E.coli* and further tested for phosphorylation by PLK1 in kinase assays. Consistent with the previous result, S457A/T465V abolished the phosphorylation of EBNA2 fragment 246-487 (Figure 14C), suggesting that S457 and T465 are the major phosphorylation sites of EBNA2 by PLK1.

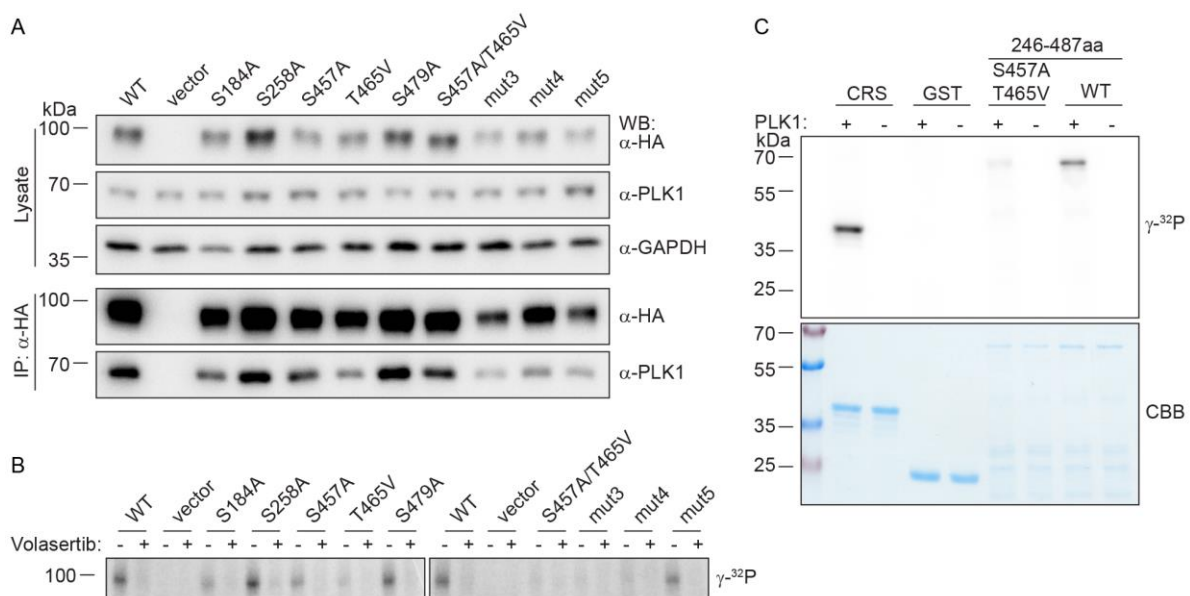


Figure 14. S457 and T465 are the major phosphorylation sites of EBNA2 by PLK1.

(A) Total cell lysates of DG75 cells exogenously expressing HA-tagged EBNA2 single and combination mutant of S184, 258, 457, 479A, or T465V were immunoprecipitation (IP) using an HA- (α -HA) specific antibody, visualized by western blotting using HA-, PLK1- (α -PLK1), and GAPDH- (α -GAPDH) specific antibodies, respectively. mut3: S457/479A/T465V, mut4: S258/457/479A/T465V, and mut5: S184/258/457/479A/T465V. (B) Immunoprecipitates described in A were submitted to kinase assay in the presence of γ - ^{32}P labeled ATP before (-) and after (+) treatment of volasertib, visualized by autoradiography. (C) Bacterially purified GST-fused EBNA2 246-487aa WT and

S457A/T465V were submitted to kinase assay in the presence of γ -³²P labeled ATP before (-) and after (+) recombinant PLK1 treatment, visualized by autoradiography and Coomassie Brilliant Blue staining, respectively. GST-CRS and GST were used as positive and negative controls.

4.2.4. Impact of PLK1-dependent phosphorylation on EBNA2's transactivation

To test the phosphorylation mutants for their biological function, dual-luciferase assays were applied to monitor EBNA2 transactivation activities as described in chapter 3.4.5. All mutants that carried either S457A, T465V, or both mutations showed enhanced transactivation potential (Figure 15A), indicating phosphorylation of EBNA2 by PLK1 suppresses its transactivation. Furthermore, the EBNA2 S457A/T465V (PLK1 phosphorylation mutant), and the EBNA2 S379A (PLK1 docking mutant) were co-expressed with PLK1 WT or the kinase-dead mutant K82M. Kinase active PLK1 significantly inhibited EBNA2 WT activity as well as the docking site mutant (Figure 15B), thus confirming our previous results (Figure 11). The phosphorylation mutant was impaired weakly, suggesting that PLK1 phosphorylation suppresses EBNA2 transactivation. The PLK1 kinase-dead mutant did not impair the transactivation capacity of any EBNA2 protein, indicating that PLK1 binding per se is not sufficient but PLK1 kinase activity is required to inhibit EBNA2 activity (Figure 15B).

Since the C-terminal transactivation domain of EBNA2 is known to bind the histone acetylase and co-activator p300, p300 binding to EBNA2 phosphorylation mutants was tested by GST-pulldown experiments. While p300 binding of the single EBNA2 phosphorylation mutants was strongly enhanced by approximately 2 – 3 fold, binding by the double mutant S457A/T465V was increased even 8.7 fold, compared to WT (Figure 15C). Thus, enhanced p300 binding of EBNA2 phosphorylation mutants correlates well with improved transactivation activity. The finding suggests that PLK1 phosphorylation hinders p300 recruitment to EBNA2, thereby inhibiting EBNA2 transactivation.

In summary, PLK1 phosphorylates S457 and T465 of the TAD of EBNA2 to attenuate its activity. PLK1 uses PDS1 as a phosphorylation-dependent docking site and PDS2 as a phosphorylation-independent one. PDS1 phosphorylation of S379 by CDK1 primes the canonical docking site. PDS2 provides an extended region that involves multiple residues, like F440, WY444, and YIF460 (Figure 15D).

4. Results

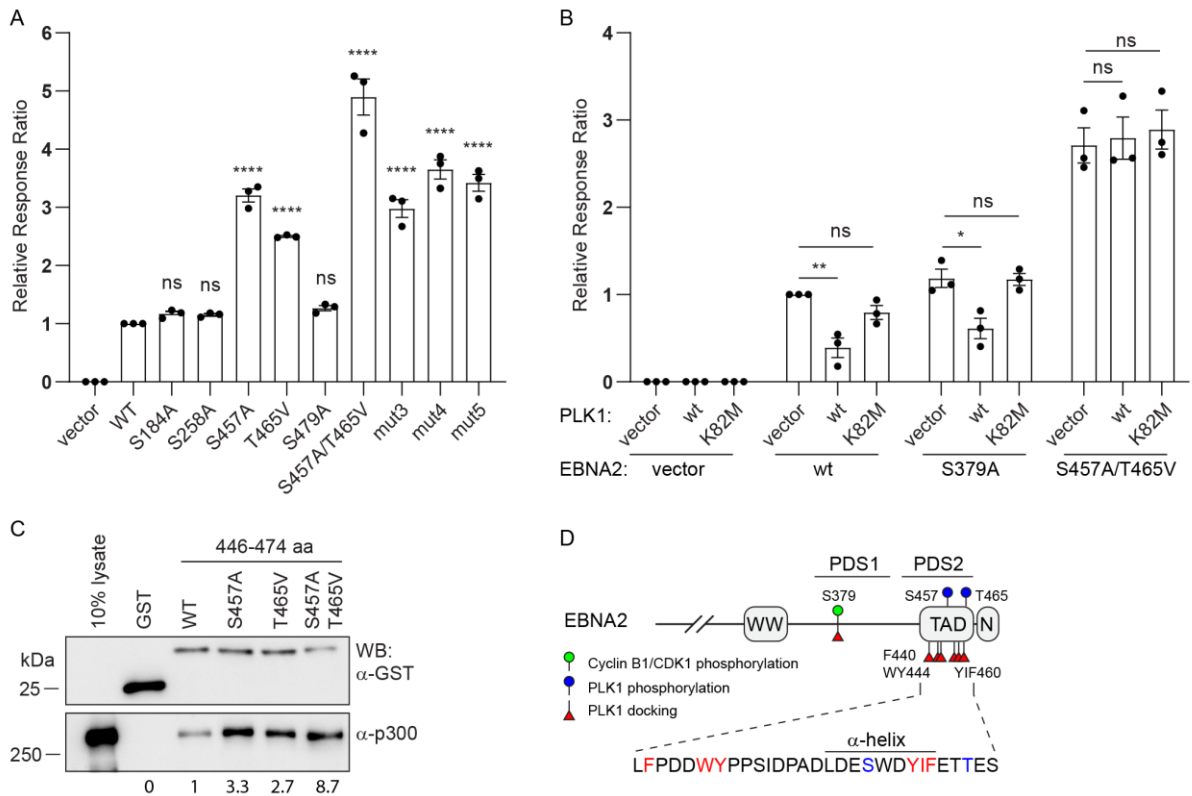


Figure 15. The phosphorylation of EBNA2 by PLK1 suppresses its transactivation.

(A) Luciferase activities of cell extracts of DG75 cells exogenously expressing firefly luciferase driven by EBNA2 single and combination mutant of S184, 258, 457, 479A, and T465V were measured by dual-luciferase assay and normalized to renilla luciferase, respectively. Data were presented as the mean \pm S.E.M. of $n = 3$ biological replicates. Statistical significance was tested by one-way ANOVA followed by a Tukey's multiple comparison test (ns: not significant, ****: $P < 0.0001$, vs WT). mut3: S457/479A/T465V, mut4: S258/457/479A/T465V, and mut5: S184/258/457/479A/T465V. (B) Luciferase activities of cell extracts of DG75 cells exogenously expressing firefly luciferase driven by EBNA2 WT, S379A, and S457A/T465V, along with PLK1 WT and K82M, were measured by dual-luciferase assay and normalized to renilla luciferase, respectively. Data were presented as the mean \pm S.E.M. of $n = 3$ biological replicates. Statistical significance was tested by two-way ANOVA followed by a Tukey's multiple comparison test (ns: not significant, *: $P < 0.05$, **: $P < 0.01$). (C) Total cell lysates of DG75 cells were GST-pulldown using GST-fused EBNA2 C-terminal fragments 446-474 WT, S457A, T465V, and S457A/T465V, visualized by western blotting using GST- (α -GST) and p300- (α -p300) specific antibodies, respectively. Normalized p300 binding efficiencies are listed below. (D) Schematic summary of PLK1 docking and phosphorylation sites at the C-terminus of EBNA2.

4.3. BACmid construction and recombinant EBV production

4.3.1. Construction of HA-tagged EBNA2 WT, S379A, or S457A/T465V in the EBV genomes

In the previous studies, PDS1 and PDS2, the two PLK1 docking regions in the C-terminal fragment of EBNA2 were identified. PDS1 carries the S379 residue, which is a substrate of Cyclin B1/CDK1 and activates EBNA2 for PLK1 binding (Figure 9). The S379A mutant is a strong transactivator and

4. Results

thus was expected to immortalize B cells. Since the PDS2 mutant inactivated the TAD of EBNA2, recombinant virus carrying this mutation was not expected to immortalize B cells (Cohen et al., 1991) and were not tested in the context of the viral genome. In contrast, the PLK1 phosphorylation site mutant S457A/T468V was a potent transactivator, a gain-of-function mutant (Figure 15A and B). Since EBNA2 S457A/T465V is not able to be detected by EBNA2-specific antibodies (1E6 and R3) because of epitope changes (data not shown), a HA tag would be necessary for the analysis of EBNA2 expression in recombinant EBV transformed B cells.

To generate a C-terminal HA-tagged EBNA2 WT, S379A (PLK1 docking mutant), or S457A/T465V (PLK1 phosphorylation mutant) in the EBV genome, respectively, the EBV BACmid, p6008 was used as an original backbone. p6008 comprises of puromycin N-acetyl-transferase (*pac*) gene for selection in eukaryotic cells, enhanced green fluorescent protein (*eGFP*) gene as a reporter, chloramphenicol acetyltransferase (*cat*) gene for selection in bacteria, and the B95.8 EBV genome inserted the 12 kb deletion with the autologous sequences of the M-ABA EBV genome to restore right-handed *OriLyt* and to express all 25 EBV-encoded pre-miRNAs as well as the LF1, LF2, and LF3 genes (Pich et al., 2019).

Recombination-mediated genetic engineering (recombineering) makes it possible to substitute, insert, or delete sequences in bacterial artificial chromosomes (BACs) precisely without leaving any unwanted sequences (Wang et al., 2009; Warming et al., 2005). In this study, *E. coli* strain SW105, a derivative of DH10B carries a mutation in the *E. coli* ribosomal S12 gene (*rpsL*) gene leading to streptomycin resistance. However, the strain will shift to be streptomycin sensitive upon a wild-type *rpsL* gene introduced, which makes it possible to use wild-type *rpsL* as either a negative or a positive selection marker in a two-step procedure (Figure S8). In addition, SW105 is incorporated with a λ -prophage-based Red recombination system in which the expression of λ Red encoded recombinase genes (*exo*, *bet*, and *gam*) is controlled by λ -cI857, a temperature-sensitive repressor. At 32°C the recombination system is inactive because of the active repressor. Upon shifting to 42°C, along with inactivating the repressor, the recombinases are expressed, allowing homologous recombination to occur. A selection marker, e.g. kanamycin resistance aminoglycoside phosphotransferase gene (*aph*) would be necessary to select correct *E. coli* recombinants.

The two-step BAC recombineering is schematically depicted in Figure 16A and described in detail in chapter 3.2.8. In brief, p6012, a prokaryotic plasmid encoding *rpsL* and *aph* genes (*rpsL/aph* cassette) both under the control of the *rpsL* promoter, is used as a template to amplify an *rpsL/aph* cassette flanked by upstream and downstream homology arms of the desired site, respectively (Pich et al., 2019). The *rpsL/aph* cassette is inserted into the desired site by homologous recombination in the first recombineering. Synthetic DNA or PCR product of the mutant allele flanked by longer homology arms replaces the *rpsL/aph* cassette in the second recombineering to yield the BACmid with the desired mutation.

4. Results

To insert an HA tag at the C-terminus of EBNA2, in the first step, both kanamycin-resistant and streptomycin-sensitive clones were ensured with an integrated *rpsL/aph* cassette via restriction endonuclease digestion and agarose gel electrophoresis (Figure 16B). In the second step, both streptomycin-resistant and kanamycin-sensitive clones were ensured with an integrated HA tag via restriction endonuclease digestion and agarose gel electrophoresis again (Figure 16B). The resulting EBV BACmid, pXZ143 was very carefully analyzed with numerous restriction endonucleases (e.g. BamH I, Bgl II, and Xho I), and DNA sequencing to confirm the HA tag and its flanking regions (Figure 16C). Based on pXZ143, EBV BACmids encoding an N-terminal HA-tagged EBNA2 S379A (pXZ203) or S457A/T465V (pXZ146) were constructed with the same protocol (Figure 16D and E). When used for establishing virus producer cells, the supercoiled EBV BACmids were isolated by CsCl density gradient ultracentrifugation as depicted in Figure S9.

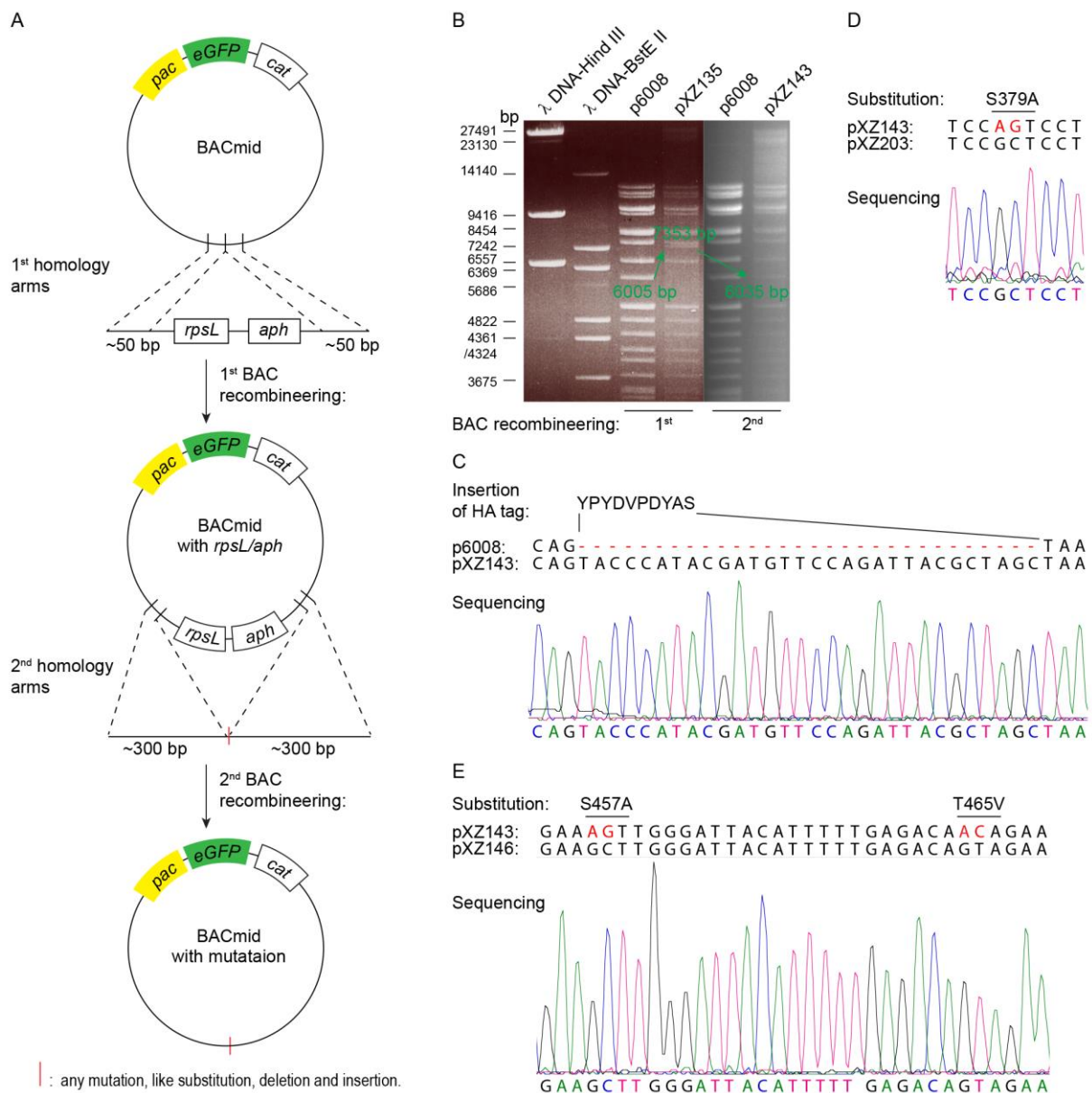


Figure 16. Construction of EBV genomic BACmids encoding C-terminal HA-tagged EBNA2 WT, S379A, or S457A/T465V.

(A) Schematic overview of the two-step BAC recombineering for precise mutation. The original EBV BACmid p6008 comprises the entire EBV genome along with puromycin N-acetyltransferase (*pac*), *eGFP*, and chloramphenicol acetyltransferase (*cat*). In the first BAC recombineering, a prokaryotic expression cassette, *rpsL/aph* flanked by two ~50 bp homology arms of the desired site were inserted into the backbone of p6008 by homologous recombination and positive/negative selection. Subsequently, in the second BAC recombineering, a mutant allele flanked by two ~300 bp homology arms of the desired site replaced the *rpsL/aph* cassette to generate the final BACmid. (B) Electrophoretic separation of BamH I digest for p6008, p6008 inserted with *rpsL/aph* cassette (pXZ135), and BACmid encoding HA-tagged EBNA2 (pXZ143). The arrows highlight specific fragments of interest since they shift in size upon *rpsL/aph* cassette insertion and deletion (6,005 bp → 7,353 bp → 6,035 bp). (C) Sanger sequencing of pXZ143 confirming the insertion of the HA tag into EBNA2 in the backbone of p6008. (D, E) Sanger sequencings of (D) pXZ203 and (E) pXZ146 confirming the substitution of S379A or S457A/T465V within HA-tagged EBNA2 in the backbone of pXZ143, respectively.

4.3.2. Recombinant EBV production and titration

The procedure of recombinant EBV production is schematically depicted in Figure 17 and described in detail in chapter 3.1.4. In this study, HEK293 cells were transfected with supercoiled EBV BACmids encoding a C-terminal HA-tagged EBNA2 WT, S379A, or S457A/T465V, and outgrowth of EBV positive cells was ensured using puromycin selection. Clonal colonies were selected using *eGFP* reporter and expanded individually. Those cell lines would produce infectious virions upon transient expression of EBV viral protein BZLF1 and BALF4. BZLF1, the lytic protein induces the switch from the latent to lytic cycle to produce large amounts of EBV progenies (Countryman and Miller, 1985; Rooney et al., 1989), and BALF4, also known as the viral glycoprotein gp110, enhances viral particle packaging and infection efficiency of B cells (Neuhierl et al., 2002). When used in mouse experiments, recombinant EBV viral particles released in the culture medium were concentrated by ultracentrifugation.

To determine viral titers, Raji cells were infected with recombinant EBV expressing EBNA2 WT, S379A, or S457A/T465V, and *eGFP* expression of the infected cells was analyzed by Flow cytometry (Figure S10A). The green Raji units per ml (GRUs/ml) were defined as recombinant EBV viral titer and calculated as demonstrated in chapter 3.1.5 (Figure S10B).

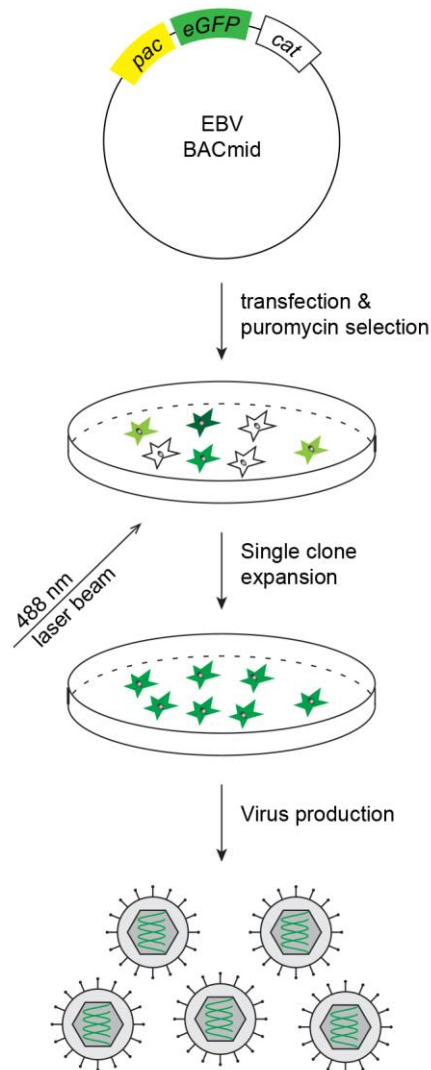


Figure 17. Schematic workflow of recombinant EBV virus production.

(A) Schematic workflow of recombinant EBV virus production. HEK293 cells were transfected with the desired EBV BACmid and selected by puromycin. Single clonal GFP positive cells were picked under a fluorescence (at least a 488 nm laser) microscope and expanded. Then, recombinant EBV viruses were produced from the clonal cells with the induction of BZLF1 and BALF4.

4.4. Characterization of human primary B cells infected with recombinant EBV

It is well studied that infection of B cells with EBV leads to immortalization of B cells. The process of immortalization or transformation of B cells to establish lymphoblastoid cell lines (LCLs) is depicted in Figure 18 (Mrozek-Gorska et al., 2019). In this study, all B cell samples were isolated from anonymous adenoids by Ficoll density gradient centrifugation (Figure S11A) and the leukocyte composition was analyzed by FACS. The B cell fraction was over 82.3% and the T cell fraction was less than 2.16% (Figure S11B). If a fraction of B cells are EBV positive, these cells spontaneously undergo proliferation driven by endogenous viruses. Thus, each B cell sample used in this study was ensured to be EBV negative by PCR (data not shown).

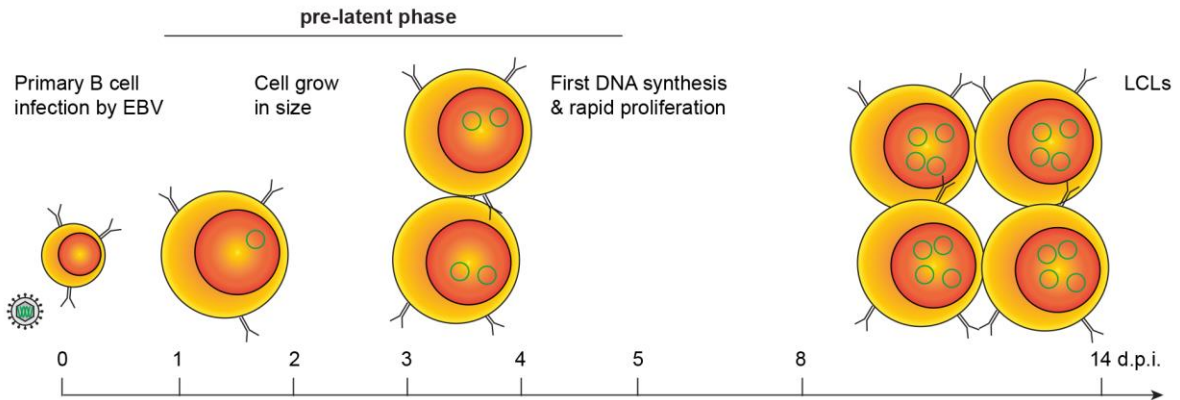


Figure 18. Schematic process of the transformation of primary B cells by EBV.

Human primary B cells infected with EBV grow in size within 2 days. Cells undergo rapid proliferation following the first DNA synthesis in the pre-latent phase. Immortalized lymphoblastoid cell lines (LCLs) are established 14 days post-infection (d.p.i.). Figure 18 is adapted from Mrozek-Gorska et al., 2019.

4.4.1. EBV strains carrying EBNA2 mutants deficient for PLK1 docking or phosphorylation transform primary B cells *in vitro*

To test if the recombinant EBV mutants could still immortalize B cells, human primary B cells were infected with recombinant infectious EBV mutants defective for PLK1 binding (S379A) or PLK1 phosphorylation (S457A/T465V) of EBNA2. EBV EBNA2 S379A or S457A/T465V infected B cells grew in size and formed cell clumps, and became cell lines in 2 weeks (Figure 19). Thus, EBV strains carrying EBNA2 mutants deficient for PLK1 docking or phosphorylation transformed primary B cells efficiently *in vitro*.

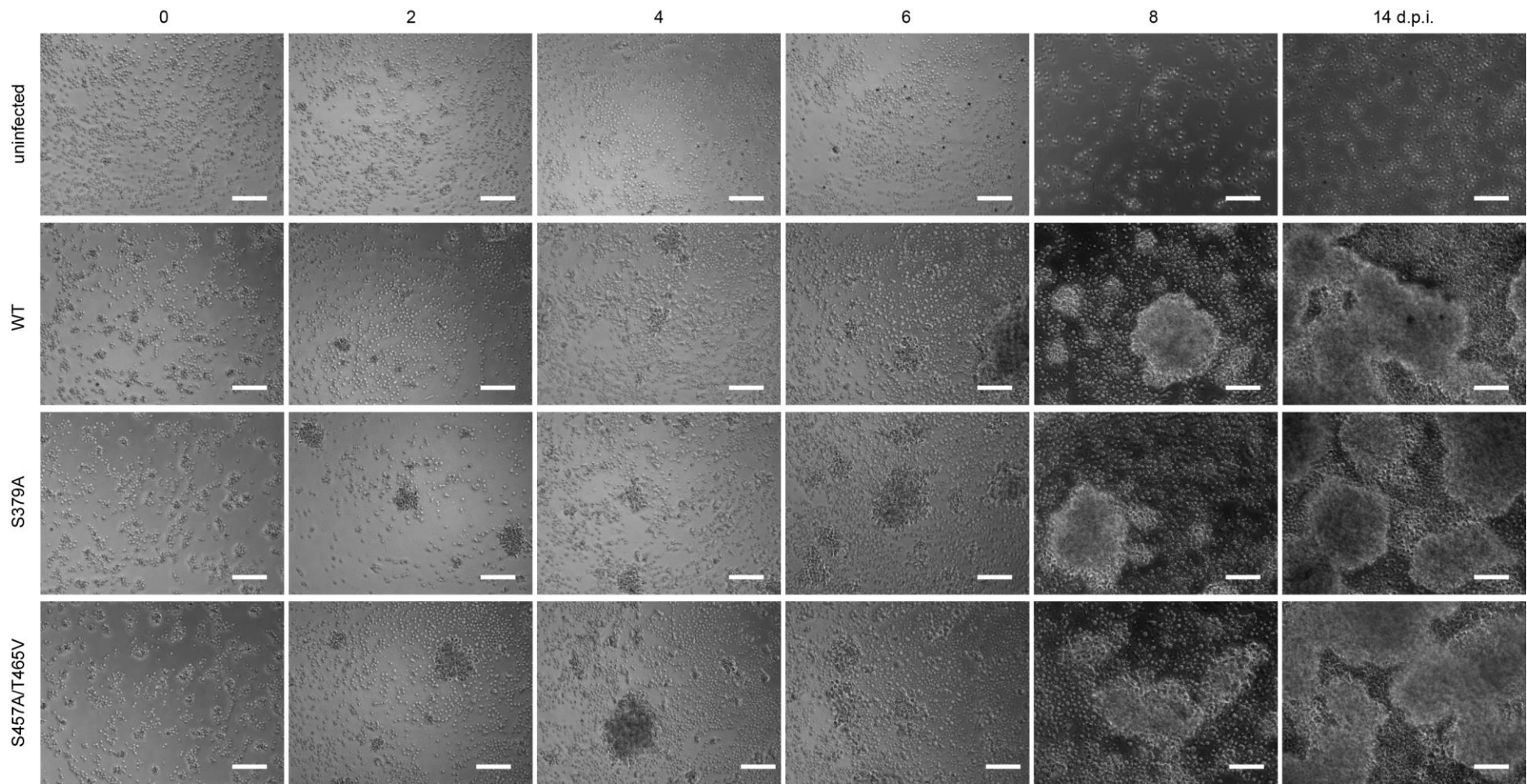


Figure 19. EBV strains carrying EBNA2 mutants deficient for PLK1 docking or phosphorylation transform primary B cells *in vitro*.

Light microscopic photos of primary B cells infected with EBV strains expressing EBNA2 WT, S379A, S457A/T465V, or left uninfected from 0 to 14 days post-infection (d.p.i.). A representative data of n = 3 biological replicates are shown. Scale bar, 100µm.

4.4.2. EBV strains expressing EBNA2 mutants deficient for PLK1 docking or phosphorylation promote B cell proliferation

To further compare the different EBV strains during the first 6 days post-infection, cell trace violet assays were applied to analyze the B cell proliferation. Cells infected with EBV EBNA2 S457A/T465V or S379A proliferated faster than WT infected counterparts (Figure S12 and Figure 20A and B). Since long-term cultures could be established as described in chapter 4.4.1, the proliferation of these LCLs was characterized by counting the cells daily. The phosphorylation mutant S457A/T465V proliferated the fastest, followed by S379A and WT infected cells (Figure 20C). These findings were in line with our previous results that EBNA2 transactivation was suppressed by PLK1 phosphorylation (Figure 11 and Figure 15A and B).

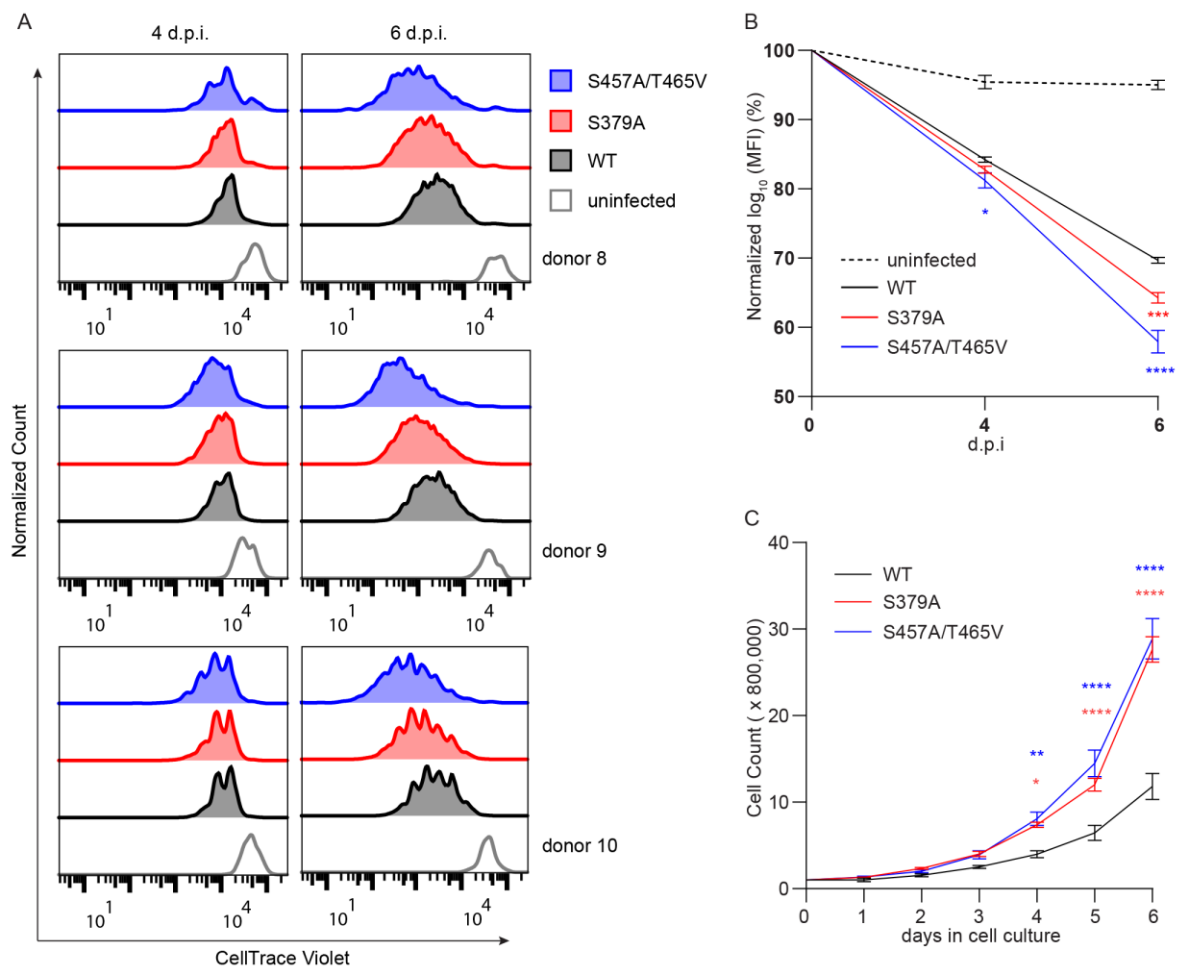


Figure 20. EBV strains expressing EBNA2 mutants deficient for PLK1 docking or phosphorylation promote B cell proliferation.

(A) Histograms showing proliferation profiles of B cells after EBV infection. Primary B cells were stained with cell trace violet, infected with EBV mutants as indicated, and then analyzed by flow cytometry 4 and 6 d.p.i. Data of 3 donors are shown. (B) Line chart showing flow-cytometric analysis of median fluorescence intensities of cell trace violet. Data were presented as the mean \pm S.E.M. of $n = 3$ biological replicates. Statistical significance was tested by two-way ANOVA followed by a Tukey's multiple comparison test (*: $P < 0.05$, ***: $P < 0.001$, ****: $P < 0.0001$, vs WT). (C) The line chart indicates cell numbers of LCLs established with indicated EBV mutants from 0 to 8 days.

4. Results

Data were presented as the mean \pm S.E.M. of $n = 4$ biological replicates. Statistical significance was tested by two-way ANOVA followed by a Tukey's multiple comparison test (*: $P < 0.05$, **: $P < 0.01$, ****: $P < 0.0001$, vs WT).

4.4.3. Upregulation of LMP1 in LCLs established by EBV strains expressing EBNA2 deficient for PLK1 docking or phosphorylation

To further analyze the viral and cellular gene expression in the LCLs established by recombinant EBV mutants, LCLs were lysed and the gene expression was analyzed by western blotting. The result revealed that EBNA2 S457A/T465V was expressed at low levels but strongly induced LMP1 expression. MYC levels were not affected in any group (Figure 21).

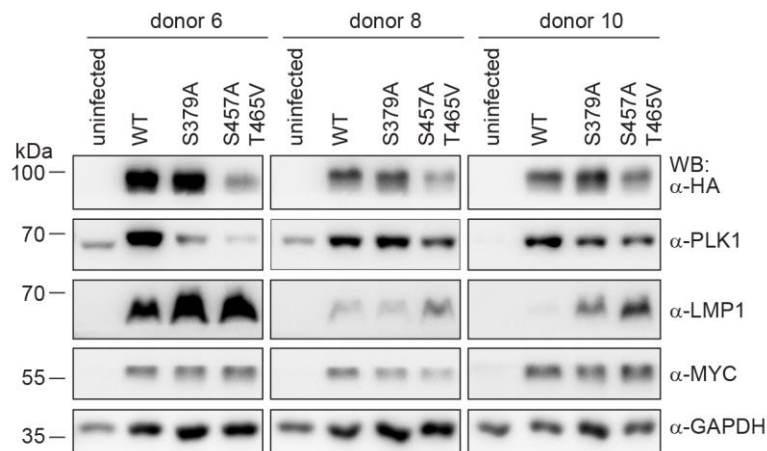


Figure 21. Expression of representative viral and cellular genes.

The viral (EBNA2 and LMP1) and cellular (PLK1, MYC, and GAPDH) genes were analyzed in LCLs established with indicated EBV mutants, visualized by western blotting using HA- (α -HA), PLK1- (α -PLK1), LMP1- (α -LMP1), MYC- (α -MYC), and GAPDH- (α -GAPDH) specific antibodies. Data of three donors are shown.

4.5. Characterization of humanized mice infected with recombinant EBV

In collaboration with Prof. Christian Münz (UZH, Zürich), humanized mice were used to characterize the recombinant EBVs. In this study, a super immunodeficient NSG (NOD-*scid* γ_c^{null}) mouse strain was used. The NOD background prevents phagocytosis of human cells by murine myeloid cells since human CD47 inhibits murine myeloid cells through interaction with the mouse signal regulatory protein α (SIRP α). The *scid* mutation abolishes murine adaptive lymphocyte development by compromising B and T cell receptor somatic recombination. The γ_c deficiency eliminates innate lymphocytes by blocking interleukin (IL) -2, -4, -7, -9, -15, and -21 signaling because the development of innate lymphoid cell precursors and the differentiation of the natural killer (NK) cells are IL-7 and -15 dependent, respectively (Münz, 2017). Therefore, NSG mice engrafted with human CD34⁺ hematopoietic progenitor cells develop a human immune system.

These chimeric humanized mice are used to study EBV-induced tumor formation and anti-viral immune mechanisms against EBV *in vivo* (Strowig et al., 2009).

I produced recombinant EBV strains expressing EBNA2 WT, S379A, or S457A/465V. The recombinant viruses were delivered to Prof. Münz's lab. Dr. Anita Murer did the first mouse experiment with the viruses and Patrick Schuhmachers did the other two experiments.

4.5.1. EBV strains carrying EBNA2 mutants deficient for PLK1 phosphorylation induce more frequently lymphomas in humanized mice

Since EBNA2 mutants S379A and S457A/T465V exhibited an enhanced transactivation capacity and LCLs generated with those virus mutants proliferated faster *in vitro*, these virus mutants were hypothesized to promote tumorigenicity in humanized mice. Hence, humanized mice were injected i.p. with 10^5 Green Raji Units (GRUs) of EBV and analyzed the immune cell composition and activation in the blood over five weeks. After five weeks of infection, humanized mice were sacrificed to analyze tumor development, viral loads, and immune cell composition in blood and spleen (Figure 22A). In two out of three experiments infection with EBV EBNA2 S457A/T465V resulted in increased mortality compared to EBV WT or S379A infected animals (66% survival in one and 20% in the second experiment; Figure 22B). In addition, mice that were infected with either of the two EBV EBNA2 mutants presented with higher incidences of tumor development in spleens or the peritoneal cavity as compared to mice infected with WT EBV (23% for WT, 36% for S379A, and 44% for S457A/T465V; Figure 22C). This is in line with the finding that EBV EBNA2 mutant infected mice presented slightly higher viral loads in spleens five weeks post-infection (Figure 22D). When comparing blood viral loads similar values across all groups irrespective of EBV mutant or WT infection were observed. Notably, the viral loads in mice within the EBNA2 S457A/T465V mutant group reached higher levels already two weeks after infection as compared to the WT or the EBNA2 S379A infected animals and started to decrease already at four weeks p.i. when high viral loads were still detected in the WT infected animals (Figure 22E).

In summary, the EBV EBNA2 mutant impairing phosphorylation of EBNA2 by PLK1 (EBNA2 S457A/T465V) leads to increased mortality and induces tumors in a higher fraction of infected mice.

4. Results

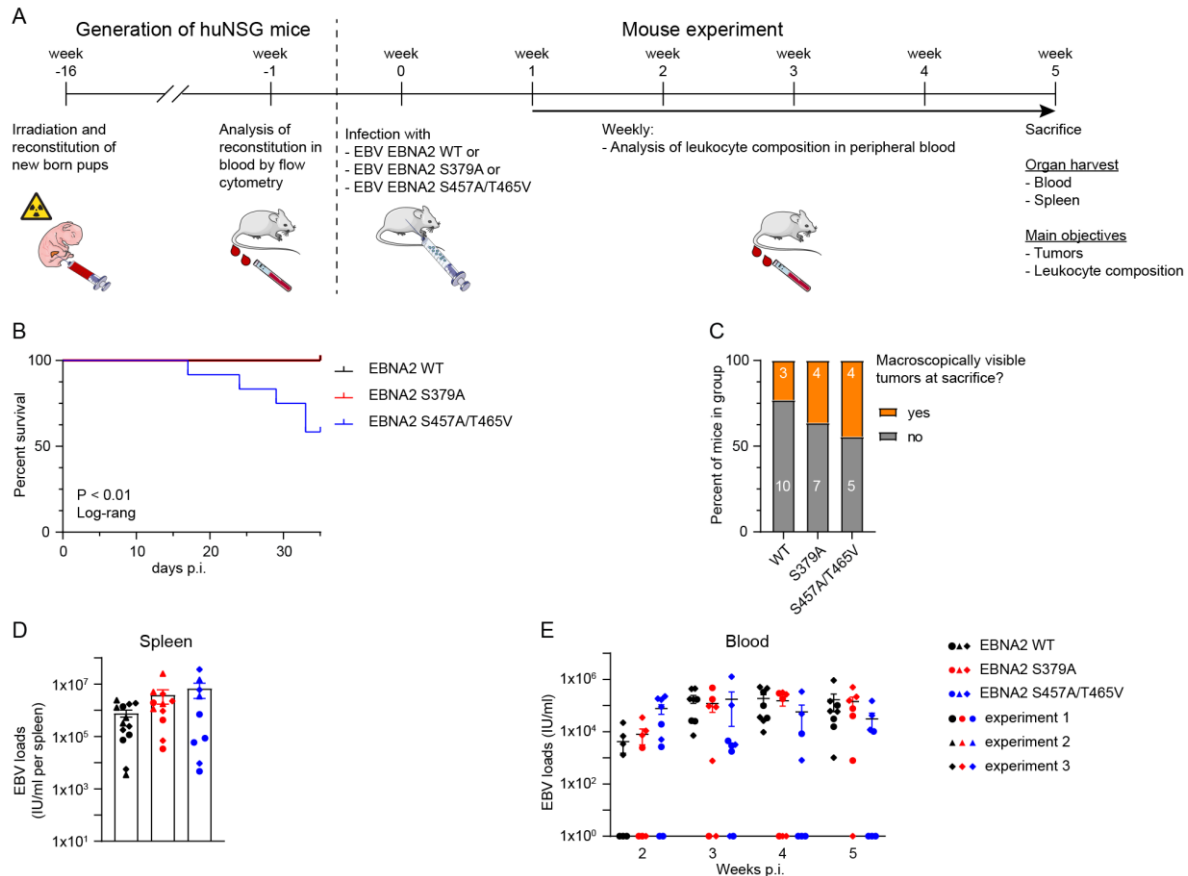


Figure 22. EBV strains expressing EBNA2 mutants deficient for PLK1 docking or phosphorylation cause more frequently lymphomas in humanized mice.

(A) Experiment set-up. Images of animals, syringes, and blood collection tubes are derived from Servier Medical Art. (B) Survival curve of humanized mice infected with EBV EBNA2 WT (n = 13), S379A (n = 11), or S457A/T465V (n = 9). Log-rank test. (C) Percentage of mice having macroscopically visible tumors at the day of sacrifice. Numbers within bars indicate the total number of mice with or without tumors in the respective groups. Fisher's Exact Test. (D) Viral loads in spleens of infected humanized mice at the day of sacrifice. Data were presented as the mean \pm S.E.M. (E) Development of viral loads in blood of infected mice over five weeks. Data were presented as the mean \pm S.E.M. Mann-Whitney U test. (B – D) Data points are derived from three independently performed experiments. (E) The graph depicts the values of two independently performed experiments. Shapes of data points indicate to which repetition of the experiments the respective animal belongs. Statistical significance tested using the Mann-Whitney U Test with Holm-Sidak correction for multiple comparisons. Figure 22 was provided by Patrick Schuhmachers (AG M \ddot{u} nz, UZH).

4.5.2. EBV strains carrying EBNA2 mutants deficient for PLK1 phosphorylation induce an earlier immune response in humanized mice

Since extensive CD8⁺ T cell expansion and activation in blood is a common trait marking EBV infection in humanized mice and normally follows with a delay of about a week rising viral loads (Chatterjee et al., 2019; Strowig et al., 2009) and correlates with these (Caduff et al., 2020; Zdimerova et al., 2021), the expansion and activation of both CD8⁺ and CD4⁺ T cells in the blood of infected animals were further analyzed. As CD8⁺ T cells expand more strongly than do CD4⁺ T

4. Results

cells upon EBV infection, a rising CD8⁺ to CD4⁺ T cell ratio indicates the extensive proliferation of CD8⁺ T cells. As compared to WT infection, The CD8⁺ to CD4⁺ T cell ratios in mice infected with the EBV EBNA2 S457A/T465V mutant were significantly increased at three weeks p.i. (mean of CD8⁺ to CD4⁺ T cell ratios in mice infected with EBV (i) EBNA2 WT: 0.37 and (ii) EBNA2 S457A/T465V: 0.99; Figure 23A and Figure S13A and B). Notably, the WT infected group did not show increased CD8⁺ to CD4⁺ T cell ratios before 4 weeks p.i. suggesting that T cells are earlier expanded during infection with the EBV EBNA2 S457A/T465V mutant. In line with this, a higher percentage of CD8⁺ T cells was earlier positive for the activation marker HLA-DR, i.e. activated, in the mice infected with the same mutant virus starting from 2 weeks p.i. A similar trend could be observed for mice infected with the EBNA2 S379A mutant (Figure 23B). Interestingly, the EBV EBNA2 S457A/T465V mutant seemed to induce also more strongly induce activation of CD4⁺ T cells in blood of mice within five weeks of infection compared to the WT group (Figure 23C). In contrast to blood, the fractions of CD8⁺ and CD4⁺ T cells in spleens of infected animals did not differ between the groups (Figure 23D) However, we still could determine a higher fraction of CD8⁺ and a significantly increased fraction of CD4⁺ T cells to be HLA-DR positive when infected with the EBV EBNA2 S457A/T465V mutant, i.e. activated (Figure 23E). The development of memory cells, i.e. effector memory (Tem), central memory (Tcm), or terminally differentiated subsets that re-express CD45RA (Temra), however, was not influenced by EBNA2 mutations (Figure S13C and D).

In summary, T cells, in particular CD8⁺ T cells, in mice infected with the EBNA2 S457A/T465V mutant virus expanded more rapidly in blood and a higher fraction of those was positive for the activation marker HLA-DR earlier after infection when compared with EBV WT. This suggests also the more rapid proliferation of EBNA2 S457A/T465V expressing B cells *in vivo*, resulting in an earlier T cell activation and expansion.

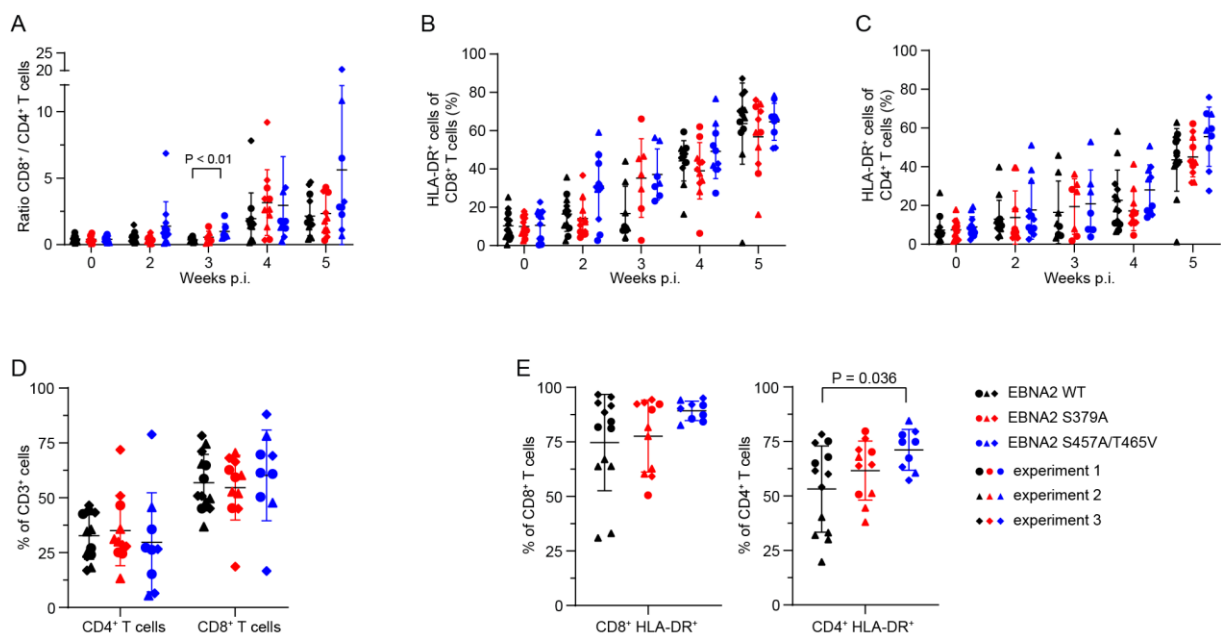


Figure 23. EBV strains expressing EBNA2 mutants deficient for PLK1 phosphorylation cause an earlier immune response in humanized mice.

4. Results

(A – C) Flow-cytometric analyses of (A) CD8⁺/CD4⁺ T cell ratios and (B) CD8⁺ or (C) CD4⁺ T cell activation in blood of mice infected with WT or mutant EBNA2 EBVs over five weeks. Data were presented as the mean \pm SD. (D, E) Analyses of (D) CD8⁺ and CD4⁺ T cell percentages, and (E) CD8⁺ and CD4⁺ T cell activation in spleens of infected mice. Data were presented as the mean \pm SD. Mann-Whitney U test. (A – E) Data points are derived from three independently performed experiments. Shapes of data points indicate to which repetition of the experiments the respective animal belongs. Statistical significance tested using the Mann-Whitney U Test with Holm-Sidak correction for multiple comparisons. Figure 23 was provided by Patrick Schuhmachers (AG M \ddot{u} nz, UZH).

5. Discussion

5.1. The interaction of EBNA2 and PLK1

The viral transactivator EBNA2 initiates cell cycle entry and maintains the proliferation of infected B cells by activating a cascade of primary and secondary cellular and viral target genes. In this thesis, it was demonstrated that EBNA2 binds directly to PLK1, a master regulator of multiple stages of cell cycle including G2/M transition, M-phase progression, and cytokinesis. It was shown that EBNA2 provides two docking sites, PDS1 and PDS2, for the polo-box domain (PBD) of PLK1 (Figure 8). The binding of PLK1 to PDS1 requires priming by the mitotic kinase CDK1, which phosphorylates EBNA2 S379. The K_D of a phospho-heptapeptide harboring pS379 in complex with PBD is 8.19 nM (Figure 9C). Compared to PLK1 substrates that have been characterized previously, this binding affinity is surprisingly high. Through phosphorylation of CDC25C1, MYT1, and WEE1, PLK1 promotes the activation of the mitotic driver Cyclin B1/CDK1 in the late G2-phase triggering prophase onset (Gheghiani et al., 2017; Nakajima et al., 2003; Watanabe et al., 2005). It remains to be tested whether EBNA2 might compete with these cellular substrates of PLK1.

Surprisingly, the EBNA2 S379A mutant shows elevated transactivation potential compared to EBNA2 WT, suggesting that PLK1 antagonizes the biological activity of EBNA2. In contrast to PDS1, PDS2 does not require substrate priming by phosphorylation to create a docking site. Indeed, PDS2 binding to PLK1 PBD was confirmed by NMR titrations. PDS2 triple mutants were designed and analyzed by ITC. The cluster mutant A (F440A and WY444AA) and C (YIF460AAA) impaired PLK1 binding individually, and almost abolished binding when combined. Comparison of PDS1 and PDS2 mutants by co-immunoprecipitations from cellular extracts confirmed that both docking sites contribute to complex formation.

PDS2 (423-474) widely overlaps with the C-terminal acidic transactivation domain (TAD: 431-474) of EBNA2. Like many other TADs, this TAD is intrinsically unstructured. In complex with a subunit of the TFIIH transcription complex, Tfb1/p62, the EBNA2 TAD forms a 9-residue α -helix that exposes W458, I461, and F462 to the hydrophobic interface that confers the interaction. Mutagenesis of EBNA2 W458, I461, and F462 impaired Tfb1 binding and transactivation of reporter genes by EBNA2 (Chabot et al., 2014). Our study shows that residues YIF460 also bind to PLK1. Thus PLK1 might also impair EBNA2 by direct interactions with its TAD. Interestingly, recent reports describe a second cryptic hydrophobic pocket within the PBD that functions as a second substrate recognition site close to the phospho-peptide docking site (Sharma et al., 2019; Śledź et al., 2011). This second substrate-binding site can be targeted by small molecules. Future biophysical studies will need to test if EBNA2 PDS2 contacts the hydrophobic second pocket of PBD.

5.2. The phosphorylation of EBNA2 by PLK1

Most importantly, it was shown that EBNA2 is a substrate of PLK1. It was reported that EBNA2 S457 is not phosphorylated by CK1 (Grässer et al., 1992), but here it shows that PLK1 phosphorylates S457 and T465 within PDS2. S457A/T465V missense mutants can still bind to PLK1 but are not phosphorylated. The phosphorylation mutant EBNA2 S457A/T465V exhibits a significantly enhanced transactivation potential. This enhanced potential might be caused in part by the elevated levels of histone acetyltransferase and co-activator p300 that bind this mutant (Figure 15C). To directly test, if PLK1 inhibits EBNA2, both binding partners were co-expressed and promoter-reporter studies were performed. Kinase active but not kinase-dead PLK1 (K82M) inhibited the transactivation of EBNA2 wild-type and the S379A docking site mutant. Since the transactivation of the phosphorylation mutant EBNA2 S457A/T465V was not inhibited by PLK1 co-expression, it was concluded that PLK1 phosphorylation rather than PLK1 binding inhibits EBNA2 transactivation potential. PDS2 could confer substrate binding in non-mitotic cells before CDK1 activity rises.

During cell cycle progression, PLK1 abundance and activity gradually increase at the G2/M transition point and peak during mitosis. In parallel, the global transcription activity is severely reduced while the chromatin condensates (Palozola et al., 2019). During mitosis, EBNA2 is hyperphosphorylated and considered to be inactive (Yue et al., 2004). The same research group reported that phosphorylation of EBNA2 S243 by Cyclin B1/CDK1 or the viral PK encoded by the BGLF4 gene impairs the transactivation of the LMP1 gene by EBNA2 (Yue et al., 2005, 2006). The viral mutant that carries an EBNA2 S243 mutant has not been studied. Thus, though a distinct molecular process is postulated in Yue's studies, the impact on EBNA2 function in mitosis is similar.

5.3. Characterization of EBV expressing EBNA2 deficient for PLK1 binding or phosphorylation *in vitro* and *in vivo*

EBV mutants were engineered to carry the PLK1 docking site (EBNA2 S379A) or phosphorylation (EBNA2 S457A/T465V) mutations. Both EBV mutants were fully immortalization competent and initiated long term proliferating B cell cultures. Cell division rates were increased in mutant cell lines early after infection as well as in long-term cultures. LMP1 expression was enhanced in both mutants but was most pronounced in the phosphorylation mutants. To study the impact of both mutations on carcinogenesis, humanized mice were infected with both EBV mutants. Blood samples were analyzed weekly for viral loads and immune responses by CD4⁺ and CD8⁺ T cell populations were characterized. Importantly, the phosphorylation mutant induced high viral loads in blood of mice already at early time points of infection which is in line with a higher replicative activity of transformed B cells *in vitro*. Additionally, splenic EBV loads seemed to be slightly elevated in both EBNA2 mutants compared to EBNA2 WT infected individuals. Viral loads were reported to usually be followed by expansion and activation of EBV-specific CD8⁺ T cells in EBV infected

humanized mice (Shultz et al., 2010; Strowig et al., 2009). Our finding that the S379A and S457A/T465V mutants induced early expansion and activation of cytotoxic T cells is therefore consistent with earlier publications and can be explained by higher antigen abundance due to higher viral loads at already two weeks post-infection. Irrespective of the early adaptive immune response to infection more EBV infected mice developed lymphomas with both EBNA2 mutants when compared to EBNA2 wildtype virus infections. These findings are consistent with the higher replicative activity of both mutants compared to the EBNA2 WT causing accelerated infection and more frequent tumor formation.

In summary, our study shows that PLK1 is an important regulator of EBNA2 activity that limits the tumorigenicity of EBV *in vitro* and *in vivo*. Since PLK1 activity peaks in mitosis, we speculate that PLK1 controls EBNA2 activities during this time window. Unfortunately, since during mitosis the global cellular transcription of the condensed chromosomes is silenced, EBNA2 activity cannot be tested reliably in this cellular environment. Interestingly, it has been shown before that PLK1 can affect the activity of transcription factors. Phosphorylation of the tumor suppressor p53 and the related p73 protein impair the transactivation activity of both transcription factors. In p73 the substrate site of PLK1 has been mapped to the TAD (Ando et al., 2004; de Cárcer, 2019; Koida et al., 2008; Martin and Strebhardt, 2006). Phosphorylation of the transcription factor FOXO1 causes its nuclear exclusion and thereby prevents its action (Yuan et al., 2014). However, PLK1-dependent phosphorylation of FoxM1 regulates a transcriptional program that mediates cell-cycle progression (Fu et al., 2008). It is tempting to speculate that, PLK1 might contribute to focus the transcriptional activity on mitosis relevant transcripts and proteins.

5.4. A proposed model

In this thesis, I can provide evidence that PLK1 suppresses EBV-associated carcinogenesis through the phosphorylation of EBNA2. Initially, Dr. Sybille Thumann found that PLK1 is significantly enriched in EBNA2 co-immunoprecipitates from DG75 cells which exogenously overexpress EBNA2. I confirmed that PLK1 and EBNA2 interact with each other in EBV-transformed B cells. Interestingly, two PLK1 binding sites (PDS1 and PDS2) of EBNA2 were mapped. The phosphorylation of S379 in PDS1 by CDK1 dramatically enhanced its PLK1 binding ability. In contrast, PDS2 provided an extended region for PLK1 binding that involves multiple residues, like F440, WY444, and YIF460. Next, I found that EBNA2 is a viral substrate of PLK1. PLK1 phosphorylated S457 and T465 of the C-terminal TAD of EBNA2 to attenuate its transactivation activity by hindering the recruitment of p300. In addition, EBV strains expressing EBNA2 mutants deficient for either PLK1 docking (S379A) or phosphorylation (S457A/465V) promoted B cell proliferation *in vitro*, indicating PLK1 phosphorylation of EBNA2 suppresses EBV-driven B cell proliferation. Even though the expression levels of EBNA2 were low in LCLs established by EBV strain with PLK1 phosphorylation site, the induction levels of the viral oncogene, LMP1 were high in these cells, indicating EBV EBNA2 S457A/465V is more tumorigenic than EBV wild-type.

Furthermore, EBV strains expressing EBNA2 mutants deficient for either PLK1 docking or phosphorylation induced more frequently lymphomas in humanized mice compared to the wild-type. EBV strain expressing EBNA2 mutant deficient for PLK1 phosphorylation induced higher mortality and caused an earlier immune response in humanized mice compared to the wild-type. In summary, PLK1 restricts the EBV tumorigenicity through the phosphorylation of EBNA2.

A model based on these findings is proposed (Figure 24). PLK1 phosphorylates EBNA2 in a pre-phosphorylation-dependent or -independent manner, which leads to the strong or weak phosphorylation of EBNA2, respectively. The phosphorylation of S379 by CDK1 functions as a switcher between these two states. The phosphorylation of S457/T465 of TAD by PLK1 suppresses the transactivation of EBNA2, which further has an impact on the expression of EBNA2 target genes, the proliferation of EBV infected B cells *in vitro*, and EBV pathogenesis *in vivo*.

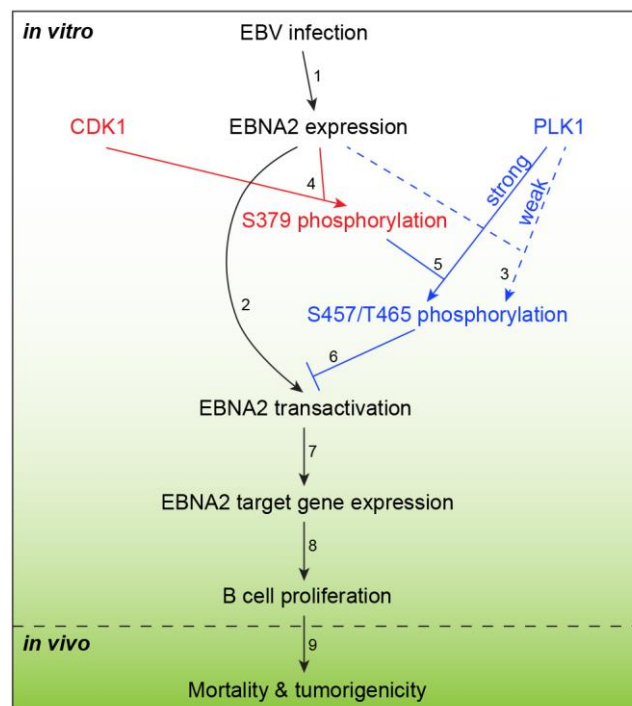


Figure 24. A model explaining how PLK1 prevents EBV-induced tumorigenesis through phosphorylation of EBNA2

(1) EBNA2 is one of the first expressed genes upon EBV infection. (2) EBNA2 transactivates its target gene expression. (3) PLK1 binds to EBNA2 through PDS2. Therefore, serine 457 and threonine 465 of EBNA2 was phosphorylated weakly. (4) CDK1 phosphorylates serine 379 of EBNA2. (5) The phosphoserine 379 enhances EBNA2 binding to PLK1. Therefore, the serine 457 and threonine 465 of EBNA2 was phosphorylated by PLK1 strongly. (6) The phosphoserine 457 and phosphothreonine 465 suppress EBNA2 transactivation. (7) EBNA2 transactivates its target genes, like C-MYC and LMP1. (8) The expression of EBNA2 target genes drives the proliferation of EBV infected B cells *in vitro*. (9) The B cell proliferation induces lymphomas *in vivo*.

5.5. The relevance of this study for the use of PLK1 inhibitors in cancer treatment

In healthy immunocompetent hosts, EBNA2 is expressed in a short time window immediately post-infection before either EBNA2 expression is silenced or the EBNA2 expressing cell is eliminated by the immune system. Immunodeficient patients can develop aggressive EBNA2 positive B lymphomas and EBNA2 is a driving force for these tumor entities. It is well established that high-level expression of PLK1 promotes carcinogenesis in multiple tissues (Strebhardt, 2010; Strebhardt and Ullrich, 2006). Currently, clinical trials evaluate the safety and efficacy of PLK1 inhibitors for patient treatment. However, PLK1 has tumor-suppressive potential in APC-truncated colon cancer cells (Raab et al., 2018) and high-level PLK1 induced aneuploidies and chromosome instability can suppress cancerogenesis in some mouse models (de Cárcer, 2019). Thus, inhibition of PLK1 activity might have opposing effects in the context of the specific transformed cell. Here we show that PLK1 is an important cellular control factor that restrains the proliferation and transformation of latently infected B cells driven by a growth program that depends on EBNA2. Both S379A and S457/T465V of EBNA2 mutants are gain-of-function variants of this viral oncogene. Based on our results the development and therapeutic use of PLK1 inhibitors should be considered and closely monitored for potential adverse effects in the context of the prevalent EBV infections in the population.

6. References

1. Ando, K., Ozaki, T., Yamamoto, H., Furuya, K., Hosoda, M., Hayashi, S., Fukuzawa, M., and Nakagawara, A. (2004). Polo-like kinase 1 (Plk1) inhibits p53 function by physical interaction and phosphorylation. *J. Biol. Chem.* *279*, 25549–25561.
2. Archambault, V., and Normandin, K. (2017). Several inhibitors of the Plk1 Polo-Box Domain turn out to be non-specific protein alkylators. *Cell Cycle* *16*, 1220–1224.
3. Archambault, V., Lépine, G., and Kachaner, D. (2015). Understanding the Polo Kinase machine. *Oncogene* *34*, 4799–4807.
4. Asteriti, I.A., De Mattia, F., and Guarguaglini, G. (2015). Cross-Talk between AURKA and Plk1 in Mitotic Entry and Spindle Assembly. *Front. Oncol.* *5*, 283.
5. Baer, R., Bankier, A.T., Biggin, M.D., Deininger, P.L., Farrell, P.J., Gibson, T.J., Hatfull, G., Hudson, G.S., Satchwell, S.C., Séguin, C., et al. (1984). DNA sequence and expression of the B95-8 Epstein - Barr virus genome. *Nature* *310*, 207–211.
6. Bar-Or, A., Pender, M.P., Khanna, R., Steinman, L., Hartung, H.P., Maniar, T., Croze, E., Aftab, B.T., Giovannoni, G., and Joshi, M.J. (2020). Epstein–Barr Virus in Multiple Sclerosis: Theory and Emerging Immunotherapies. *Trends Mol. Med.* *26*, 296–310.
7. Barr, F.A., Silljé, H.H.W., and Nigg, E.A. (2004). Polo-like kinases and the orchestration of cell division. *Nat. Rev. Mol. Cell Biol.* *5*, 429–441.
8. Barth, S., Liss, M., Voss, M.D., Dobner, T., Fischer, U., Meister, G., and Grässer, F.A. (2003). Epstein-Barr Virus Nuclear Antigen 2 Binds via Its Methylated Arginine-Glycine Repeat to the Survival Motor Neuron Protein. *J. Virol.* *77*, 5008–5013.
9. Ben-bassats, H., Goldblum, N., Mitrani, S., Goldblum, T., Yoffey, J.M., Cohen, M.M., Bentwich, Z., Ramot, B., Klein, E., and Klein, G. (1977). Establishment in continuous culture of a new type of lymphocyte from a “burkitt-like” malignant lymphoma (line d.g.-75). *Int. J. Cancer* *19*, 27–33.
10. Bornkamm, G.W., Berens, C., Kuklik-Roos, C., Bechet, J.-M., Laux, G., Bachl, J., Korndoerfer, M., Schlee, M., Hölzel, M., Malamoussi, A., et al. (2005). Stringent doxycycline-dependent control of gene activities using an episomal one-vector system. *Nucleic Acids Res.* *33*, e137–e137.
11. Van den Bossche, J., Lardon, F., Deschoolmeester, V., De Pauw, I., Vermorken, J., Specenier, P., Pauwels, P., Peeters, M., and Wouters, A. (2016). Spotlight on Volasertib: Preclinical and Clinical Evaluation of a Promising Plk1 Inhibitor. *Med. Res. Rev.* *36*, 749–786.
12. Burkitt, D. (1958). A sarcoma involving the jaws in african children. *Br. J. Surg.* *46*, 218–223.
13. Caduff, N., McHugh, D., Murer, A., Rämer, P., Raykova, A., Landtwing, V., Rieble, L., Keller, C.W., Prummer, M., Hoffmann, L., et al. (2020). Immunosuppressive FK506 treatment leads to more frequent EBV-associated lymphoproliferative disease in humanized mice. *PLOS Pathog.* *16*, e1008477.
14. de Cárcer, G. (2019). The Mitotic Cancer Target Polo-Like Kinase 1: Oncogene or Tumor

6. References

- Suppressor? *Genes (Basel)*. *10*, 208–222.
15. de Cárcer, G., Manning, G., and Malumbres, M. (2011). From Plk1 to Plk5. *Cell Cycle* *10*, 2255–2262.
 16. de Cárcer, G., Venkateswaran, S.V., Salgueiro, L., Bakkali, A. El, Somogyi, K., Rowald, K., Montañés, P., Sanclemente, M., Escobar, B., Martino, A. de, et al. (2018). Plk1 overexpression induces chromosomal instability and suppresses tumor development. *Nat. Commun.* *9*, 1–14.
 17. Cen, O., and Longnecker, R. (2015). Latent Membrane Protein 2 (LMP2). In *Current Topics in Microbiology and Immunology*, (Springer International Publishing), pp. 151–180.
 18. Chabot, P.R., Raiola, L., Lussier-Price, M., Morse, T., Arseneault, G., Archambault, J., and Omichinski, J.G. (2014). Structural and Functional Characterization of a Complex between the Acidic Transactivation Domain of EBNA2 and the Tfb1/p62 Subunit of TFIIH. *PLOS Pathog.* *10*, e1004042.
 19. Chatterjee, B., Deng, Y., Holler, A., Nunez, N., Azzi, T., Vanoaica, L.D., Müller, A., Zdimerova, H., Antsiferova, O., Zbinden, A., et al. (2019). CD8+ T cells retain protective functions despite sustained inhibitory receptor expression during Epstein-Barr virus infection in vivo. *PLoS Pathog.* *15*, e1007748.
 20. Chen, Y.P., Chan, A.T.C., Le, Q.T., Blanchard, P., Sun, Y., and Ma, J. (2019). Nasopharyngeal carcinoma. *Lancet* *394*, 64–80.
 21. Cheng, K.-Y., Lowe, E.D., Sinclair, J., Nigg, E.A., and Johnson, L.N. (2003). The crystal structure of the human polo-like kinase-1 polo box domain and its phospho-peptide complex. *EMBO J.* *22*, 5757–5768.
 22. Cho, Y.-G., Gordadze, A. V., Ling, P.D., and Wang, F. (1999). Evolution of Two Types of Rhesus Lymphocryptovirus Similar to Type 1 and Type 2 Epstein-Barr Virus. *J. Virol.* *73*, 9206–9212.
 23. Chua, M.L.K., Wee, J.T.S., Hui, E.P., and Chan, A.T.C. (2016). Nasopharyngeal carcinoma. *Lancet* *387*, 1012–1024.
 24. Le Clorennec, C., Youlyouz-Marfak, I., Adriaenssens, E., Coll, J., Bornkamm, G.W., and Feuillard, J. (2006). EBV latency III immortalization program sensitizes B cells to induction of CD95-mediated apoptosis via LMP1: role of NF- κ B, STAT1, and p53. *Blood* *107*, 2070–2078.
 25. Cohen, J.I., and Kieff, E. (1991). An Epstein-Barr virus nuclear protein 2 domain essential for transformation is a direct transcriptional activator. *J. Virol.* *65*, 5880–5885.
 26. Cohen, J.I., Wang, F., Mannick, J., and Kieff, E. (1989). Epstein-Barr virus nuclear protein 2 is a key determinant of lymphocyte transformation. *Proc. Natl. Acad. Sci.* *86*, 9558–9562.
 27. Cohen, J.I., Wang, F., and Kieff, E. (1991). Epstein-Barr virus nuclear protein 2 mutations define essential domains for transformation and transactivation. *J. Virol.* *65*, 2545–2554.
 28. Countryman, J., and Miller, G. (1985). Activation of expression of latent Epstein-Barr herpesvirus after gene transfer with a small cloned subfragment of heterogeneous viral DNA. *Proc. Natl. Acad. Sci.* *82*, 4085–4089.
 29. Dai, Y., Tang, Y., He, F., Zhang, Y., Cheng, A., Gan, R., and Wu, Y. (2012). Screening and

6. References

- functional analysis of differentially expressed genes in EBV-transformed lymphoblasts. *Viol. J.* 9, 1–9.
30. Delaglio, F., Grzesiek, S., Vuister, G., Zhu, G., Pfeifer, J., and Bax, A. (1995). NMRPipe: a multidimensional spectral processing system based on UNIX pipes. *J. Biomol. NMR* 6, 277–293.
31. Dharnidharka, V.R., Webster, A.C., Martinez, O.M., Preiksaitis, J.K., Leblond, V., and Choquet, S. (2016). Post-transplant lymphoproliferative disorders. *Nat. Rev. Dis. Prim.* 2, 1–20.
32. Dierickx, D., and Habermann, T.M. (2018). Post-Transplantation Lymphoproliferative Disorders in Adults. *N. Engl. J. Med.* 378, 549–562.
33. Donhuijsen-Ant, R., Abken, H., Bornkamm, G., Donhuijsen, K., Grosse-Wilde, H., Neumann-Haefelin, D., Westerhausen, M., and Wiegand, H. (1988). Fatal Hodgkin and non-Hodgkin lymphoma associated with persistent Epstein-Barr virus in four brothers. *Ann. Intern. Med.* 109, 946–952.
34. Draborg, A.H., Duus, K., and Houen, G. (2012). Epstein-barr virus and systemic lupus erythematosus. *Clin. Dev. Immunol.* 2012, 1–10.
35. Elia, A.E.H., Cantley, L.C., and Yaffe, M.B. (2003a). Proteomic Screen Finds pSer/pThr-Binding Domain Localizing Plk1 to Mitotic Substrates. *Science* (80-.). 299, 1228–1231.
36. Elia, A.E.H., Rellos, P., Haire, L.F., Chao, J.W., Ivins, F.J., Hoepker, K., Mohammad, D., Cantley, L.C., Smerdon, S.J., and Yaffe, M.B. (2003b). The Molecular Basis for Phosphodependent Substrate Targeting and Regulation of Plks by the Polo-Box Domain. *Cell* 115, 83–95.
37. Epstein, M., Achong, B., and Barr, Y.. (1964). Virus Particles in Cultured Lymphoblasts from Burkitt's Lymphoma. *Lancet* 283, 702–703.
38. Farrell, P.J. (2015). Epstein–Barr Virus Strain Variation. In *Current Topics in Microbiology and Immunology*, (Springer International Publishing), pp. 45–69.
39. Francis, M.S., Amer, A.A.A., Milton, D.L., and Costa, T.R.D. (2017). Site-Directed Mutagenesis and Its Application in Studying the Interactions of T3S Components. *Methods Mol. Biol.* 1531, 11–31.
40. Frappier, L. (2015). EBNA1. In *Current Topics in Microbiology and Immunology*, (Springer International Publishing), pp. 3–34.
41. Friberg, A., Thumann, S., Hennig, J., Zou, P., Nössner, E., Ling, P.D., Sattler, M., and Kempkes, B. (2015). The EBNA-2 N-Terminal Transactivation Domain Folds into a Dimeric Structure Required for Target Gene Activation. *PLOS Pathog.* 11, e1004910.
42. Fu, Z., Malureanu, L., Huang, J., Wang, W., Li, H., van Deursen, J., Tindall, D., and Chen, J. (2008). Plk1-dependent phosphorylation of FoxM1 regulates a transcriptional programme required for mitotic progression. *Nat. Cell Biol.* 10, 1076–1082.
43. Gheghiani, L., Loew, D., Lombard, B., Mansfeld, J., and Gavet, O. (2017). PLK1 Activation in Late G2 Sets Up Commitment to Mitosis. *Cell Rep.* 19, 2060–2073.
44. Glaser, L. V., Rieger, S., Thumann, S., Beer, S., Kuklik-Roos, C., Martin, D.E., Maier, K.C.,
-

6. References

- Harth-Hertle, M.L., Grüning, B., Backofen, R., et al. (2017). EBF1 binds to EBNA2 and promotes the assembly of EBNA2 chromatin complexes in B cells. *PLOS Pathog.* *13*, e1006664.
45. Gordadze, A., Onunwor, C., Peng, R., Poston, D., Kremmer, E., and Ling, P. (2004). EBNA2 amino acids 3 to 30 are required for induction of LMP-1 and immortalization maintenance. *J. Virol.* *78*, 3919–3929.
46. Goroshchuk, O., Kolosenko, I., Vidarsdottir, L., Azimi, A., and Palm-Apergi, C. (2019). Polo-like kinases and acute leukemia. *Oncogene* *38*, 1–16.
47. Goroshchuk, O., Vidarsdottir, L., Björklund, A.-C., Hamil, A.S., Kolosenko, I., Dowdy, S.F., and Palm-Apergi, C. (2020). Targeting Plk1 with siRNAs in primary cells from pediatric B-cell acute lymphoblastic leukemia patients. *Sci. Rep.* *10*, 1–10.
48. Grässer, F.A., Haiss, P., Göttel, S., and Mueller-Lantzsch, N. (1991). Biochemical characterization of Epstein-Barr virus nuclear antigen 2A. *J. Virol.* *65*, 3779–3788.
49. Grässer, F.A., Göttel, S., Haiss, P., Boldyreff, B., Issinger, O.G., and Mueller-Lantzsch, N. (1992). Phosphorylation of the Epstein-Barr virus nuclear antigen 2. *Biochem. Biophys. Res. Commun.* *186*, 1694–1701.
50. Hammerschmidt, W., and Sugden, B. (1989). Genetic analysis of immortalizing functions of Epstein-Barr virus in human B lymphocytes. *Nature* *340*, 393–397.
51. Harada, S., and Kieff, E. (1997). Epstein-Barr virus nuclear protein LP stimulates EBNA-2 acidic domain-mediated transcriptional activation. *J. Virol.* *71*, 6611–6618.
52. Harada, S., Yalamanchili, R., and Kieff, E. (2001). Epstein-Barr Virus Nuclear Protein 2 Has at Least Two N-Terminal Domains That Mediate Self-Association. *J. Virol.* *75*, 2482–2487.
53. zur Hausen, H., Schulte-Holthausen, H., Klein, G., Henle, W., Henle, G., Clifford, P., and Santesson, L. (1970). Epstein-Barr virus in Burkitt's lymphoma and nasopharyngeal carcinoma: EBV DNA in biopsies of Burkitt tumours and anaplastic carcinomas of the nasopharynx. *Nature* *228*, 1056–1058.
54. Henkel, T., Ling, P., Hayward, S., and Peterson, M. (1994). Mediation of Epstein-Barr virus EBNA2 transactivation by recombination signal-binding protein J kappa. *Science* (80-). *265*, 92–95.
55. Henle, G., Henle, W., and Diehl, V. (1968). Relation of Burkitt's tumor-associated herpes-type virus to infectious mononucleosis. *Proc. Natl. Acad. Sci.* *59*, 94–101.
56. Hille, A., Badu-Antwi, A., Holzer, D., and Grässer, F.A. (2002). Lysine residues of Epstein-Barr virus-encoded nuclear antigen 2 do not confer secondary modifications via ubiquitin or SUMO-like proteins but modulate transcriptional activation. *J. Gen. Virol.* *83*, 1037–1042.
57. Hochberg, D., Souza, T., Catalina, M., Sullivan, J.L., Luzuriaga, K., and Thorley-Lawson, D.A. (2004). Acute Infection with Epstein-Barr Virus Targets and Overwhelms the Peripheral Memory B-Cell Compartment with Resting, Latently Infected Cells. *J. Virol.* *78*, 5194–5204.
58. Hsieh, J.J., Henkel, T., Salmon, P., Robey, E., Peterson, M.G., and Hayward, S.D. (1996). Truncated mammalian Notch1 activates CBF1/RBPJk-repressed genes by a mechanism resembling that of Epstein-Barr virus EBNA2. *Mol. Cell. Biol.* *16*, 952–959.
-

6. References

59. Hummeler, K., Henle, G., and Henle, W. (1966). Fine structure of a virus in cultured lymphoblasts from Burkitt lymphoma. *J. Bacteriol.* *91*, 1366–1368.
60. Jackstadt, R., Röh, S., Neumann, J., Jung, P., Hoffmann, R., Horst, D., Berens, C., Bornkamm, G.W., Kirchner, T., Menssen, A., et al. (2013). AP4 is a mediator of epithelial–mesenchymal transition and metastasis in colorectal cancer. *J. Exp. Med.* *210*, 1331–1350.
61. Jang, Y.-J., Ma, S., Terada, Y., and Erikson, R.L. (2002). Phosphorylation of Threonine 210 and the Role of Serine 137 in the Regulation of Mammalian Polo-like Kinase. *J. Biol. Chem.* *277*, 44115–44120.
62. Jones, J.F., Shurin, S., Abramowsky, C., Tubbs, R.R., Sciotto, C.G., Wahl, R., Sands, J., Gottman, D., Katz, B.Z., and Sklar, J. (1988). T-Cell Lymphomas Containing Epstein–Barr Viral DNA in Patients with Chronic Epstein–Barr Virus Infections. *N. Engl. J. Med.* *318*, 733–741.
63. Joukov, V., and Nicolo, A. De (2018). Aurora-PLK1 cascades as key signaling modules in the regulation of mitosis. *Sci. Signal.* *11*, 4195.
64. Kaiser, C., Laux, G., Eick, D., Jochner, N., Bornkamm, G.W., and Kempkes, B. (1999). The Proto-Oncogene c- myc Is a Direct Target Gene of Epstein-Barr Virus Nuclear Antigen 2 . *J. Virol.* *73*, 4481–4484.
65. Kempkes, B., and Ling, P.D. (2015). EBNA2 and Its Coactivator EBNA-LP. In *Current Topics in Microbiology and Immunology*, (Springer International Publishing), pp. 35–59.
66. Khan, G., and Hashim, M.J. (2014). Global burden of deaths from epstein-barr virus attributable malignancies 1990-2010. *Infect. Agent. Cancer* *9*, 1–11.
67. Kleylein-Sohn, J., Westendorf, J., Clech, M. Le, Habedanck, R., Stierhof, Y.-D., and Nigg, E.A. (2007). Plk4-Induced Centriole Biogenesis in Human Cells. *Dev. Cell* *13*, 190–202.
68. Koida, N., Ozaki, T., Yamamoto, H., Ono, S., Koda, T., Ando, K., Okoshi, R., Kamijo, T., Omura, K., and Nakagawara, A. (2008). Inhibitory role of Plk1 in the regulation of p73-dependent apoptosis through physical interaction and phosphorylation. *J. Biol. Chem.* *283*, 8555–8563.
69. Küppers, R. (2008). The biology of Hodgkin’s lymphoma. *Nat. Rev. Cancer* *9*, 15–27.
70. Kwiatkowski, B., Chen, S.Y.J., and Schubach, W.H. (2004). CKII Site in Epstein-Barr Virus Nuclear Protein 2 Controls Binding to hSNF5/Ini1 and Is Important for Growth Transformation. *J. Virol.* *78*, 6067–6072.
71. Laichalk, L.L., and Thorley-Lawson, D.A. (2005). Terminal Differentiation into Plasma Cells Initiates the Replicative Cycle of Epstein-Barr Virus In Vivo. *J. Virol.* *79*, 1296–1307.
72. Lee, K.H., Hwang, J.-A., Kim, S.-O., Kim, J.H., Shin, S.C., Kim, E.E., Lee, K.S., Rhee, K., Jeon, B.H., Bang, J.K., et al. (2018). Phosphorylation of human enhancer filamentation 1 (HEF1) stimulates interaction with Polo-like kinase 1 leading to HEF1 localization to focal adhesions. *J. Biol. Chem.* *293*, 847–862.
73. Lee, K.S., Park, J.-E., Kang, Y.H., Kim, T.-S., and Bang, and J.K. (2014). Mechanisms Underlying Plk1 Polo-Box Domain-Mediated Biological Processes and Their Physiological Significance. *Mol. Cells* *37*, 286–294.
74. Li, Z., Li, J., Bi, P., Lu, Y., Burcham, G., Elzey, B.D., Ratliff, T., Konieczny, S.F., Ahmad, N.,

6. References

- Kuang, S., et al. (2014). Plk1 Phosphorylation of PTEN Causes a Tumor-Promoting Metabolic State. *Mol. Cell. Biol.* 34, 3642–3661.
75. Ling, P.D., and Hayward, S.D. (1995). Contribution of conserved amino acids in mediating the interaction between EBNA2 and CBF1/RBPJk. *J. Virol.* 69, 1944–1950.
76. Ling, P.D., Ryon, J.J., and Hayward, S.D. (1993). EBNA-2 of herpesvirus papio diverges significantly from the type A and type B EBNA-2 proteins of Epstein-Barr virus but retains an efficient transactivation domain with a conserved hydrophobic motif. *J. Virol.* 67, 2990–3003.
77. Liu, Z., Sun, Q., and Wang, X. (2017). PLK1, A Potential Target for Cancer Therapy. *Transl. Oncol.* 10, 22–32.
78. Llamazares, S., Moreira, A., Tavares, A., Girdham, C., Spruce, B.A., Gonzalez, C., Karess, R.E., Glover, D.M., and Sunkel, C.E. (1991). polo encodes a protein kinase homolog required for mitosis in *Drosophila*. *Genes Dev.* 5, 2153–2165.
79. Lu, L.-Y., Wood, J.L., Minter-Dykhouse, K., Ye, L., Saunders, T.L., Yu, X., and Chen, J. (2008). Polo-Like Kinase 1 Is Essential for Early Embryonic Development and Tumor Suppression. *Mol. Cell. Biol.* 28, 6870–6876.
80. Luzuriaga, K., and Sullivan, J.L. (2010). Infectious Mononucleosis. *N. Engl. J. Med.* 362, 1993–2000.
81. de Martel, C., Georges, D., Bray, F., Ferlay, J., and Clifford, G.M. (2020). Global burden of cancer attributable to infections in 2018: a worldwide incidence analysis. *Lancet Glob. Heal.* 8, e180–e190.
82. Martin, B.T., and Strebhardt, K. (2006). Polo-Like Kinase 1: Target and Regulator of Transcriptional Control. *Cell Cycle* 5, 2881–2885.
83. Maruo, S., Johannsen, E., Illanes, D., Cooper, A., and Kieff, E. (2003). Epstein-Barr Virus Nuclear Protein EBNA3A Is Critical for Maintaining Lymphoblastoid Cell Line Growth. *J. Virol.* 77, 10437–10447.
84. Möhl, B.S., Chen, J., Sathiyamoorthy, K., Jardetzky, T.S., and Longnecker, R. (2016). Structural and Mechanistic Insights into the Tropism of Epstein-Barr Virus. *Mol. Cells* 39, 286–291.
85. Mourão, A., Bonnal, S., Soni, K., Warner, L., Bordonné, R., Valcárcel, J., and Sattler, M. (2016). Structural basis for the recognition of spliceosomal SmN/B/B' proteins by the RBM5 OCRE domain in splicing regulation. *Elife* 5, 1–26.
86. Mrozek-Gorska, P., Buschle, A., Pich, D., Schwarzmayr, T., Fechtner, R., Scialdone, A., and Hammerschmidt, W. (2019). Epstein-Barr virus reprograms human B lymphocytes immediately in the prelatent phase of infection. *Proc. Natl. Acad. Sci.* 116, 16046–16055.
87. Münz, C. (2017). Humanized mouse models for Epstein Barr virus infection. *Curr. Opin. Virol.* 25, 113–118.
88. Münz, C. (2019). Latency and lytic replication in Epstein–Barr virus-associated oncogenesis. *Nat. Rev. Microbiol.* 17, 691–700.
89. Nakajima, H., Toyoshima-Morimoto, F., Taniguchi, E., and Nishida, E. (2003). Identification of a consensus motif for Plk (Polo-like kinase) phosphorylation reveals Myt1 as a Plk1 substrate.
-

6. References

- J. Biol. Chem. 278, 25277–25280.
90. Neef, R., Gruneberg, U., Kopajtich, R., Li, X., Nigg, E.A., Sillje, H., and Barr, F.A. (2007). Choice of Plk1 docking partners during mitosis and cytokinesis is controlled by the activation state of Cdk1. *Nat. Cell Biol.* 9, 436–444.
 91. Neuhierl, B., Feederle, R., Hammerschmidt, W., and Delecluse, H.J. (2002). Glycoprotein gp110 of Epstein–Barr virus determines viral tropism and efficiency of infection. *Proc. Natl. Acad. Sci.* 99, 15036–15041.
 92. Palozola, K., Lerner, J., and Zaret, K. (2019). A changing paradigm of transcriptional memory propagation through mitosis. *Nat. Rev. Mol. Cell Biol.* 20, 55–64.
 93. Pan, S.-H., Tai, C.-C., Lin, C.-S., Hsu, W.-B., Chou, S.-F., Lai, C.-C., Chen, J.-Y., Tien, H.-F., Lee, F.-Y., and Wang, W.-B. (2009). Epstein-Barr virus nuclear antigen 2 disrupts mitotic checkpoint and causes chromosomal instability. *Carcinogenesis* 30, 366–375.
 94. Park, J.-E., Li, L., Park, J., Knecht, R., Strebhardt, K., Yuspa, S.H., and Lee, K.S. (2009). Direct quantification of polo-like kinase 1 activity in cells and tissues using a highly sensitive and specific ELISA assay. *Proc. Natl. Acad. Sci.* 106, 1725–1730.
 95. Pavlovsky, A.G., Liu, X., Faehnle, C.R., Potente, N., and Viola, R.E. (2012). Structural Characterization of Inhibitors with Selectivity against Members of a Homologous Enzyme Family. *Chem. Biol. Drug Des.* 79, 128–136.
 96. Peng, R., Moses, S.C., Tan, J., Kremmer, E., and Ling, P.D. (2005). The Epstein-Barr Virus EBNA-LP Protein Preferentially Coactivates EBNA2-Mediated Stimulation of Latent Membrane Proteins Expressed from the Viral Divergent Promoter. *J. Virol.* 79, 4492–4505.
 97. Petti, L., Sample, C., and Kieff, E. (1990). Subnuclear localization and phosphorylation of Epstein-Barr virus latent infection nuclear proteins. *Virology* 176, 563–574.
 98. Pich, D., Mrozek-Gorska, P., Bouvet, M., Sugimoto, A., Akidil, E., Grundhoff, A., Hamperl, S., Ling, P.D., and Hammerschmidt, W. (2019). First Days in the Life of Naive Human B Lymphocytes Infected with Epstein-Barr Virus. *MBio* 10, e01723-19.
 99. Pope, J.H., Horne, M.K., and Scott, W. (1968). Transformation of foetal human leukocytes in vitro by filtrates of a human leukaemic cell line containing herpes-like virus. *Int. J. Cancer* 3, 857–866.
 100. Pulvertaft, R.J.V. (1964). Cytology of Burkitt’s Tumour (African Lymphoma). *Lancet* 283, 238–240.
 101. Raab-Traub, N. (2015). Nasopharyngeal Carcinoma: An Evolving Role for the Epstein–Barr Virus. In *Current Topics in Microbiology and Immunology*, (Springer International Publishing), pp. 339–363.
 102. Raab, M., Sanhaji, M., Matthes, Y., Hörlin, A., Lorenz, I., Dötsch, C., Habbe, N., Waidmann, O., Kurunci-Csacsco, E., Firestein, R., et al. (2018). PLK1 has tumor-suppressive potential in APC-truncated colon cancer cells. *Nat. Commun.* 2018 91 9, 1–17.
 103. Reindl, W., Gräber, M., Strebhardt, K., and Berg, T. (2009). Development of high-throughput assays based on fluorescence polarization for inhibitors of the polo-box domains of

6. References

- polo-like kinases 2 and 3. *Anal. Biochem.* 395, 189–194.
104. Rickinson, A.B., Young, L.S., and Rowe, M. (1987). Influence of the Epstein-Barr virus nuclear antigen EBNA 2 on the growth phenotype of virus-transformed B cells. *J. Virol.* 61, 1310–1317.
105. Rochford, R., and Moormann, A.M. (2015). Burkitt's Lymphoma. In *Current Topics in Microbiology and Immunology*, (Springer International Publishing), pp. 267–285.
106. Romero-Masters, J.C., Ohashi, M., Djavadian, R., Eichelberg, M.R., Hayes, M., Bristol, J.A., Ma, S., Ranheim, E.A., Gumperz, J., Johannsen, E.C., et al. (2018). An EBNA3C-deleted Epstein-Barr virus (EBV) mutant causes B-cell lymphomas with delayed onset in a cord blood-humanized mouse model. *PLOS Pathog.* 14, e1007221.
107. Rooney, C.M., Rowe, D.T., Ragot, T., and Farrell, P.J. (1989). The spliced BZLF1 gene of Epstein-Barr virus (EBV) transactivates an early EBV promoter and induces the virus productive cycle. *J. Virol.* 63, 3109–3116.
108. Rosenblum, D., Gutkin, A., Kedmi, R., Ramishetti, S., Veiga, N., Jacobi, A.M., Schubert, M.S., Friedmann-Morvinski, D., Cohen, Z.R., Behlke, M.A., et al. (2020). CRISPR-Cas9 genome editing using targeted lipid nanoparticles for cancer therapy. *Sci. Adv.* 6, eabc9450.
109. Sattler, M., Schleucher, J., and Griesinger, C. (1999). Heteronuclear multidimensional NMR experiments for the structure determination of proteins in solution employing pulsed field gradients. *Prog. Nucl. Magn. Reson. Spectrosc.* 34, 93–158.
110. Schlee, M., Krug, T., Gires, O., Zeidler, R., Hammerschmidt, W., Mailhammer, R., Laux, G., Sauer, G., Lovric, J., and Bornkamm, G.W. (2004). Identification of Epstein-Barr Virus (EBV) Nuclear Antigen 2 (EBNA2) Target Proteins by Proteome Analysis: Activation of EBNA2 in Conditionally Immortalized B Cells Reflects Early Events after Infection of Primary B Cells by EBV. *J. Virol.* 78, 3941–3952.
111. Schmucker, S., and Sumara, I. (2014). Molecular dynamics of PLK1 during mitosis. *Mol. Cell. Oncol.* 1, 954–957.
112. Seki, A., Coppinger, J.A., Jang, C.-Y., Yates, J.R., and Fang, G. (2008). Bora and the Kinase Aurora A Cooperatively Activate the Kinase Plk1 and Control Mitotic Entry. *Science* (80-). 320, 1655–1658.
113. Sharma, P., Mahen, R., Rossmann, M., Stokes, J., Hardwick, B., Huggins, D., Emery, A., Kunciw, D., Hyvönen, M., Spring, D., et al. (2019). A cryptic hydrophobic pocket in the polo-box domain of the polo-like kinase PLK1 regulates substrate recognition and mitotic chromosome segregation. *Sci. Rep.* 9, 1–15.
114. Shevchenko, A., Wilm, M., Vorm, O., and Mann, M. (1996). Mass Spectrometric Sequencing of Proteins from Silver-Stained Polyacrylamide Gels. *Anal. Chem.* 68, 850–858.
115. Shultz, L., Saito, Y., Najima, Y., Tanaka, S., Ochi, T., Tomizawa, M., Doi, T., Sone, A., Suzuki, N., Fujiwara, H., et al. (2010). Generation of functional human T-cell subsets with HLA-restricted immune responses in HLA class I expressing NOD/SCID/IL2r gamma(null) humanized mice. *Proc. Natl. Acad. Sci.* 107, 13022–13027.
-

6. References

116. Skalsky, R.L., and Cullen, B.R. (2015). EBV Noncoding RNAs. In *Current Topics in Microbiology and Immunology*, (Springer International Publishing), pp. 181–217.
117. Śledź, P., Stubbs, C.J., Lang, S., Yang, Y.-Q., McKenzie, G.J., Venkitaraman, A.R., Hyvönen, M., and Abell, C. (2011). From Crystal Packing to Molecular Recognition: Prediction and Discovery of a Binding Site on the Surface of Polo-Like Kinase 1. *Angew. Chemie Int. Ed.* *50*, 4003–4006.
118. Strebhardt, K. (2010). Multifaceted polo-like kinases: drug targets and antitargets for cancer therapy. *Nat. Rev. Drug Discov.* *2010* *9*, 643–660.
119. Strebhardt, K., and Ullrich, A. (2006). Targeting polo-like kinase 1 for cancer therapy. *Nat. Rev. Cancer* *6*, 321–330.
120. Strowig, T., Gurer, C., Ploss, A., Liu, Y.F., Arrey, F., Sashihara, J., Koo, G., Rice, C.M., Young, J.W., Chadburn, A., et al. (2009). Priming of protective T cell responses against virus-induced tumors in mice with human immune system components. *J. Exp. Med.* *206*, 1423–1434.
121. Sunkel, C., and Glover, D. (1988). polo, a mitotic mutant of *Drosophila* displaying abnormal spindle poles. *J. Cell Sci.* *89*, 25–38.
122. Syed, N., Smith, P., Sullivan, A., Spender, L.C., Dyer, M., Karran, L., O’Nions, J., Allday, M., Hoffmann, I., Crawford, D., et al. (2006). Transcriptional silencing of Polo-like kinase 2 (SNK/PLK2) is a frequent event in B-cell malignancies. *Blood* *107*, 250–256.
123. Takada, K. (2012). Role of EBER and BARF1 in nasopharyngeal carcinoma (NPC) tumorigenesis. *Semin. Cancer Biol.* *22*, 162–165.
124. Takai, N., Hamanaka, R., Yoshimatsu, J., and Miyakawa, I. (2005). Polo-like kinases (Plks) and cancer. *Oncogene* *24*, 287–291.
125. Thorley-Lawson, D.A. (2001). Epstein-Barr virus: Exploiting the immune system. *Nat. Rev. Immunol.* *1*, 75–82.
126. Thorley-Lawson, D.A. (2005). EBV the prototypical human tumor virus - Just how bad is it? *J. Allergy Clin. Immunol.* *116*, 251–261.
127. Thorley-Lawson, D.A. (2015). EBV persistence-introducing the virus. In *Current Topics in Microbiology and Immunology*, (Springer International Publishing), pp. 151–209.
128. Thorley-Lawson, D.A., and Allday, M.J. (2008). The curious case of the tumour virus: 50 years of Burkitt’s lymphoma. *Nat. Rev. Microbiol.* *6*, 913–924.
129. Thorley-Lawson, D.A., and Gross, A. (2004). Persistence of the Epstein–Barr Virus and the Origins of Associated Lymphomas. *N. Engl. J. Med.* *350*, 1328–1337.
130. Thumann, S. (2016). Transcriptional regulation by the EBV nuclear antigen 2. Ludwig Maximilian University of Munich.
131. Tong, X., Wang, F., Thut, C.J., and Kieff, E. (1995a). The Epstein-Barr virus nuclear protein 2 acidic domain can interact with TFIIB, TAF40, and RPA70 but not with TATA-binding protein. *J. Virol.* *69*, 585–588.
132. Tong, X., Drapkin, R., Yalamanchili, R., Mosialos, G., and Kieff, E. (1995b). The Epstein-

6. References

- Barr virus nuclear protein 2 acidic domain forms a complex with a novel cellular coactivator that can interact with TFIIE. *Mol. Cell. Biol.* *15*, 4735–4744.
133. Tong, X., Drapkin, R., Reinberg, D., and Kieff, E. (1995c). The 62- and 80-kDa subunits of transcription factor IIH mediate the interaction with Epstein-Barr virus nuclear protein 2. *Proc. Natl. Acad. Sci.* *92*, 3259–3263.
134. Uchida, J., Yasui, T., Takaoka-Shichijo, Y., Muraoka, M., Kulwichit, W., Raab-Traub, N., and Kikutani, H. (1999). Mimicry of CD40 Signals by Epstein-Barr Virus LMP1 in B Lymphocyte Responses. *Science (80-.)*. *286*, 300–303.
135. Vranken, W.F., Boucher, W., Stevens, T.J., Fogh, R.H., Pajon, A., Llinas, M., Ulrich, E.L., Markley, J.L., Ionides, J., and Laue, E.D. (2005). The CCPN data model for NMR spectroscopy: Development of a software pipeline. *Proteins Struct. Funct. Bioinforma.* *59*, 687–696.
136. Wagner, H.J., Bein, G., Bitsch, A., and Kirchner, H. (1992). Detection and quantification of latently infected B lymphocytes in Epstein-Barr virus-seropositive, healthy individuals by polymerase chain reaction. *J. Clin. Microbiol.* *30*, 2826–2829.
137. Wang, F., Tsang, S.F., Kurilla, M.G., Cohen, J.I., and Kieff, E. (1990). Epstein-Barr virus nuclear antigen 2 transactivates latent membrane protein LMP1. *J. Virol.* *64*, 3407–3416.
138. Wang, L., Grossman, S.R., and Kieff, E. (2000). Epstein-Barr virus nuclear protein 2 interacts with p300, CBP, and PCAF histone acetyltransferases in activation of the LMP1 promoter. *Proc. Natl. Acad. Sci.* *97*, 430–435.
139. Wang, S., Zhao, Y., Leiby, M., and Zhu, J. (2009). A New Positive/Negative Selection Scheme for Precise BAC Recombineering. *Mol. Biotechnol.* *42*, 110–116.
140. Warming, S., Costantino, N., Court, D.L., Jenkins, N.A., and Copeland, N.G. (2005). Simple and highly efficient BAC recombineering using galK selection. *Nucleic Acids Res.* *33*, e36–e36.
141. Watanabe, N., Arai, H., Iwasaki, J., Shiina, M., Ogata, K., Hunter, T., and Osada, H. (2005). Cyclin-dependent kinase (CDK) phosphorylation destabilizes somatic Wee1 via multiple pathways. *Proc. Natl. Acad. Sci.* *102*, 11663–11668.
142. White, R.E., Rämer, P.C., Naresh, K.N., Meixlsperger, S., Pinaud, L., Rooney, C., Savoldo, B., Coutinho, R., Bödör, C., Gribben, J., et al. (2012). EBNA3B-deficient EBV promotes B cell lymphomagenesis in humanized mice and is found in human tumors. *J. Clin. Invest.* *122*, 1487–1502.
143. Xu, J., Shen, C., Wang, T., and Quan, J. (2013). Structural basis for the inhibition of Polo-like kinase 1. *Nat. Struct. Mol. Biol.* *20*, 1047–1053.
144. Yuan, C., Wang, L., Zhou, L., and Fu, Z. (2014). The function of FOXO1 in the late phases of the cell cycle is suppressed by PLK1-mediated phosphorylation. *Cell Cycle* *13*, 807–819.
145. Yue, W., Davenport, M.G., Shackelford, J., and Pagano, J.S. (2004). Mitosis-Specific Hyperphosphorylation of Epstein-Barr Virus Nuclear Antigen 2 Suppresses Its Function. *J. Virol.* *78*, 3542–3552.
146. Yue, W., Gershburg, E., and Pagano, J.S. (2005). Hyperphosphorylation of EBNA2 by Epstein-Barr Virus Protein Kinase Suppresses Transactivation of the LMP1 Promoter. *J. Virol.*
-

6. References

- 79, 5880–5885.
147. Yue, W., Shackelford, J., and Pagano, J.S. (2006). cdc2/Cyclin B1-Dependent Phosphorylation of EBNA2 at Ser243 Regulates Its Function in Mitosis. *J. Virol.* *80*, 2045–2050.
148. Yun, S.-M., Moulaei, T., Lim, D., Bang, J.K., Park, J.-E., Shenoy, S.R., Liu, F., Kang, Y.H., Liao, C., Soung, N.-K., et al. (2009). Structural and functional analyses of minimal phosphopeptides targeting the polo-box domain of polo-like kinase 1. *Nat. Struct. Mol. Biol.* *16*, 876–882.
149. Zdimerova, H., Murer, A., Engelmann, C., Raykova, A., Deng, Y., Gujer, C., Rühl, J., McHugh, D., Caduff, N., Naghavian, R., et al. (2021). Attenuated immune control of Epstein-Barr virus in humanized mice is associated with the multiple sclerosis risk factor HLA-DR15. *Eur. J. Immunol.* *51*, 64–75.
150. Zimmerman, W.C., and Erikson, R.L. (2007a). Polo-like kinase 3 is required for entry into S phase. *Proc. Natl. Acad. Sci.* *104*, 1847–1852.
151. Zimmerman, W.C., and Erikson, R.L. (2007b). Finding Plk3. *Cell Cycle* *6*, 1314–1318.
152. Zitouni, S., Nabais, C., Jana, S.C., Guerrero, A., and Bettencourt-Dias, M. (2014). Polo-like kinases: structural variations lead to multiple functions. *Nat. Rev. Mol. Cell Biol.* *2014* *157* *15*, 433–452.

7. Appendices

7.1. Supplemental information

Table S1. Oligos used in plasmid construction.

Plasmid	Usage	Oligo	Sequence (5' → 3')	Annealing (°C)
pCKR656	PCR primers	xz54-F	ACGACCAACAATTACATCATCTACCCT	57
		xz317-R	ATTAGCTAGCGTAATCTGGAACATCGTATGGGTATCCCCGGCTCTGGCCTTG	57
pCKR657	PCR primers	xz54-F	ACGACCAACAATTACATCATCTACCCT	57
		xz318-R	ATTAGCTAGCGTAATCTGGAACATCGTATGGGTAATAATCTTCATCTGAGCTAGGAGATTCTGT	57
pXZ140	PCR primers	xz72-F	ATATGAATTCCATCATGCCAGAGCCAAACACCTCCAGTCC	57
		xz129-R	CAAAAATGTAATCCCAAGCTTCGTCTAAGTCTG	57
	PCR primers	xz129-F	CAGACTTAGACGAAGCTTGGGATTACATTTTTG	57
		xz53-R2	ATCTTTAGCTAGCGTAATCTGGAAC	57
pXZ141	PCR primers	xz72-F	ATATGAATTCCATCATGCCAGAGCCAAACACCTCCAGTCC	57
		xz130-R	GAGCTAGGAGATTCTACTGTCTCAAAAATG	57
	PCR primers	xz130-F	CATTTTTGAGACAGTAGAATCTCCTAGCTC	57
		xz53-R2	ATCTTTAGCTAGCGTAATCTGGAAC	57
pXZ142	PCR primers	xz72-F	ATATGAATTCCATCATGCCAGAGCCAAACACCTCCAGTCC	57
		xz130-R	GAGCTAGGAGATTCTACTGTCTCAAAAATG	57
	PCR primers	xz129-F	CAGACTTAGACGAAGCTTGGGATTACATTTTTG	57
		xz53-R2	ATCTTTAGCTAGCGTAATCTGGAAC	57
pXZ153	PCR primers	xz53-F1	AGCCCCTCAGGCCAGGTTGGTCCAG	57
		xz153-R1	CTGGATCATTGGGACGGCTTGATGAGTAAG	57
	PCR primers	xz153-F2	CTTACTCATCAAGCCGTCCCAAATGATCCAG	57
		xz52-R	CTCTGGTCTCCAAGGTCCACCG	57
pXZ154	PCR primers	xz54-F	ACGACCAACAATTACATCATCTACCCT	57
		xz154-R1	AGGCATGCTAGGAGCGGCGACGTTTGGCTCTGG	57
	PCR primers	xz154-F2	CCAGAGCCAAACGTGCGCGCTCCTAGCATGCCT	57
		xz53-R2	ATCTTTAGCTAGCGTAATCTGGAAC	57
pXZ155	PCR primers	xz54-F	ACGACCAACAATTACATCATCTACCCT	57
		xz155-R1	CATAATCTTCATCTGCGGCAGGAGCTTCTGTTGTCTC	57
		xz155-F2	GAGACAACAGAAGCTCCTGCCGCAGATGAAGATTATG	57

	PCR primers	xz53-R2	ATCTTTAGCTAGCGTAATCTGGAAC	57
pXZ179	PCR primers	xz54-F	ACGACCAACAATTACATCATCTACCCT	57
		xz179-R1	AGGCATGCTAGGAGCGGAGGTGTTTGGCTCTGG	57
	PCR primers	xz179-F2	CCAGAGCCAAACACCTCCGCTCCTAGCATGCCT	57
		xz53-R2	ATCTTTAGCTAGCGTAATCTGGAAC	57
pCKR675	PCR primers	xz51-F	ATTAGAATTCCATCATGGGGCATGGACCTCTAGCATCTG	57
		xz346-R	TAAGCCTCGGTTGTGCCAGAGGTGACAAAATGGTGGG	57
	PCR primers	xz346-F	TTGTCACCTCTGGCACAACCGAGGCTTACCCCTC	57
		xz53-R1.1	ATTAGGTCTCAGGCATGCGTGGTGGTGATGGT	57
pCKR676	PCR primers	xz203-Fwd Seq	CTCCTACCCCTCTGCCACCTGCAAC	57
		xz347-R	TAAGAGGGTGCATTGCTTGGTCTGGCACATGCAAGACA	57
	PCR primers	xz347-F	CATGTGCCAGACCAAGCAATGCACCCTCTTACTCATCAAAG	57
		xz317-R	ATTAGCTAGCGTAATCTGGAACATCGTATGGGTATCCCCGGCTCTGGCCTTG	57
pCKR677	PCR primers	xz53-F2.2	ATTAGGTCTCATGCCAGAGCCAAACACCTCCA	57
		xz348-R	GGGCGAGGTCTTTTAGCGGGTCCCTCCACATAATCTTCA	57
	PCR primers	xz348-F	TATGTGGAGGGACCCGCTAAAAGACCTCGCCCCT	57
		xz53-R2	ATCTTTAGCTAGCGTAATCTGGAAC	57
pCKR678	PCR primers	xz53-F2.2	ATTAGGTCTCATGCCAGAGCCAAACACCTCCA	57
		xz348-R	GGGCGAGGTCTTTTAGCGGGTCCCTCCACATAATCTTCA	57
	PCR primers	xz348-F	TATGTGGAGGGACCCGCTAAAAGACCTCGCCCCT	57
		xz53-R2	ATCTTTAGCTAGCGTAATCTGGAAC	57
pXZ288	PCR primers	xz72-F	ATATGAATTCCATCATGCCAGAGCCAAACACCTCCAGTCC	57
		xz261-R	AGCCGCATCATCGGGGCGAGAATGGGAGCCTCT	57
	PCR primers	xz261-F	GCCCCGATGATGCGGCTCCTCCATCTATAGACCCC	57
		xz263-R	AGCAGCGGCATCCCAACTTTCGTCTAAGTCT	57
	PCR primers	xz263-F	GCCGCTGCTGAGACAACAGAATCTC	57
	xz53-R2	ATCTTTAGCTAGCGTAATCTGGAAC	57	

pXZ229	PCR primers	xz190-F	ATTAGGATCCGGACAGAGCAGG	57
		xz229-R	ATTATCTAGACGTTAGGGG	57
pXZ150	PCR primers	xz150-F	TATA GGATCCATCTGCGACCCCCCGCAAC	57
		xz150-R	ATTA TCTAGA TCACTGGATGGAGGGGCGAGGT	57
pXZ151	PCR primers	xz150-F	TATA GGATCCATCTGCGACCCCCCGCAAC	57
		xz151-R	ATTA TCTAGA TCAATTGGATGGGCCAGGAGTTGG	57
pXZ152	PCR primers	xz152-F	TATA GGATCCAATGCCGCCCCCGTTTGTA	57
		xz150-R	ATTA TCTAGA TCACTGGATGGAGGGGCGAGGT	57
pCKR661	PCR primers	xz162-F	ATTAGGATCCCCAATACATGAACCG	57
		xz331-R	AATTTCTAGACTAATAATCTTCATC	57
pCKR672	PCR primers	xz190-F	ATTAGGATCCGGACAGAGCAGG	57
		xz331-R	AATTTCTAGACTAATAATCTTCATC	57
pXZ92	PCR primers	XZ92-F	ATTAGTCGACTGGACAGAGCAGG	57
		XZ92-R	ATTAGCGGCCGCTACTGGATGGA	57
pXZ93	PCR primers	XZ92-F	ATTAGTCGACTGGACAGAGCAGG	57
		XZ93-R	ATTAGCGGCCGCTAAACGTTAGG	57
pXZ94	PCR primers	XZ94-F	ATTAGTCGACTTCACCAATACATGAAC	57
		XZ92-R	ATTAGCGGCCGCTACTGGATGGA	57
pXZ109	PCR primers	XZ94-F	ATTAGTCGACTTCACCAATACATGAAC	57
		xz111-R	AATTGCGGCCGCTAATAATCTTCATC	57
pXZ110	PCR primers	XZ94-F	ATTAGTCGACTTCACCAATACATGAAC	57
		xz110-R	AATTGCGGCCGCTAATACCAATCA	57
pXZ111	PCR primers	xz111-F	ATTAGTCGACTCCTCCATCTATAGACC	57
		xz111-R	AATTGCGGCCGCTAATAATCTTCATC	57
pXZ112	PCR primers	xz112-F	ATTAGTCGACTGTGGAGGGACCCAG	57
		XZ92-R	ATTAGCGGCCGCTACTGGATGGA	57
pXZ113	PCR primers	xz111-F	ATTAGTCGACTCCTCCATCTATAGACC	57
		XZ92-R	ATTAGCGGCCGCTACTGGATGGA	57
pXZ162	PCR primers	xz162-F	ATTAGGATCCCCAATACATGAACCG	57
		xz111-R	AATTGCGGCCGCTAATAATCTTCATC	57

pXZ190	PCR primers	xz190-F	ATTAGGATCCGGACAGAGCAGG	57
		xz93-R	ATTAGCGGCCGCTAAACGTTAGG	57
pXZ198	PCR primers	xz198-F	ATTAGTGCAGCTCGCATGCATCTCCCTGTCTTG	57
		XZ92-R	ATTAGCGGCCGCTACTGGATGGA	57
pXZ299	PCR primers	xz299-F	ATTAGGATCCCGTGACTTAGACGAAAGTTGG	57
		xz299-R	TATAGCGGCCGCTAATAATCACGTTTCATCTGAGCTAGGAG	57
pXZ191	PCR primers	xz190-F	ATTAGGATCCGGACAGAGCAGG	57
		xz93-R	ATTAGCGGCCGCTAAACGTTAGG	57
pXZ261	PCR primers	xz162-F	ATTAGGATCCCCAATACATGAACCG	57
		xz261-R	AGCCGCATCATCGGGGCGGAGAATGGGAGCCTCT	57
	PCR primers	xz261-F	GCCCCGATGATGCGGCTCCTCCATCTATAGACCCC	57
		xz111-R	AATTGCGGCCGCTAATAATCTTCATC	57
pXZ262	PCR primers	xz162-F	ATTAGGATCCCCAATACATGAACCG	57
		xz262-R	GGCTGCAGCTGGAGGATACCAATCATCG	57
	PCR primers	xz262-F	GCTGCAGCCCCCGCAGACTTAGACGA	57
		xz111-R	AATTGCGGCCGCTAATAATCTTCATC	57
pXZ263	PCR primers	xz162-F	ATTAGGATCCCCAATACATGAACCG	57
		xz263-R	AGCAGCGGCATCCCAACTTTCGTCTAAGTCT	57
	PCR primers	xz263-F	GCCGCTGCTGAGACAACAGAATCTC	57
		xz111-R	AATTGCGGCCGCTAATAATCTTCATC	57
pXZ264	PCR primers	xz162-F	ATTAGGATCCCCAATACATGAACCG	57
		xz264-R	GGCTGCAGCTGGAGGAGCCGCATC	57
	PCR primers	xz262-F	GCTGCAGCCCCCGCAGACTTAGACGA	57
		xz111-R	AATTGCGGCCGCTAATAATCTTCATC	57
pXZ265	PCR primers	xz162-F	ATTAGGATCCCCAATACATGAACCG	57
		xz263-R	AGCAGCGGCATCCCAACTTTCGTCTAAGTCT	57
	PCR primers	xz263-F	GCCGCTGCTGAGACAACAGAATCTC	57
		xz111-R	AATTGCGGCCGCTAATAATCTTCATC	57
pXZ266	PCR primers	xz162-F	ATTAGGATCCCCAATACATGAACCG	57
		xz264-R	GGCTGCAGCTGGAGGAGCCGCATC	57

	PCR primers	xz262-F	GCTGCAGCCCCCGCAGACTTAGACGA	57
		xz111-R	AATTGCGGCCGCTAATAATCTTCATC	57
pXZ304	PCR primers	xz302-F	ATTACGTCTCACATGAGGATGCCTACATTCTATCTTGCG	57
		xz51-R	GCAAATAAGGCCCGGTCA	57
	PCR primers	xz302-F	ATTACGTCTCACATGAGGATGCCTACATTCTATCTTGCG	57
		xz213-R	ATTACTCGAGTCACTGGATGGAGGGGCGAG	57
pXZ161	PCR primers	xz161-F	ATTAGAATTCATGAGTGCTGCAGTGAAGTGCAGG	57
		xz161-R	AATTAAGCTTAGGAGGCCTTGAGACGGTT	57
	Sanger sequencing	xz161-1456R22	CCGAATAGTCCACCCACTTGC	63
pXZ164	PCR primers	xz164-F	ATTAACATGTTAGCACCGGCCGACCCTG	57
		xz164-R	AATTAAGCTTATTTATTGAGGACTGTGAGGGGCTTC	57
pXZ165	PCR primers	xz165-F	ATTACCATGGCGAAAGGCTTGGAGAACCCCTGCCTG	57
		xz165-R	AATTAAGCTTAGGAGGCCTTGAGACGGTTGCTGG	57

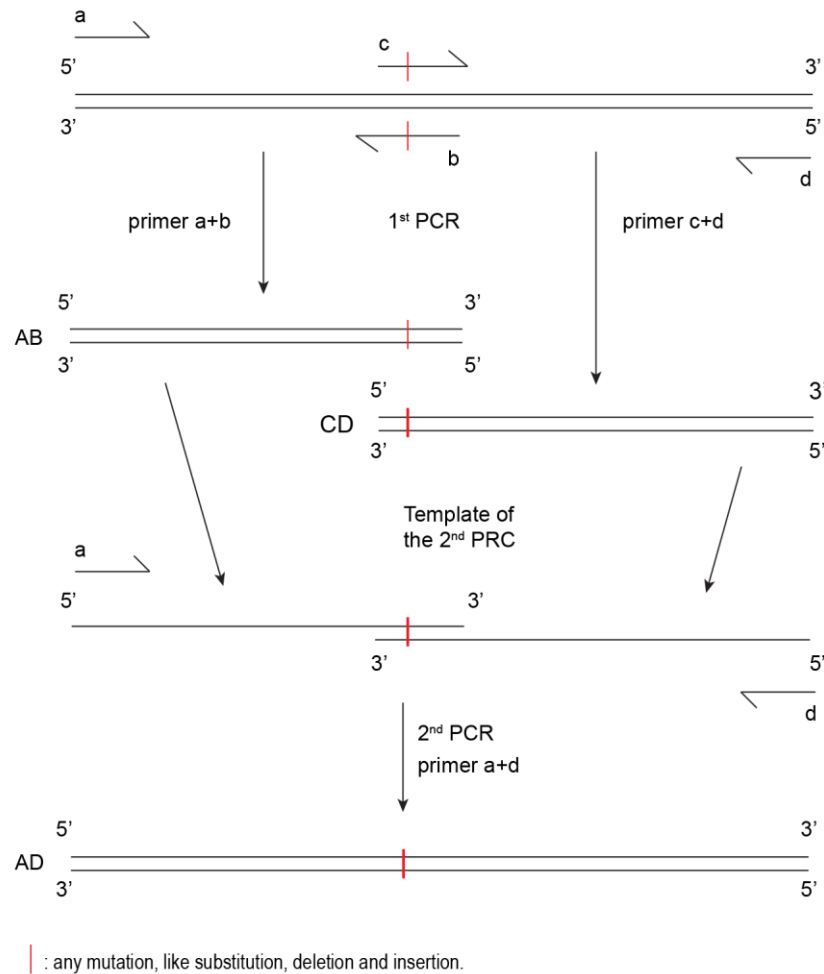
Table S2. Oligos used in BAC recombineering.

BACmid	Usage	Oligo	Sequence (5' → 3')	Annealing (°C)
pXZ135	PCR primers	xz135-F	ATGAAGATTATGTGGAGGGACCCAGTAAAAGACCTCGCCCCTCCATCCAGGGCCTG GTGATGATGGCGGGATCG	57
		xz135-R	GTAACATTTATTTGGGATACATTGGTTGCTGGAGAGGGCAAGGGTTTTTATCAGAAG AACTCGTCAAGAAGGCG	57
pXZ143	PCR primers	xz143-F	CCAGGGACAAGCAACGCAAG	57
		xz143-R	ACAGGTTTTGGCAACGAGAGC	57
pXZ201	PCR primers	xz201-F	TATAGACCCCGCAGACTTAGACGAAAGTTGGGATTACATTTTTGAGACAGGGCCTG GTGATGATGGCGGGATCG	57
		xz201-R	TCTTTTACTGGGTCCCTCCACATAATCTTCATCTGAGCTAGGAGATTCTATCAGAAG AACTCGTCAAGAAGGCG	57
pXZ146	PCR primers	xz146-F	GGAGACCAGAGCCAAACACC	57
		xz130-R	GAGCTAGGAGATTCTACTGTCTCAAAAATG	57

pXZ202	PCR primers	xz130-F	CATTTTTGAGACAGTAGAATCTCCTAGCTC	57
		xz146-R	TTGGGACTGGGGTAAAAGTGG	57
	Sanger sequencing	xz143-F	CCAGGGACAAGCAACGCAAG	63
		xz143-R	ACAGGTTTTGGCAACGAGAGC	63
PCR primers	xz202-F	CAAGCAACGCAAGCCCGGTGGACCTTGGAGACCAGAGCCAAACACCTCCAGGCCT GGTGATGATGGCGGGATCG	57	
	xz202-R	TTGTCCCTGATGAAGACCGAGGACTGGACTTAGTTCAGGCATGCTAGGACTCAGAA GAACTCGTCAAGAAGGCG	57	
pXZ203	PCR primers	xz203-F	TGCCAGACCAATCAATGCACCCTC	57
		xz203-R	GGGCGAGGTCTTTTACTGGGTCCCT	57
	Sanger sequencing	xz203-Fwd Seq	CTCCTACCCCTCTGCCACCTGCAAC	63
		xz143-R	ACAGGTTTTGGCAACGAGAGC	63
pXZ204	PCR primers	xz203-F	TGCCAGACCAATCAATGCACCCTC	57
		xz203-R	GGGCGAGGTCTTTTACTGGGTCCCT	57
	Sanger sequencing	xz203-Fwd Seq	CTCCTACCCCTCTGCCACCTGCAAC	63
		xz143-R	ACAGGTTTTGGCAACGAGAGC	63

Table S3. Oligos used in pathogen diagnosis.

Pathogen	Usage	Oligo	Sequence (5' → 3')	Annealing (°C)
EBV	PCR primers	BamHI W-F	TCGCGTTGCTAGGCCACCTT	57
		BamHI W-R	CTTGGATGGCGGAGTCAGCG	57

**Figure S1. Schematic diagram of overlap PCR-based mutagenesis.**

In the first round of PCR reactions, DNA of interest served as templates, using primer pairs “a” with “b” and “c” with “d”, respectively. The resulting amplified short fragment AB and CD worked as a new template when mixed with the flanking primer pair “a” and “d” in the second round of PCR, which results in amplification of the final long fragment AD with the desired mutation. Red bars annotate a mutation of interest, e.g. a substitution, a deletion, or an insertion. The figure is adapted from Francis et al., 2017

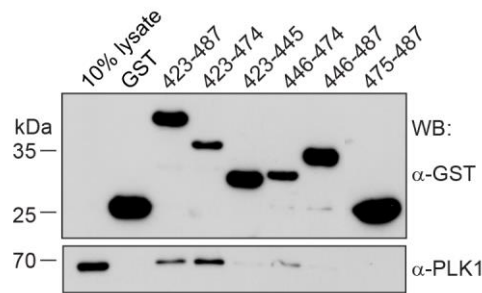


Figure S2. EBNA2 423-474 (PDS2) is sufficient for its binding to PLK1.

DG75 cell extracts were GST-pull-down using GST-fused EBNA2 C-terminal fragments 423-487, 423-474, 423-445, 446-474, 446-487, and 475-487, visualized by western blotting using GST- and PLK1- specific antibodies, respectively.

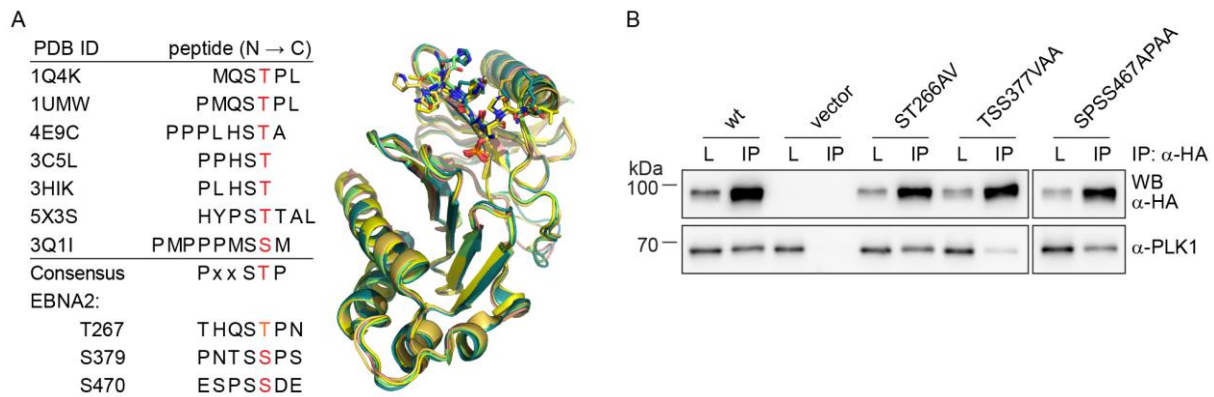


Figure S3. S379 is a canonical PLK1 docking site.

(A) Multiple sequence alignment (left) of seven phosphopeptides present in crystal structures of PLK1-PBD. Phosphorylated residues are in red. EBNA2 docking site candidates are listed below. Superposition (right) of crystal structures of the PLK1-PBD in complex with the seven peptides (MQSpTPL (PDB: 1Q4K) (Cheng et al., 2003), PMQSpTPL (PDB: 1UMW) (Elia et al., 2003a), PPPLHSpTA (PDB: 4E9C) (Śledź et al., 2011), PPHSpT (PDB: 3C5L), PLHSpT (PDB: 3HIK) (Yun et al., 2009), HYPSpTTAL (PDB: 5X3S) (Lee et al., 2018) and PMPPPMSpSM (PDB: 3Q11) (Pavlovsky et al., 2012)) show that the positively charged groove of PBD docks in a similar fashion to the negatively charged phosphopeptides. (B) Total cell lysates (L) of DG75 cells exogenously expressing HA-tagged EBNA2 mutants ST266AV, TSS377VAA, or SPSS467APAA were immunoprecipitation (IP) using an HA-specific antibody, visualized by western blotting using HA- and PLK1- specific antibodies, respectively. Figure S3A was provided by Dr. André Mourão (AG Sattler, HMGU).

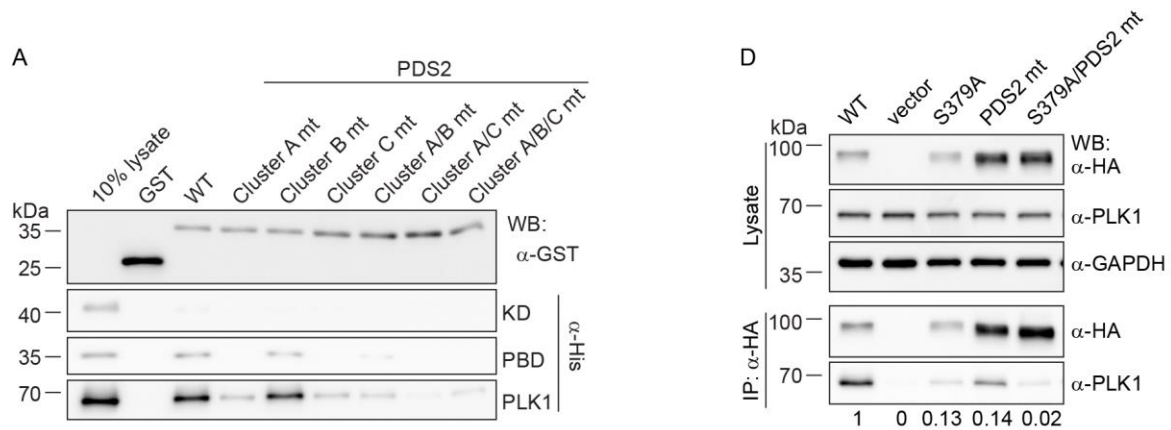


Figure S4. S379 and Cluster A/C are involved in PLK1 binding.

(A) Cluster A and C are essential for PDS2/PBD interaction. 6x His-tagged KD, PBD (both purified from *E. coli*), or PLK1 (purified from insect cells) were GST-pulldown using GST-fused EBNA2 PDS2 mutants cluster A mt (F440A/WY444AA), cluster B mt (SID448AAA), cluster C mt (YIF460AAA), cluster A/B mt (F440A/WY444AA/SID448AAA), cluster A/C mt (F440A/WY444AA/YIF460AAA), or cluster A/B/C mt (F440A/WY444AA/SID448AAA/YIF460AAA), visualized by western blotting using GST- and His- (α -His) specific antibodies, respectively. (B) Total cell lysates (L) of DG75 cells exogenously expressing HA-tagged EBNA2 mutants S379A, PDS2 mt, or S379A/PDS2 mt were immunoprecipitation (IP) using an HA-specific antibody, visualized by western blotting using HA-, PLK1- and GAPDH- specific antibodies, respectively.

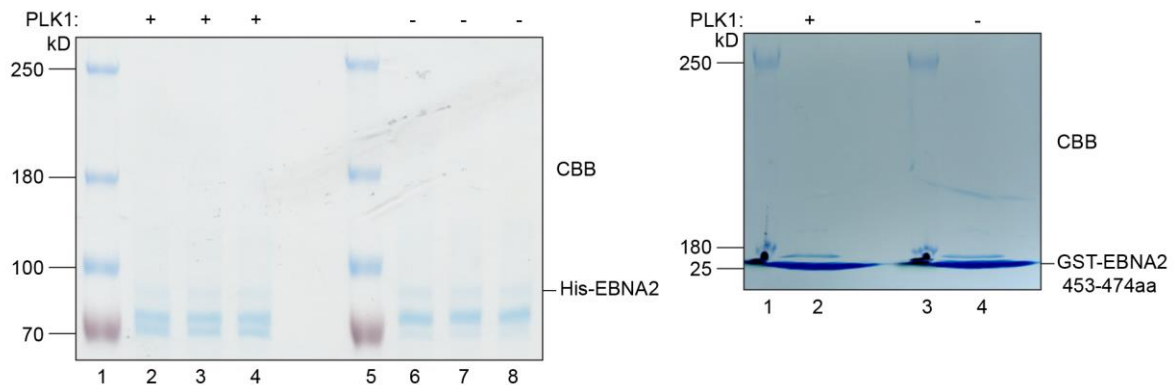


Figure S5. Electrophoresis separation of EBNA2 for LC-MS/MS.

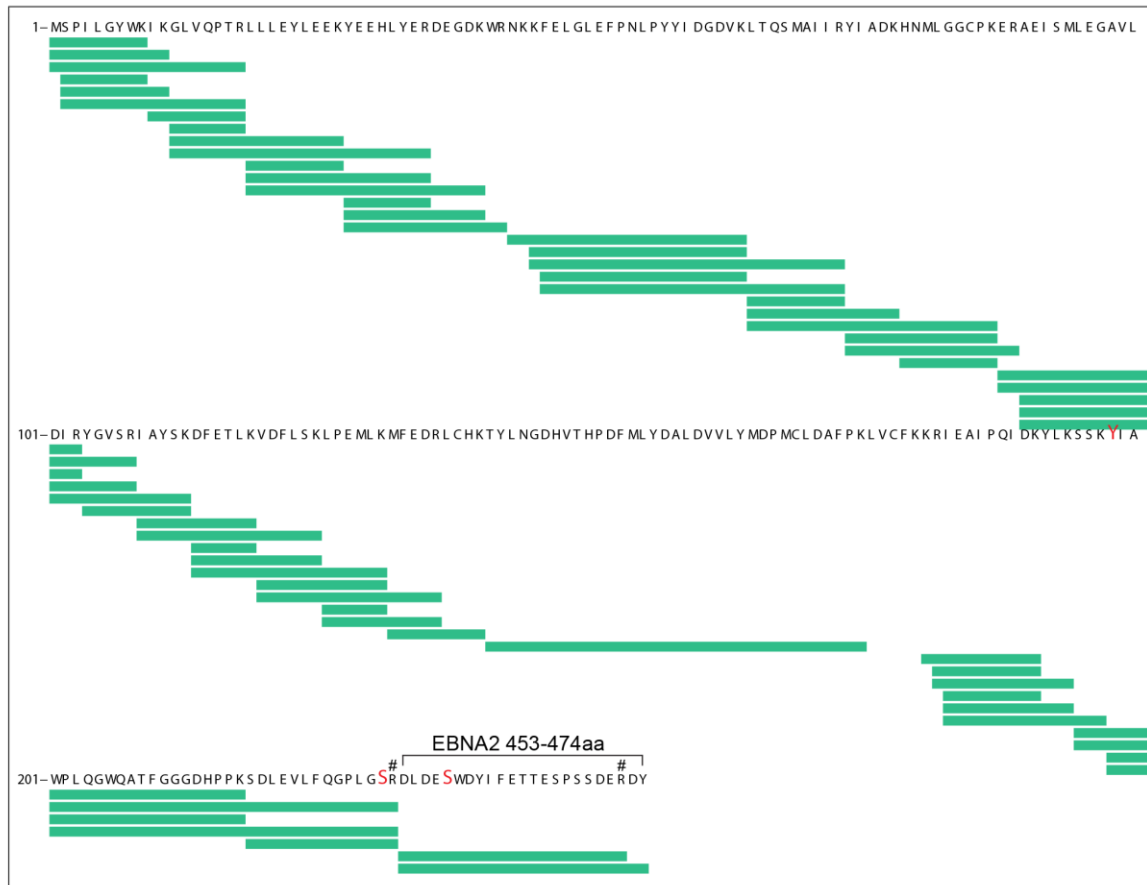
SDS-PAGE separation of 6x His-tagged EBNA2 (left) and GST-fused EBNA2 fragment 453-474 before (-) and after (+) PLK1 treatment, visualized by Coomassie Brilliant Blue staining.

Figure S6. Identification of phosphorylation sites of EBNA2 treated with PLK1.

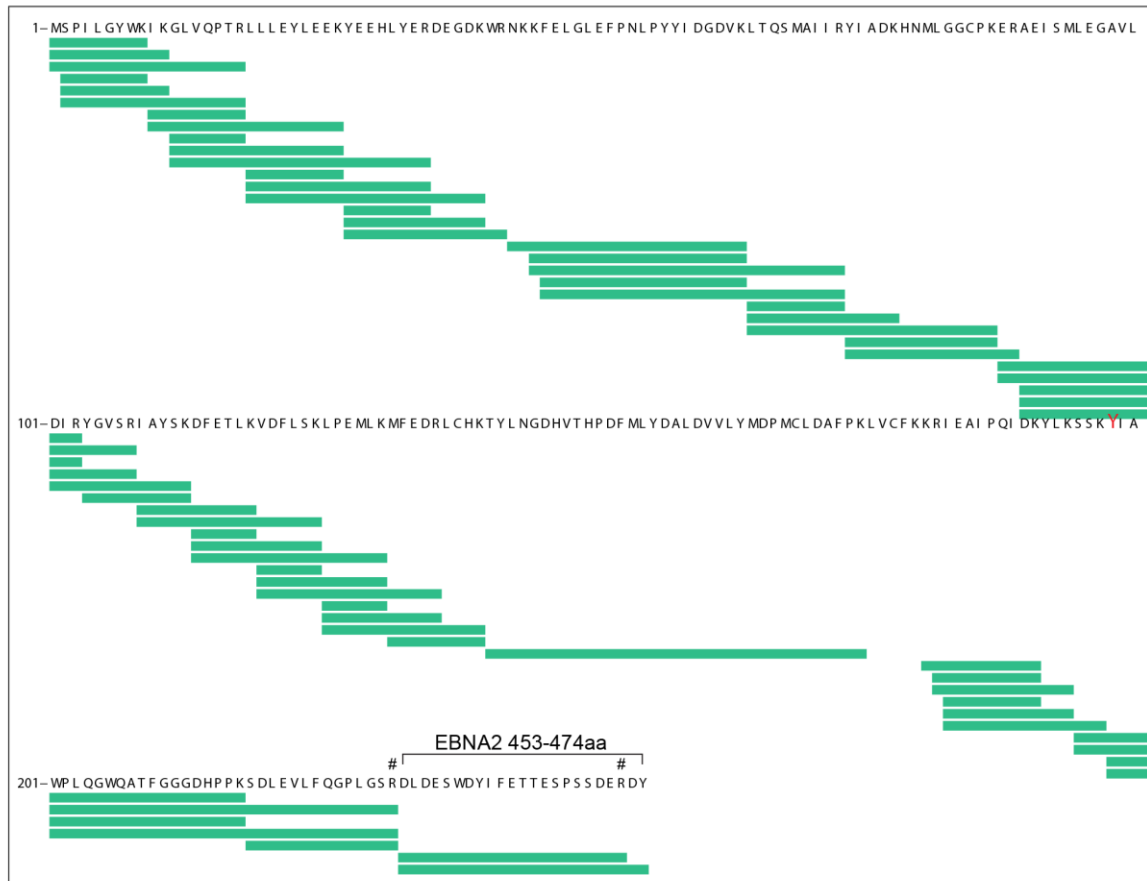
Overview of sequence coverage and phosphorylation sites (larger letters in red or purple) of 6× His-tagged EBNA2 before (-) and after (+) recombinant PLK1 treatment. Proteins of interest were extracted after SDS-PAGE separation, digested by trypsin (green bar) and V8 (blue bar) in parallel, and submitted to LC-MS/MS analysis. The number sign (#) denotes Arg (R) inserted to facilitate fragmentation. The asterisk (*) denotes the initial Met (M) of EBNA2.

7. Appendices

+ PLK1



- PLK1

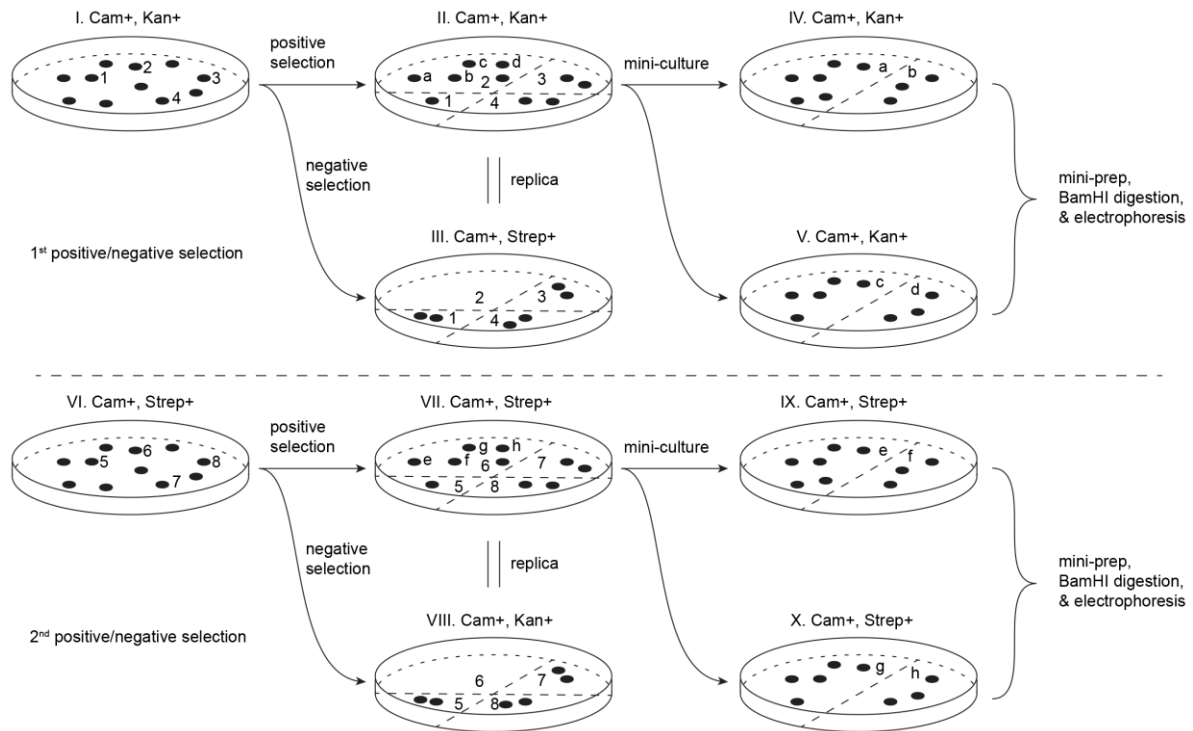


Enzyme: ■ Trypsin

Localization probability: ■ Localized

Figure S7. Identification of phosphorylation sites of EBNA2 fragment 453-474aa by PLK1.

Overview of sequence coverage and phosphorylation sites (larger letters in red) of GST-EBNA2 453-474aa before (-) and after (+) recombinant PLK1 treatment. Proteins of interest were extracted after SDS-PAGE separation, digested by trypsin (green bar), and submitted to LC-MS/MS analysis. The number sign (#) denotes Arg (R) inserted to facilitate fragmentation.

**Figure S8. Schematic diagram of positive/negative selection used in BAC recombineering.**

In the first recombineering, single E.coli SW105 clone #1, 2, 3, and 4 from plate I (Cam⁺ and Kan⁺) were streaked on area #1, 2, 3, and 4 of plate II (Cam⁺/Kan⁺), respectively, with plate III (Cam⁺/Strep⁺) as a replica of plate II. Because clone #2 could grow on plate II (positive selection) but not on plate III (negative selection), clones from area #2 were further identified. Clone #a, b, c, and d from plate II were streaked on area #a, b, c, and d of plate IV and V (Cam⁺/Kan⁺), respectively. Mini-prep of BACs were isolated from the bacteria, digested with BamH I, and analyzed using agarose electrophoresis. In the second recombineering, a similar protocol was applied. However, Cam⁺/Strep⁺ plates were used in positive selection and Cam⁺/Kan⁺ plates were used in negative selection.

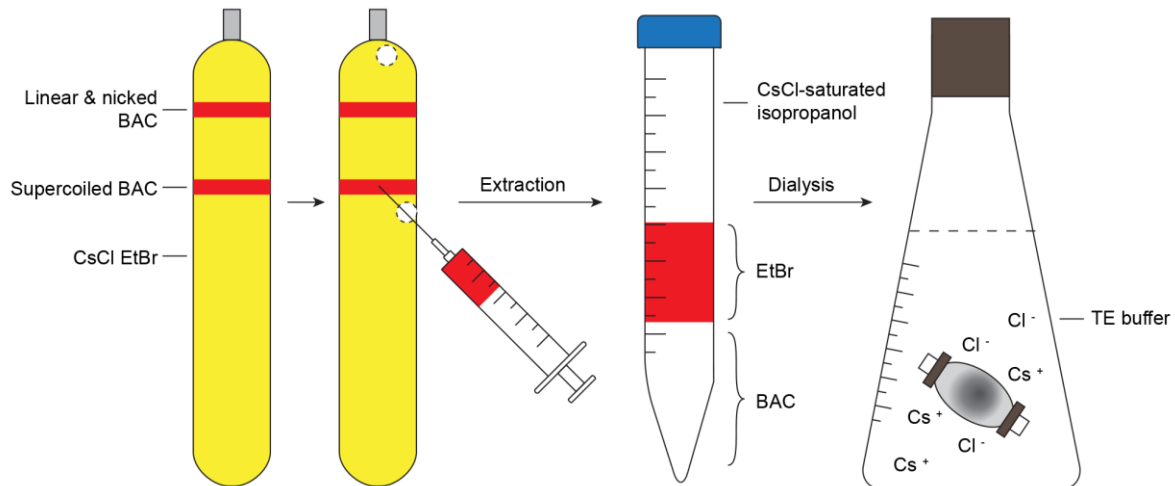


Figure S9. Schematic overview of supercoiled BACmid isolation.

Maxi-prep of the desired BACmid was separated by CsCl density gradient ultracentrifugation. The band of supercoiled BACmid was transferred to a 15 ml Falcon tube, followed by Ethidium bromide (EtBr) exclusion using CsCl-saturated isopropanol extraction. Subsequently, the BAC DNA phase was packed in a dialysis membrane and desalted with TE buffer to isolate the supercoiled BACmid.

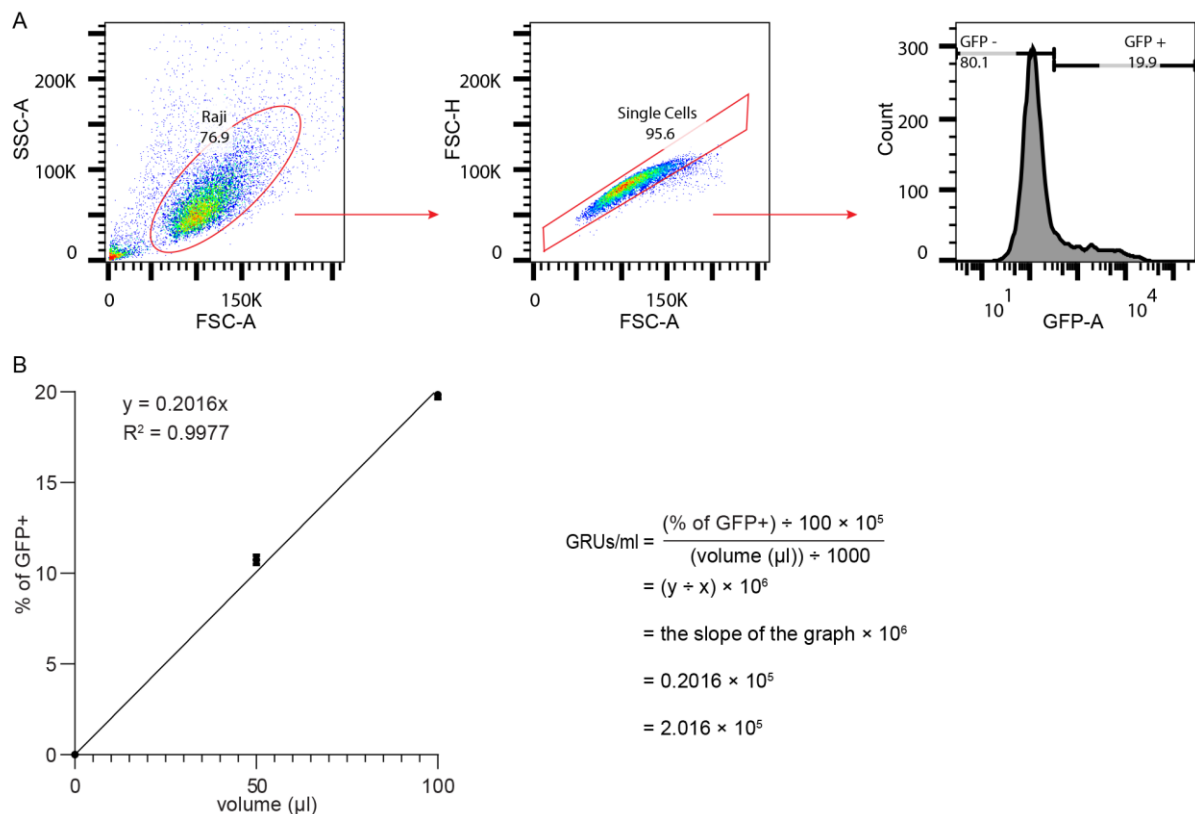


Figure S10. Recombinant EBV virus titration.

(A) Gating strategy of recombinant EBV-infected Raji cells. Raji cells were included in a “Raji” gate on an FSC-A vs SSC-A dot plot and depleted of doublets using a “Single Cells” gate on an FSC-A vs FSC-H dot plot. The single-cell fraction was further analyzed for eGFP expression using a “GFP+” gate on a GFP-A histogram. (B) Calculation of the titer of recombinant EBV. Graph of the percentages of GFP positive cells versus the volumes (μl) of recombinant EBV used to infect Raji cells with a linear regression line ($y = 0.2016x$, $R^2 = 0.9977$), showing data of 3 technical

7. Appendices

replicates of EBV EBNA2 S457A/T465V infection. The calculation of the virus titer (GRUs/ml) was presented on the right of the graph.

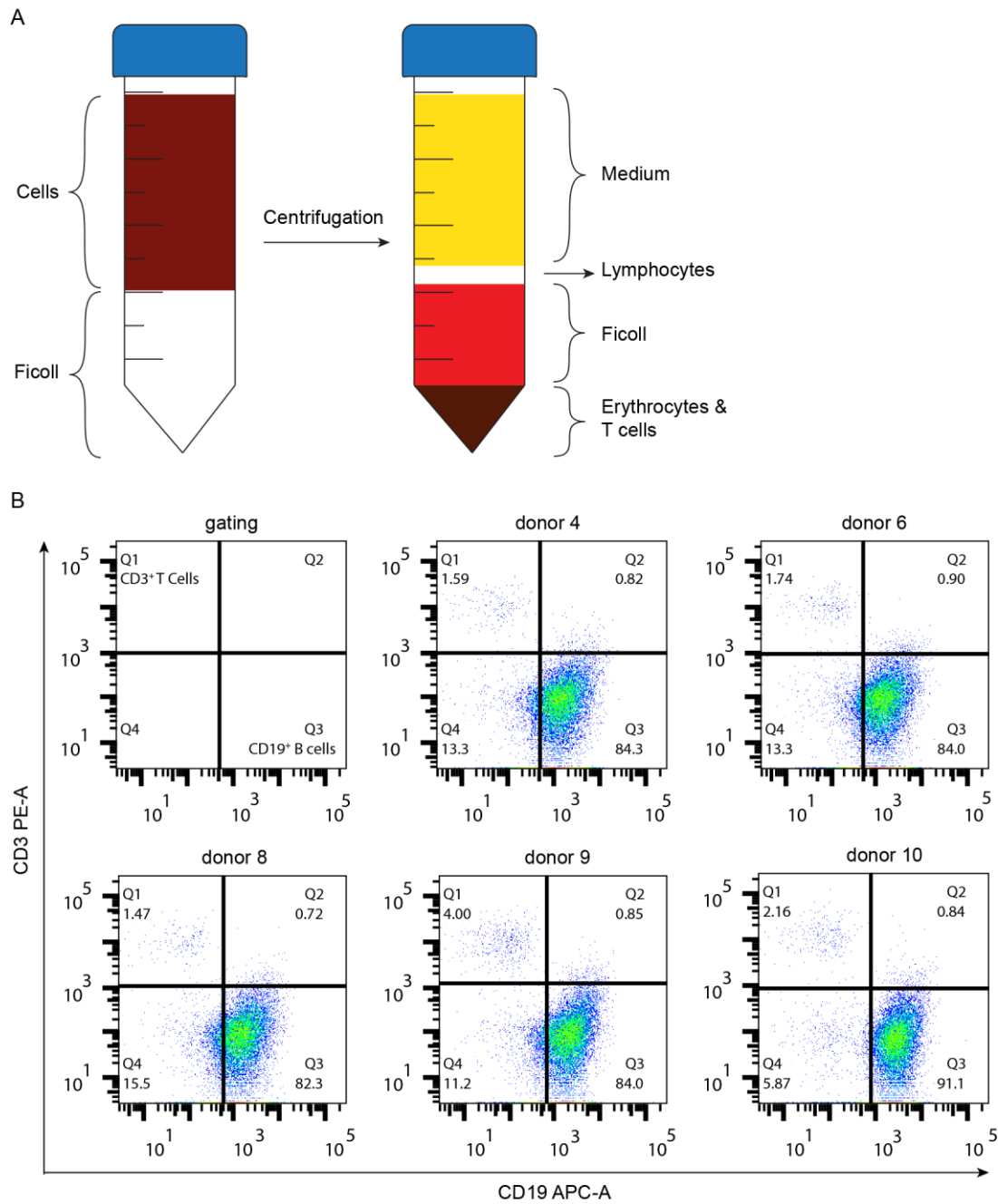


Figure S11. Preparation of human primary B cells.

(A) Schematic overview of human primary B cell isolation. Cells isolated from an adenoid were separated by Ficoll density gradient centrifugation. The lymphocyte phase containing human primary B cells was collected. Subsequently, several washing-and-centrifugation steps were applied to purify human primary B cells. (B) Flow cytometric analyses of the percentages of CD3⁺ T (Q1) and CD19⁺ B (Q3) cells. Data of 5 donors are shown.

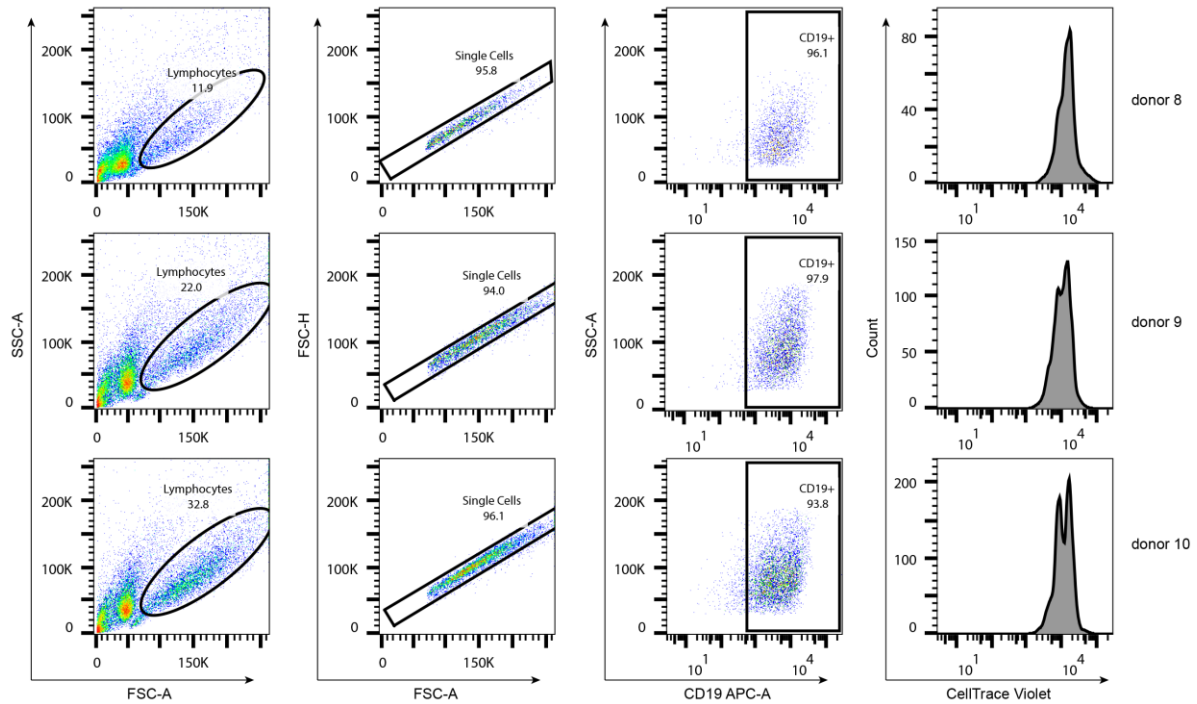


Figure S12. FACS profiles of cell trace violet proliferation assay of B cells after infection.

Gating strategy of B cells after EBV infection. Primary B cells were stained with cell trace violet, infected with EBV, and then analyzed by flow cytometry. EBV activated cells were included in a “Lymphocytes” gate on an FSC-A vs SSC-A dot plot, depleted of doublets using a “Single Cells” gate on an FSC-A vs FSC-H dot plot, and B cells were included in a “CD19+” gate on a CD19 APC-A vs SSC-A dot plot. The B cell fraction was further analyzed for cell trace violet dilution on a CellTrace Violet histogram. Data of 3 donors 4 d.p.i. are shown.

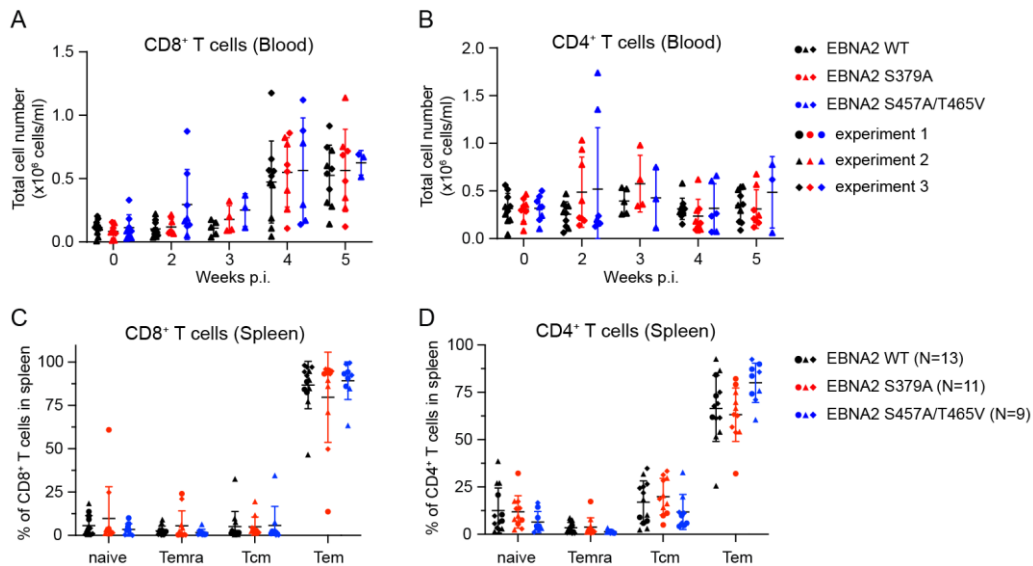


Figure S13. Infection with EBV strains expressing EBNA2 mutants deficient for PLK1 docking or phosphorylation leads to earlier CD8⁺ T cell expansion.

(A, B) Total cell numbers of (A) CD8⁺ T cells and (B) CD4⁺ T cells in blood of infected individuals over five weeks. Data were presented as the mean \pm SD. Multiple Mann-Whitney U test. Graphs show data points of two independently performed experiments. (C, D) Percentages of (C) CD8⁺ and (D) CD4⁺ T cell subsets in spleens of infected mice. Graphs show data points of three independently performed experiments. Error bars indicate mean \pm

SD. Shapes of data points indicate to which repetition of the experiments the individual belongs. Figure S13 was provided by Patrick Schuhmachers (AG Münz, UZH).

7.2. Comments on figures

Table S4. Collaborators' contributions to the figures in this thesis

Figure	Collaborator	Their contribution
8E and S4	Dr. André Mourão (AG Sattler, HMGU)	PLK1 purification
9A	Dr. André Mourão (AG Sattler, HMGU)	PDS1 purification
15B	Cornelia Kuklik-Roos (AG Kempkes, HMGU)	Transfection and dual-luciferase assay

Table S5. My contributions to the figures provided by my collaborators

Figure	Provider	My contribution
9C and S3A	Dr. André Mourão (AG Sattler, HMGU)	Plasmid construction of PLK1 PBD
10	Dr. André Mourão (AG Sattler, HMGU)	Plasmid construction of EBNA2 PDS2 WT, Cluster A mt, Cluster C mt, and Cluster A/C mt and PLK1 PBD
13, S6 and S7	Dr. Piero Giansanti (AG Küster, TUM)	Plasmid construction, protein purification, kinase assay, and protein separation of 6x His-tagged EBNA2 and GST fused-EBNA2 fragment 453-474aa
22, 23 and S13	Patrick Schuhmachers (AG Münz, UZH)	BACmid recombineering, virus production, virus concentration, virus titration of recombinant EBV EBNA2 WT, S379A, and S457A/465V

The results show in all figures which are not listed in Table S4 and Table S5 were generated by me. Schematic figures adapted from elsewhere were annotated in the figure legends.

7.3. Affirmation

Eidesstattliche Erklärung

Ich versichere hiermit an Eides statt, dass die vorliegende Dissertation mit dem Titel

“Inhibition of PLK1-dependent phosphorylation of EBNA2 promotes
EBV-induced carcinogenesis in humanized mice”

von mir selbstständig und ohne unerlaubte Hilfe angefertigt ist.

München, 02.02.2021

Xiang Zhang

Erklärung

Hiermit erkläre ich,

dass die Dissertation nicht ganz oder in wesentlichen Teilen einer anderen
Prüfungskommission vorgelegt worden ist.

dass ich mich anderweitig einer Doktorprüfung ohne Erfolg nicht unterzogen habe.

München, 02.02.2021

Xiang Zhang

